Physicochemical Properties of Skimmed Milks, Milk Gels, and Sodium Caseinates from Bovine A1A2 and A2 Milks

Weam Sameer Banjar

A thesis submitted in fulfilment of the requirements for the degree of Doctor of Philosophy in Food Science, The University of Auckland, 2020

Dedication

I dedicate this thesis to my parents, family and to everyone who supported me with immense gratitude. Thank you for making me see my dream become true.

Abstract

Globally, milk and the Dairy Industry is an important part of the food sector. Many studies have been conducted to investigate the behaviour of dairy products and their ingredients. The appearance of commercial A2 milk in the recent years has sparked a huge number of debates on the health benefits of A2 β-casein (A2 β-CN) compared to the regular cow's milk containing both A1 and A2 β-CN variants. As the consumption of the A2 milk is increased due to its claimed health benefits, more research on the physicochemical properties of this milk is needed. The main aim of this thesis is to compare some physicochemical properties of A2 and A1A2 milks to determine if they are different when utilised as milk products or as dairy ingredients such as sodium caseinate. Additionally, the structural alterations of A2 and A1A2 milks under processing should be also compared in order to reveal their effects on the properties of these two milks.

In this thesis, sodium caseinates (SC) were extracted from regular A1A2 and A2 milks, and compared in terms of their physicochemical properties using different methods. Rheological analysis revealed that the viscosity of SC increased with increasing total solid concentration, especially with the concentrations > 1wt%. Moreover, an increase in the particle size of SC was observed with increasing their concentrations, likely due to the presence of large aggregate, as measured by dynamic light scattering (DLS). The analysis of SC adsorption behaviour onto the latex particles showed that the adsorbed layer of SC was around 10 nm and the protein full protein surface coverage attained at around 16.5 mg/m^2. The internal structure of SC by small angle X-ray scattering (SAXS) revealed that the radius of gyration (R_g) of SC particles is around 7 nm and consist of protein inhomogeneities (~ 3 nm) within the particles. The results of SAXS and DSL are not in agreement due likely to the sensitivity of DLS to large aggregates. This study showed that there is no difference in the investigated physicochemical properties of the SCs extracted from regular A1A2 and A2 milks.

Milk gels were prepared by acidifying heated and non-heated A1A2 and A2 milks using glucono-δ-lactone (GDL) with the milk concentration ranging from 5 to 20 wt%. Both these acid milk gels and selected commercial stirred yoghurts were examined by diffusing-wave apectroscopy (DWS) coupled with multiple speckle diffusing-wave spectroscopy (MSDWS). DWS and MSDWS were both designed and developed in-house. It is found that the measurement of acid milk gels samples was extremely difficult due to the nature of the samples

and the structural characteristics of the gels. It is found that the structure of the milk gels continues to evolve, which leads to the importance of time when the measurement was taken. Two dynamics were detected for the milk gels; a first fast dynamic with a relaxation time at around 2 ms due to the diffusion of the individual protein aggregates, and a second slow dynamic (>10 s) associated with the dynamic of the whole system. DWS-MSDWS was found to be very adequate to measure the stirred commercial yoghurts. Only a slow relaxation time which seems to be dependent of the product of the viscosity by the protein aggregate size is observed. Based on the experimental results, it was difficult to differentiate the dynamic behaviour of acid milk gels prepared from A1A2 and A2 milks.

In-situ study on the impact of high hydrostatic pressure (HHP) on milk was presented in the last part of this thesis. The first experiment was conducted using SAXS coupled a diamond anvil cell (DAC) to elucidate the effect of the pressure on the substructures of the casein micelles. The dissociation of casein micelles was monitored with the pressure increasing up to approximately 1 GPa. The results indicate that casein micelles, under high pressure, dissociate into smaller "sub-micelles" and individual casein molecules. Moreover, the partial reversible structural changes of casein micelles were observed upon releasing the pressure to the atmospheric pressure. The second experiment was performed on purpose-built apparatus, which is assembled by connecting a simple turbidity measurement system with a commercially available HHP unit (up to 700 MPa) fitted with two spectroscopic windows. Reconstituted A1A2 and A2 milk samples with different pH values (from 5.5 to 10.5) were investigated. The result indicated that increasing the pH from 5.7 to 8.7, the pressure threshold value required for milk dissociation is increased from 180 MPa to 250 MPa. Increasing the pH of the sample from 8.7 to >10 did not result in the change in the pressure threshold (250 MPa). These findings did not show any differences in the behaviour of A1A2 and A2 milks under pressure at different pHs.

Overall, the findings of this thesis indicate that the physicochemical properties of A1A2 and A2 milks under high pressure, when acidified to form gels, and made into SCs, are similar. This is likely because the fraction of A1β-CN present in the A1A2 milks is low to impart noticeable differences in the physicochemical properties these two different milks.

Acknowledgements

I cannot express enough my deepest appreciation to Associate professor Yacine Hemar for his help, support, dexterous guidance, and immense knowledge. I was extremely lucky to meet him in 2010 and start my high educational journey under his supervision. I am very proud to be one of his students and get the chance to learn and improve my knowledge and experiences with him. During my journey I have been through extremely hard times and he was always next to me and motivated me to carry on. Assoc. Prof. Hemar is more than a teacher for me; he is the one who taught me how to be stronger and how to deal with life pressures. Without his honest nursing, patience, and wise supervision, it would have been impossible for me to complete my thesis or to reach the spot where I am now.

Also, I deeply indebted to Dr. Pascal Hebraud for his time, help, and generous hospitality in Strasbourg (France). Without his assistances and support, it would have been very difficult for me to complete my DWS/MSDWS works. It was my pleasure to get a chance to work with him personally. Regardless of my fascination with his genius, he is one of the kindness gentlemen in the world. Moreover, I cannot forget to thanks Dr. Loic Hilliou and Dr. Zhi Yang for their time, assistances and valuable suggestions in my research works. Despite Dr. Yang's busyness, he was checking my works and writing generously. Moreover, I would like to acknowledge my current supervisor Dr. Fan Zhu for accepting me to be one of his team members.

Special thanks for many researchers and technicians for their assistances and technical supports. These included Roger Van Ryn (Laboratory Electronics Technician), Mr. Martin Middleditch (Liquid Chromatography-Tandem Mass Spectrometry, LC-MS/MS), Mr. Tony Chen (Liquid Chromatography-Tandem Mass Spectrometry, LC-MS), Ms. Sreeni Pathrana (Food Science Lab), and Dr. Don Otter for helping me to reach lab technicians in Massy University, Ms. Fliss Jackson and Ms. Leiza Turnbull (Nutrition Laboratory, Massy University).

Many thanks for my research colleagues and friends who were always supporting me, Dr. Elisa Lam, Dr. Zhao Li, Dr. Mona Alzahrani, Dr. Fithri Nisa, Dr. Da Chen, Dr. Guantian, Dr. Norliza Julmohammad, Dr. Anise, Dr. Dongxing Li, Rasangi Sabaragamuwa, Jessica Sudam, Cheng Xu, Robin Wu, Xu Xu, Brooke Eastwood, Yiran Wang, Qinchen Li, Wing Kiu Sea, Ravnit Singh, Ronbin Cui, Jiecheng Li, Noor Febrianto, and Mejo Kuzhithariel, I'm extremely grateful

for their encouragement in my difficult before the happy moments during my study. A special thanks for my special friend Hussam Alzubidi who was backing me solidly and helping me with everything he could since the beginning of my PhD journey and until now.

Finally, I owe my deepest gratitude to my parents, siblings, and family members for their endless supports, cares, prays, and unconditional love. They have never given up on me and always carry on looking after me in my weirdest mood and behaviours during my PhD journey. I will treasure their supports all my life.

List of Contents

Dedication ..... **i**

Abstract ..... **ii**

Acknowledgements ..... **iv**

List of Contents ..... **vi**

List of Figures ..... **xi**

List of Tables ..... **xv**

Chapter 1. ..... **1**

Introduction and thesis aim and objectives **1**

1.1. Introduction 2

1.1.1. The objectives of the research 3

1.2. Thesis structure 4

Chapter 2. ..... **5**

Literature Review **5**

2.1. Milk 6

2.2. Composition of Milk 6

2.3. Protein 8

2.3.1. Casein 9

2.3.1.1 αs1-caseins (αs1-CN) 13

2.3.1.2. αs_2-caseins (αs2-CN) 13

2.3.1.3. Beta-caseins (β-CN) 13

2.3.1.3.1. The genetic variants of β-CN 14

2.3.1.3.1.1. A1 and A2 β-CN 15

2.3.1.4. Kappa-caseins (κ-CN) 16

2.3.2. Whey proteins 17

2.3.2.1. β-lactoglobulin (β-lg) 18

2.3.2.2. α-lactalbumin (α-lac) 18

2.4. Casein micelles 19

2.4.1. Structure of casein micelles 20

2.4.1.1. Dual-binding model 20

2.4.1.2. Sub-micelle or subunit model 21

2.5. Caseinate 23
2.5.1. Sodium caseinate (SC) 25
2.6. Factors influencing the physicochemical properties of milk 27
2.6.1. Acidification 28
2.6.2. Alkalisation 30
2.6.3. Heat treatment 31
2.6.4. High pressure (HP) treatment 34
2.7. Summary 36

Chapter 3. 37
Materials and Methods 37
3.1. Materials 38
3.1.1. Raw Materials 38
3.1.2. Minor chemicals 39
3.2. Methods 39
3.2.1. Solutions and samples preparation methods 39
3.2.1.1. Preparation of Imidazole-HCl (pH 7.0) Buffer 39
3.2.1.2. Skimming the untreated milk 39
3.2.1.3. Preparation of sodium caseinate (SC) 39
3.2.1.4 Reconstitution of SC samples 41
3.2.1.5 Reconstitution of milk samples 41
3.2.1.6 Preparation of acid milk gels 41
3.2.1.7 Preparation of milk samples used in the high pressure experiments 41
3.2.2. Physical methods 43
3.2.2.1. Rheological measurements 43
3.2.2.1.1. Frequency sweep 44
3.2.2.1.2. Time sweep 44
3.2.2.1.3. Strain sweep 44
3.2.2.2. Viscosity measurements 45
3.2.2.3. Capillary viscometry 46
3.2.2.4. Particle sizing measurements 47
3.2.2.4.1. Dynamic light scattering (DLS) 47
3.2.2.4.2. Static light scattering (SLS) 48
3.2.2.5. Diffusing Wave Spectroscopy (DWS) and Multi Speckle Diffusing

Wave Spectroscopy (MSDWS) 48
3.2.2.6. High pressure treatments 50
3.2.2.6.1. Pressure treatment using High Pressure Food Processing System (HPP) 50
3.2.2.6.2. Pressure treatment using a diamond anvil cell (DAC) 51
3.2.2.6.3. High pressure system with an optical spectroscopic cell 52
3.2.3. Chemical methods 54
3.2.3.1. Sodium dodecyl sulfate-polyacrylamide gel electrophoresis (SDS-PAGE) 54
3.2.3.1.1. Preparation of sodium dodecyl sulfate polyacrylamide gels 56
3.2.3.1.2. Instrumentation and characterisation 56
3.2.3.2. Determination of β-CN Gens Fractions Using Liquid Chromatography Coupled with Tandem Mass Spectrometry (LC− MS/MS) 56
3.2.3.2.1. Digestion the β-CN gel band 57
3.2.3.2.2. LC− MS/MS instrumentation and characterisation 58

Chapter 4. 60
Are dilute sodium caseinate solutions made from A1A2 and A2 milks different? Comparison between their viscosity, size, structure, and interfacial properties 60
4.1. Introduction 61
4.2. Materials and methods 62
4.2.1. Materials 62
4.2.2. Preparation of sodium caseinates (SCs) 62
4.2.3. Sample preparation 63
4.2.4. Viscosity measurements 63
4.2.5. Particle size measurements 64
4.2.5.1. SC solutions 64
4.2.5.2. Determination of the adsorbed SC layer on the of polystyrene spheres surface 64
4.2.6. Small-angle X-ray (SAXS) scattering 65
4.2.6.1. SAXS experiments 65
4.2.6.2. SAXS analysis 65
4.2.7. Statistical analysis 67
4.3. Results and Discussion 67

4.3.1 Viscosity and particle size measurements 67
4.3.2. SAXS investigation 70
4.3.3. Adsorption of SCs into latex particles 80
4.4. Summary 82

Chapter 5. 83
Application of DWS-MSDWS to model skim milk set gels and commercial stirred yoghurts 83
5.1. Introduction 84
5.2. Materials and Methods 85
5.2.1. Materials and sample preparation 85
5.2.2. DWS and MSDWS experimental setups 87
5.2.3. Particle size and viscosity measurements 88
5.3. Results and Discussion 88
5.4. Summary 92

Chapter 6. 94
Effect of high pressure on milks 94
6.1. Introduction 95
6.2. Materials and methods 99
6.2.1. Materials 99
6.2.2. Samples and experimental methods 99
6.3. Results and discussion 100
6.3.1. Physical appearance of milks 100
6.3.2. Sodium Dodecyl Sulfate Polyacrylamide Gel Electrophoresis (SDS-PAGE) 102
6.3.3. *In-situ* study of milk structure changes under HHP using synchrotron SAXS 103
6.3.4. *In-situ* investigation of the change in milks at different pHs using a high-pressure unit fitted with an optical cell 108
6.4. Summary 111

Chapter 7. 113
Conclusions and Future works 113
7.1. General Conclusions 114
7.2. Future Works 116

7.2.1 Comparing A2 milk to A1 milk (rather than A2 milk to A1A2 milk).....116
7.2.2. Improving the DWS-MSDWS setup 116
7.2.3. Study the effect of β-CN variant on the physicochemical properties and sensory attributes of model milk products......117
7.2.4 Study the effect of thermal processing on the physicochemical properties and structural characteristics of milks with different β-CN genotypes......117
7.2.5. Investigate the effect of β-CN variant on the digestion behaviours and nutrients absorption in dairy products including milk, yoghurt and cheese......117
7.2.6. In-situ study the milks with different β-CN genotypes under various external stressors 118
7.2.7. Effect of enzymatic and chemical cross-linking on milks with different β-CN genotypes.....118

References.....**119**
Appendix 1.....**135**
Appendix 2.....**136**

List of Figures

Figure 2. 1. Schematic depiction of gross composition of milk with its major constituents (Chandan, 1997).....7

Figure 2. 2. The total solids percentages of different components in skim and whole fat milk (Chandan, 1997).....8

Figure 2. 3. Detailed schematic depiction of the fractions of milk proteins (O'Connor, 1994). 9

Figure 2. 4. Structure of casein fractions adsorbed on planar hydrophobic interfaces. P, hydrophilic regions; B, hydrophobic region; and C denotes C-terminal block without SerP residues attached (Horne, 2002). 11

Figure 2. 5. Self-association of individual caseins generated by interaction of hydrophobic regions on neighbouring molecules (Horne, 2002).....12

Figure 2. 6. Detailed schematic features of the primary structure of β-CN (Jenness et al., 1988). 14

Figure 2. 7. Schematic representation of the positions of the diverse amino acids in A1 and A2 β-CN chains in bovine milk. 15

Figure 2. 8. Schematic representation of the differences between the amino acid structure in A2 β-CN and A1 β-CN, and the formation of BCM-7 during the digestion process of milk (Pal et al., 2015). 16

Figure 2. 9. Schematic diagram of dual binding model of casein micelles. Individual caseins α_{s1}-CN, α_{s2}-CN, β-CN and κ-CN are shown as monomers. B represents hydrophobic regions and P represents the hydrophilic regions (Horne, 2003).....21

Figure 2. 10. Schematic diagram of the structure of casein micelle based on the sub-micelle model (Horne, 2006).....22

Figure 2. 11. Schematic representation of the manufacture process of caseinates (Badem & Uçar, 2017). 24

Figure 2. 12. Schematic representation of the exchanges of minerals, water and casein molecules as a function of various physicochemical conditions (Broyard & Gaucheron, 2015). 28

Figure 3. 1. Schematic representation of the steps involved in the preparation of SC. 40

Figure 3. 2. (A) Anton-Paar Physica MCR 301 stress-controlled rheometer used. (B) The side view of the cup (left) and bob (right) geometry. (C) Schematic of the coaxial cylinders

measuring system of the geometry. (D) The top view of the cup (up) and bob (down) geometry. 45
Figure 3. 3. (A) The side view of the Cone-Plate CP50-2 geometry. (B) The top view of the Cone-Plate CP50-2 geometry. (C) The coaxial cylinders measuring system of the geometry. 46
Figure 3. 4. (A) Capillary viscometry experimental setup (A) Ubbelohde viscometer (filling tube and suction tube). 47
Figure 3. 5. (A) The covered DWS and MSDWS setup used at the University of Auckland, Auckland, NZ. (B) DWS and MSDWS detection systems.....49
Figure 3. 6. The DWS and MSDWS setup used at Institute Physical and Chemistry Materials De Strasbourg (IPCMS), Strasbourg, France.....50
Figure 3. 7. Schematic representation of the Avure 2L High Pressure Food Processing System. 51
Figure 3. 8. Schematic representation of the light scattered method connected to a laboratory High-pressure system with optical cell for spectroscopy (Model 765.0570, SITEC-Sieber Engineering AG, Maur (Zurich), SWITZERLAND). 53
Figure 3. 9. Schematic representation of the Red Helium Neon Laser system and compact spectrometer detector. 53

Figure 4. 1. Viscosity as a function of concentration for SC solutions obtained from A1A2 milks (●, ○) and A2 milks (■,□). Solid symbols and open symbols correspond to first and second batch, respectively. Error bars correspond to standard deviations. Inset is the data replotted for concentrations varying between 0.1 and 1 wt%.....68
Figure 4. 2. Intensity average diameter as a function of concentration for SC solution obtained from A1A2 milks (●, ○) and A2 milks (■,□). Solid symbols and open symbols correspond to first and second batch, respectively. Error bars correspond to standard deviations. 69
Figure 4. 3. Intensity size distribution for CS solution at concentration of 0.1% (■,□), 1% (●,○), and 10% (▲,△). Solid symbols are SC obtained from A2-B1 milk and open symbols are for SC obtained from A1A2-B2 milk. 70
Figure 4. 4. SAXS curves of the different sodium caseinates at different concentrations. The scattering profiles are vertically shifted for clarity. The model fits are demonstrated as a solid black line in each plot. 71
Figure 4. 5. SAXS data of A2B1 type SC of 0.6 wt% (A) and 6 wt% (B). The overall fits to the experimental SAXS data are demonstrated as solid black lines and individual levels are

depicted as brown and dark red dashed lines for levels 1 and 2, respectively.....73
Figure 4. 6. Fit parameters of (A) A1A2-B1, (B) A1A2-B2, (C) A2-B1, and (D) A2-B2 type of SCs defining the hard spheres structure factor, r the hard spheres radius, and η the volume fraction occupied by the protein hard spheres. The lines represent least-square fits to the data (excluding the value for η at 8 and 10 w/w% SC). 74
Figure 4. 7. Example of number particle size distribution of latex spheres alone (■, □), and in the presence of 0.02% (●,○) and 0.1 % (▲, △) SCs. Solid Symbols are for A1A2-B1 and open symbols are for A2-B1. 80
Figure 4. 8. Diameter of the latex particles mixed with SCs as a function of SCs concentration. Symbols represent: A1A2-B1 (■), A1A2-B2 (□), A2-B1 (●), A2-B2 (○) milks. Bars represent standard deviations.....81

Figure 5. 1. Example of DWS (open symbols) and MSDWS (solid symbols) autocorrelation functions for model acid milk gels made using unheated (black symbols) milk and heated (red and blue symbols) A1A2 milks. Inset: DWS-MSDWS of unheated milk gels made with milks with a concentration of 10% (black symbols) and 20% (red symbols). 89
Figure 5. 2. Slow half-life τ_{slow} for different acid gels made with unheated milks (black symbols) and heated milks (red symbols) as a function of the time at which the measurements were carried out (after incubation at 30 ^{o}C and 30 min equilibration to room temperature). Milks are A2 (open symbols) and A1A2 (solid symbols). Milk concentrations are: 5 (■), 10 (●), 15 (▲), and 20 (▼) %. 90
Figure 5. 3. Typical DWS and MSDWS correlation function of a commercial stirred yoghurt. Inset: slow relaxation τ_{long} measured by MSDWS as the function of the product of the viscosity and the mean volume size ($\eta \times D_{4,3}$). 92

Figure 6. 1. Flow diagram of the experimental procedures used in this chapter. 100
Figure 6. 2. Reconstituted freeze dried Anchor skim milk samples treated by different pressure (0, 100, 200, 400, and 600 MPa) using the Avure 2L high pressure food processing system (QFP 2L-700, Avure Technologies, Ohio, USA). Picture was taken at atmospheric pressure after 1 hour after pressure treatment. 101
Figure 6. 3. SDS-PAGE of 10% (w/w) reconstituted freeze-dried Anchor skim milk samples after pressure treatment at 0, 100, 200, 400, and 600 MPa at room temperature (~25°C) for 30 min 102

Figure 6. 4. (A) *In-situ* synchrotron SAXS patterns of skim milk solution (10 wt%) under various pressures. Inset: the isosbestic points are indicated by arrows. The scattering curves are vertically shifted for clarity. (B) Normalized scattering intensities at low-q (0.003 $Å^{-1}$) and high-q (0.08 $Å^{-1}$) with increasing pressures from atmospheric pressure to 960 MPa.....104
Figure 6. 5. (A) Example of SAXS scattering curve at 570 MPa (black symbol) with fit (solid red line) through two-state analysis using equation (6.1) mentioned below, along with the initial (270 MPa) and final (960 MPa) scattering curves. The scattering curves are vertically shifted for clarity. (B) Fitting parameters F(P) and 1-F(P) plotted as a function of pressure.....106
Figure 6. 6. (A) Time-evolution of the SAXS patterns after release of a pressure from 960 MPa to atmospheric pressure. The scattering curves are vertically shifted for clarity. (B) Values of the ambient normalized scattering intensities at low- (0.003 Å1) and high-q (0.08 Å1) at different time after pressure release to ambient pressure.....107
Figure 6. 7. Transmitted intensity as a function of wavelength for A1A2 milk at pH 6.7 for different applied pressures as indicated in the legend in MPa.....109
Figure 6. 8. Transmitted maximal intensities as a function of pressure for A1A2 milk at different pHs. 110
Figure 6. 9. Pressure threshold as a function of A1A2 (Westland, and Fonterra milks) and A2 milk's initial pH. 111

Figure A. 1. SDS-PAGE of normal A1A2 and A2 milks and extracted SCs from both types of milks.....135
Figure A. 2. Liquid chromatography–tandem mass spectrometry chromatograms (LCMS/MS) of β-CN fractions in A2 and A1A2 SC samples. 136

List of Tables

Table 2. 1. Some physicochemical properties of the different types of casein in milk (Chandan & Kilara, 2011). 10

Table 2. 2. Explanatory table of the amino acid sequences of β-CN variants (Farrell et al., 2002). 15

Table 2. 3. Typical composition of caseinates manufactured by diverse methods (all the values are presented on a dry basis) (Sarode et al., 2016). 26

Table 2. 4. Examples of typical heat treatment techniques utilised in the dairy industry (Fox et al., 2015). 32

Table 3. 1. Information of fresh milk collection. 38

Table 3. 2. Composition of A1A2 (Westland and Fonterra milks) and A2 milk powder. 38

Table 3. 3. Composition of the SCs obtained from two different batches (B1 and B2) of A1A2 and A2 milks 40

Table 3. 4. Different amounts of stock milk solution (15%), NaOH, and Milli-Q water (containing 0.02% sodium azide) used to obtain milk samples (10%) with different acidic pHs. 42

Table 3. 5. Different amounts of stock milk solution (15%), NaOH, and MilliQ water (containing 0.02% sodium azide) used to obtain milk samples (10%) with different alkaline pHs. 43

Table 3. 6. elution conations for LC-MS/MS. 58

Table 3. 7. Parameters for peptide identification by LC− MS/MS. 59

Table 4. 1. Chemical composition (wt%) of the A1A2 and A2 SCs. 63

Table 4. 2. SAXS model fit structural parameters of A1A2B1 type SC at different concentrations (w/w%). 76

Table 4. 3. SAXS model fit structural parameters of A1A2B2 type SC at different concentrations (w/w%). 77

Table 4. 4. SAXS model fit structural parameters of A2B1 type SC at different concentrations (w/w%). 78

Table 4. 5. SAXS model fit structural parameters of A2B2 type SC at different concentrations (w/w%). 79

Table 5. 1. Composition of the different commercial yoghurts (%) and their pHs.....86

Chapter 1.

Introduction and thesis aim and objectives

1.1. Introduction

Milk and dairy products are a big part of people's diet around the world since a long time ago. Consequently, milk has been given much attention scientifically to understand the behaviour of its components (Harding, 1995). Cow's milk contains a lot of components such as proteins, fats, vitamins, and minerals making it a very nutritious drink for human. Around 80% of the total protein in the milk is casein and it is divided to three types: α-casein (α-CN), β-casein (β-CN), and κ-casein (κ-CN). Each type of casein has diverse genetic variants, which decides its properties, functions and structure. The characteristics of these caseins are very significant in the process of making cheese and yoghurt (Nguyen et al., 2018). The percentage of the milk used to produce dairy products such as yoghurt, cheese, condensed milk, butter, flavoured milk and dry products is only about 7% in the world, and 22% of it is imported between countries. In order to increase the consumption of milk, attention given to dairy product development has significantly increased.

As one of the major caseins in milk, β-CN contains 13 different types of genetic variants and A1 and A2 genes are the most common variants among them (Farrell et al., 2002; Huppertz et al., 2018; Ward & Bastian, 1998; Woodford, 2007). It is reported that A2 was the original β-CN in bovine milk, with A1 being a result of mutations (Woodford, 2007). Regular cow's milk contains both gene variants A1 and A2, while A2 milk contains only A2 β-CN variant. The ratio of the A1 β-CN or A2 β-CN genes in the regular milk varies depending on the number of times the cows have been crossed to another breed. The only difference between those two genes is the amino acid in β-CN chain at position 67. Proline is the amino acid in this position in A2 β-CN, whereas histidine is the amino acid in this position in A1 β-CN (Kamiński et al., 2007).

It was reported that around 500 New Zealand dairy farmers were converting their herds to A2 milk to eliminate the production of A1 β-CN (Woodford, 2007). It was reported that the consuming A1 β-CN can lead to specific immunological processes that cause type I diabetes (Woodford, 2007). The bond of proline in A2 β-CN chain is stronger and more stable during the digestion process than the bond of histidine in A1 β-CN chain. A1 and A2 β-CN variants generate a lot of interest due to the creation of β-casomorphin7 (BCM7) from the cleavage of histidine bond in A1, while proline in A2 β-CN milk prevents splitting at this particular site and generates peptide BCM-9. BCM 7 is reported as a dangerous opioid peptide for developing

risky diseases for human including cardiovascular diseases and type I diabetes (Miluchová et al., 2016; Nguyen et al., 2017). In 2005, Truswell stated that consuming A1 β-CN might have an impact on the immune system by increasing the chance of type I diabetes in genetically susceptible children due to the release of BCM-7. However, there is no proven correlation between consuming A1 or A2 milk and having diabetes or other diseases (Truswell, 2005).

Even though there is a huge debate on the health benefits of consuming A2 milk compared to the regular A1A2 milk, limited research has been done on comparing the physicochemical properties between A1 β-CN and A2 β-CN variants. In 2015, the physicochemical properties of A1 β-CN, and A2 β-CN such as hydrodynamic radii and aggregation properties have been investigated using dynamic light scattering (DLS) and small-angle X-ray scattering (SAXS). It was indicated that A2 β-CN has smaller size than A1 β-CN, which may lead to some differences in their functionalities (Raynes et al., 2015). A1 β-CN was reported to be less soluble, highly hydrophobic, and has lower chaperone activity than A1 β-CN variant at the natural pH of milk (Darewicz & Dziuba, 2007; Nguyen et al., 2018; Raynes et al., 2015). In studies on the coagulation of the A2 and A1 milks, A2 milk showed weaker coagulation properties compared to the A1 milk (Nguyen et al., 2018; Poulsen et al., 2013).

Dairy processing requires milk systems to be subjected to various environmental conditions that may significantly influence the technological functionalities and the structure of both the casein molecules and casein micelles. Under the impact of acidification, alkalinisation, temperature treatment and pressure treatment, the structure and stability of casein micelles are modified, which lead to variations in physicochemical properties of the casein micelles and the milk (such as changes in turbidity, viscosity, texture and particle size). Therefore, investigating the physicochemical properties of milk is very important for understanding the function and behaviours of milk and assessing the quality of the resulting dairy products. However, only few research works comparing the physicochemical properties between regular milk containing A1A2 and A2 milks, are reported in the published literatures.

1.1.1. The objectives of the research

The scope of this research is to compare and investigate the differences in physicochemical properties between regular milk containing A1 and A2 β-CN variants, and milk containing only A2 β-CN variant, when they are used as ingredients such as sodium caseinates (SCs), products

(acid milk gels), or milk under various environmental conditions such as acidification, alkalinization, heating and pressure treatments. More specifically, the following objectives are addressed:

- Firstly, investigating the key differences in the physicochemical properties of sodium caseinates (SCs) made from regular A1A2 and A2 milks.
- Secondly, understanding the structural properties of stirred and unstirred different acidified milk gels prepared from A1A2 and A2 milks with different methods (with and without heat treatment) and at different milk concentrations. A diffusing wave spectroscopy coupled with multiple speckle diffusing wave spectroscopy (DWS-MSDWS) technique is implemented. Commercially available stirred yoghurt is also investigated using DWS-MSDWS.
- Thirdly, studying the structural changes of casein micelles in regular A1A2 and A2 milks at diverse pHs under different high hydrostatic pressures.

These objectives might help determine if there are differences in the behaviours of regular A1A2 and A2 milks, and their SCs, from a physicochemical viewpoint.

1.2. Thesis structure

In addition to this introductory chapter, this thesis comprises:

Chapter 2 which introduces general information on the contents of milk, with a main focus on caseins and the factors that affect the properties of milk. Some information will be repeated briefly in the working chapters.

Chapter 3 illustrates the materials and experimental methods used.

Chapter 4 the physicochemical properties of SCs extracted from regular A1A2 and A2 milks are investigated.

Chapter 5 investigates the structural properties of stirred and unstirred acid milk gels made with and without pre-heat treatment at 85^{o}C for 30 min and with different milk concentrations. A1A2 and A2 milks were used. Commercial stirred yoghurts were also investigated.

Chapter 6 explores the influence of different high hydrostatic pressures on the appearance of milk, the structure of the casein micelles, and the dissociation point of the casein micelles at diverse pHs for both A1A2 and A2 milks.

Chapter 7 is the general conclusion. Future works are also offered.

Chapter 2.

Literature Review

2.1. Milk

Milk is a white liquid generated via the female mammary glands of lactating animals (Horne, 2014). It is a fundamental and complex food source for the newborn, as it is designed to fulfil its nutritional needs. Many of the milk micro-constituents, additionally to providing the nutritional needs of the newborn, also serve a protective role. For example, milk contains immunoglobulins, which aid in the development of an effective immune system (Gerosa & Skoet, 2012). Milk has to be consumed at regular intervals by the newborn to maintain hydration and overall wellbeing, and to promote good health. The composition of milk depends on factors such as health status of the animal, genetic factors, stage of lactation and various environmental factors such as the climatic conditions of the place where the animal is located.

Milk is a complete nutritious food, and in most cases, it can be consumed without further processing. Economic growth in the developing world has led to an increase in consumption and supply of dairy products where approximately 740 million tonnes of milk were produced in 2011 (FAO, 2013). Common sources of milk are cows, buffaloes, sheep and goat. Bovine milk is the most commonly consumed globally, accounting for approximately 85% of the total milk consumed (Gerosa & Skoet, 2012). It contains nutrients required for development and growth and is a source of lipids, proteins, carbohydrates (lactose), vitamins and minerals. The milk composition undergoes a marked change over the course of lactation in order to adapt to the requirements of the newborn and its subsequent growth. For example, cows have a high protein content to account for the calves' weight doubling within 35 days, whereas human milk protein content is approximately lower to accommodate doubling of infant weight over the course of 165 days (Du & Yarema, 2010).

2.2. Composition of Milk

Milk has more than 100 different substances that are in either suspension, liquid, or emulsion in water. The composition of milk within any species varies between breeds, individual animals, feeding regime, age and health of the animal, stage of lactation, intervals of milking, season, weather, different quarters of udder, gestation period, environmental temperature, and many other factors. The major components of cow's milk are water (87.5%) and milk solids (12.5%).

Milk solids are divided to ~4% of milk solid fats (MSF) and ~9% milk solids-non-fat (MSNF). The MSNFs include proteins (~3.4%), carbohydrates (~4.8%), mineral substances (~0.7%), miscellaneous (salts, enzymes, gases and vitamins) and organic acids (Walstra et al., 2006). These MSNF components are distributed amongst the liquid phases and the casein micelles in the milk. Figure 2.1 presents the major constituents of milk. MSNFs are also referred to as the serum solids or skim solids. The meaning of "total solids" is the milk fat plus the skim solids (Chandan, 1997).

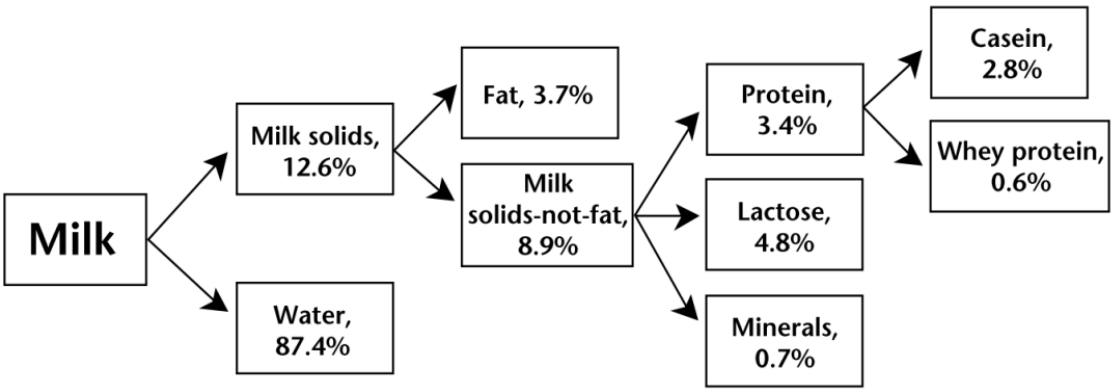

Figure 2. 1. Schematic depiction of gross composition of milk with its major constituents (Chandan, 1997).

The percentage comparison between the compositions of the skim and full fat milk is presented in Figure 2.2. It should be noted that the principal constituents of milk vary less widely in pooled market milk than in individual cow's milk. Non-fat milk or skim milk is milk that contains at least 8.25% of MSNF, in which the fat is reduced to no more than 0.5 g per one serving. Low-fat milk is milk that contains at least 8.25% MSNF in which the fat is no more than 3 g of milk fat per one serving. The dominant feature of non-fat milk is the casein micelles (Farrell et al., 2002).

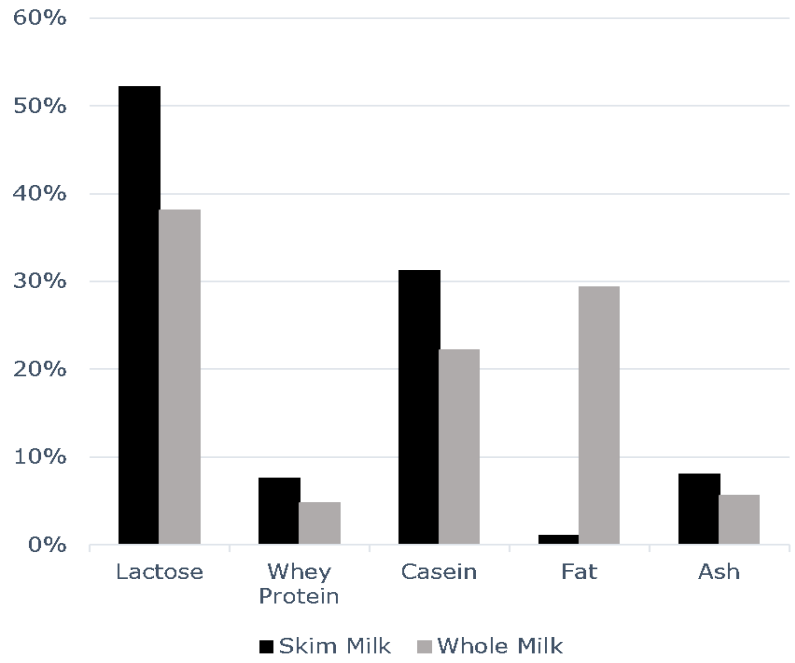

Figure 2. 2. The total solids percentages of different components in skim and whole fat milk (Chandan, 1997).

The concentrations of the other constituents, including magnesium, calcium, ash and phosphorus also vary significantly. In the case of cow milk, 0.78 g/100 mL was found as the average concentration of ash in milks of all breeds. Whereas, the total concentration of ash in specific milk lies in the range of 0.49 g/100 mL for the Holstein breed to 0.98 g/100 mL for the Jersey and Guernsey breeds (Chen et al., 2017). An interesting seasonal pattern can be observed in commercial milk that is used by food processors. There is about 10% variation in protein and fat in milk received during summer months (July and August) compared to milk received in late autumn (October and November). Variation in fat and protein can significantly affect cheese (Amenu & Deeth, 2007) and yoghurt manufacture (Atamian, et al., 2014), as well as the production of whey protein (Cintineo et al., 2018).

2.3. Protein

Proteins make up approximately 32 g/L (Haug et al., 2007) or 3.8% of total solid content of milk (Augustin et al., 2011). Milk proteins are a valuable source of amino acids; hence they are of significant biological value. The total protein component of milk is made of various specific proteins with functions ranging from antimicrobial, acting as growth factors, hormones, enzymes and antibodies, to enhancing nutrient adsorption.

Proteins are nitrogen-based compounds which comprises of three types: casein, whey, and non-protein nitrogen (NPN). Caseins are the primary group of milk proteins (78%), followed by whey (17%) and NPN (5%) (Jenkins & McGuire, 2006). The main fractions that make up whey proteins are α-lactalbumin (α-lac), β-lactoglobulin (β-lg), bovine serum albumin and immunoglobulins (Haug et al., 2007). Moreover, the main fractions of casein proteins are κ-casein (κ-CN), β-casein (β-CN), α_{S1}-casein (α_{S1}-CN) and α_{S2}-casein (α_{S2}-CN) (Augustin et al., 2011). In addition, enzymes and other minor proteins also make up the total content of protein in milk. The different types of proteins are summarised in Figure 2.3 (O'Connor, 1994).

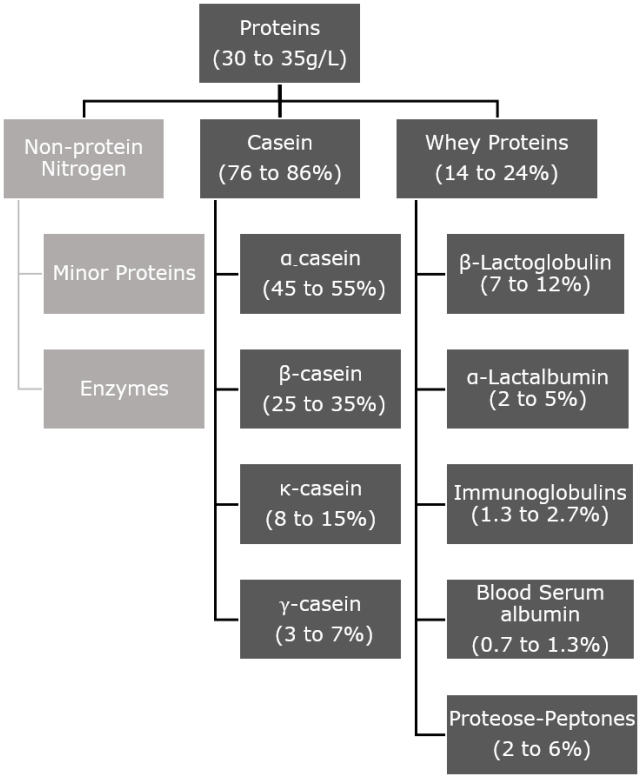

Figure 2. 3. Detailed schematic depiction of the fractions of milk proteins (O'Connor, 1994).

2.3.1. Casein

The approximate ratio of the major four types of caseins α_{S1}-CN, α_{S2}-CN, β-CN, and κ-CN are 4: 1: 4: 1 weight ratio in bovine milk. γ-casein (γ-CN) is a fragmentation of casein protein caused by plasmin action found in milk. The caseins are well-known in terms of their molecular weight, amino acid composition, major physicochemical properties and their concentrations in milk of various species. Moreover, all casein molecules possess good calcium phosphate-binding capacity, since all of them are phosphorylated to some extent. The presence of phosphate group is a unique feature which is common for all groups of individual caseins

(Augustin et al., 2011). Caseins are rheomorphic and are known for their excellent stabilizing and surface-active properties due to their high flexibility (Broyard & Gaucheron, 2015). A rheomorphic protein is the protein that has an open conformation with a vast number of side chains (de Kruif & Holt, 2003). The main casein fractions differ with regards to their phosphoserine (SerP) residues, proline residues and hydrophobicity, with these differences impacting their behavioural characteristics (Chandan & Kilara, 2011). Table 2.1 below summarizes the general physicochemical properties of the main caseins in milk.

Table 2. 1. Some physicochemical properties of the different types of casein in milk (Chandan & Kilara, 2011).

Protein	% Total casein	Molecular weight	Phosphate residues (mol/mol protein)	Proline residues (mol/mol protein)	Hydrophobic regions	Sulfhydryl groups
α_{s1}-CN	44 to 46	22,068 to 23,724	8 to 10	17	1 to 44, 90 to 113, 132 to 199	-
α_{s2}-CN	12	25,230	10 to 13	10	90 to 120, 160 to 207	2
β-CN	32 to 35	23,944 to 24,092	4 to 5	35	2/3 of C terminal end	-
κ-CN	8 to 12	19,007 to 19,039	1	20	5 to 65, 105 to 115	2

Caseins are referred to as phosphoproteins due to the presence of phosphate groups which are chemically bonded to the casein. These phosphate groups are esterified to SerP residues and to a lesser extent to the threoline (Thr) residue. The amount of phosphate groups in casein determines as to how reactive the calcium is, as these phosphate groups bind calcium in the form of calcium phosphate clusters. α_{s2}-CN is considered as the most phosphorylated casein, which contains 10 to 13 SerP residues. It is followed by α_{s1}-CN and β-CN with 8 to 10, and 4 to 5 phosphoserine residues, respectively. κ-CN only has one SerP and it is considered as the least phosphorylated casein (Augustin et al., 2011). As a result, α_{s1}-CN, α_{s2}-CN, and β-CN are deemed to be calcium-sensitive caseins, where it has been reported that the presence of calcium in concentration greater than ~6 mM at 20°C could lead to precipitation of these highly

phosphorylated caseins (Chandan & Kilara, 2011). In contrast, κ-CN is termed as calcium-insensitive due to the presence of only one phosphate group in its structure. Combining κ-CN with the calcium-sensitive caseins is known to stabilize and prevent the calcium-sensitive caseins from precipitating by developing colloidal particles known as casein micelles (Augustin et al., 2011). The amount of propyl residues can also have a significant impact on the structure of casein. This has been attributed to proline (Pro) residues being able to interrupt the formation of both α-helical and β-sheets. As β-CN has the highest number of Pro residues in its primary structure; its secondary structure undergoes the most disruption, followed by κ-CN, α_{s1}-CN and α_{s2}-CN (Swaisgood, 1992).

Another important feature of caseins is that they are amphiphilic due to the presence of both hydrophobic (non-polar) and hydrophilic regions (polar). Hydrophobicity differs according to the casein type with β-CN being the most hydrophobic casein containing a hydrophobic region which makes up approximately two thirds of the protein in the C- terminal. α_s-CN contains three hydrophobic domains along the polypeptide which counts as the greatest hydrophilic casein (Augustin et al., 2011). α_{s1}-CN has one hydrophilic domain located in the middle of two hydrophobic terminal ends (both N and C termini) (Horne, 2002). κ-CN is the only glycosylated casein with complex oligosaccharides, components of galactosamine, galactose and sialic acid (N-acetylneuraminicacid), which are bonded to the Threonine (Thr) residues in the C-terminal region. The hydrophilicity of κ-CN is enhanced as a result of this oligosaccharides attachment (Augustin et al., 2011). Casein fractions when adsorbed on planar hydrophobic interfaces exhibit different properties as indicated in Figure 2.4.

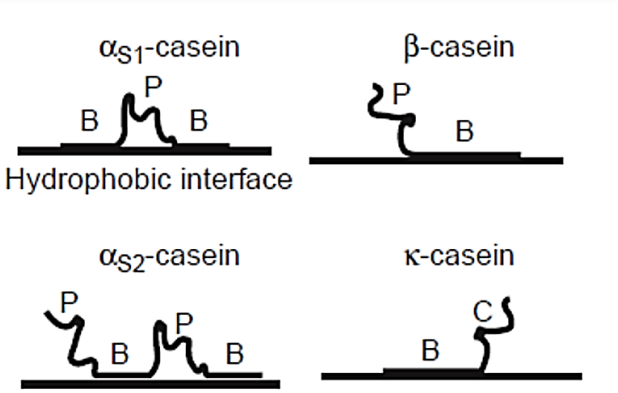

Figure 2. 4. Structure of casein fractions adsorbed on planar hydrophobic interfaces. P, hydrophilic regions; B, hydrophobic region; and C denotes C-terminal block without SerP residues attached (Horne, 2002).

As a result of these polar and non-polar regions, caseins exhibit self-association properties (Horne, 2002). For instance, α_{s1}-CN is able to create polymers facilitated by end-to-end association of its hydrophobic regions. The absence of calcium allows β-CN to form spherical particles, while κ-CN undergoes polymerization via hydrophobic and intermolecular disulphide bonds (Augustin et al., 2011). Polymer size and electrostatic repulsion can also influence casein self-association with the latter being able to limit the extent of self-association. The structures of self-associated fractions of α_{s1}-CN and β-CN are presented in Figure 2.5 below (Horne, 2002).

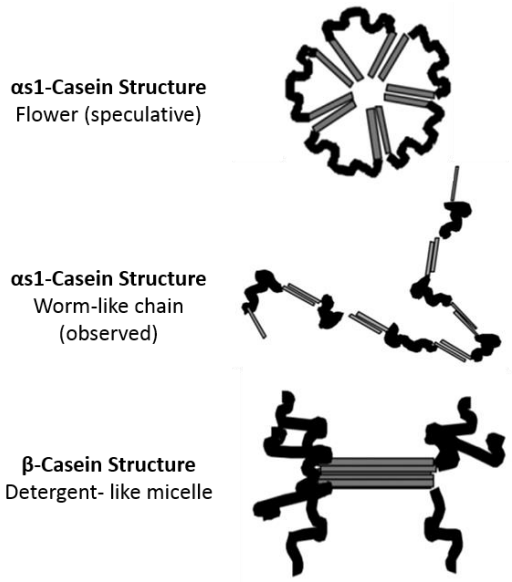

Figure 2. 5. Self-association of individual caseins generated by interaction of hydrophobic regions on neighbouring molecules (Horne, 2002).

The detergent-like micelle of β-CN and the polymer chain of α_{s1}-CN are detected experimentally (Horne, 2002). However, the flower-like ring structure is theoretically suggested (Horne, 2002). Genetic polymorphism can be observed for all the main constituents of casein proteins. In general, genetic polymorphism includes the substitution of either one or two amino acids and but rarely involves the removal of an entire protein segment. Bovine milk contains 15, 12, 9 and 4 genetic variants for κ-CN, β-CN, α_{s1}-CN and α_{s2}-CN, respectively (Othman et al., 2013). Minor components of caseins include the γ-CNs and the N-terminal fragments. γ-CNs are the β-CN's C-terminal fragments that are generated via the action of plasmin. The N-terminal fragments are exposed in the proteose peptone fraction of milk protein. With the exception of κ-CN, all caseins contain low levels of cysteine. All the constituents contain high amounts of proline and a different amount of phosphorus. The

greatest amount of proline is contained in β-CN. Since cysteine is practically absent in β-CN and α_{s1}-CN, the molecules of these basic constituents of casein proteins exhibit increased flexibility (Fox, et al., 2017).

2.3.1.1 α_{s1}-caseins (α_{s1}-CN)

α_{s1}-CN makes up the predominant casein in bovine milk (Chandan & Kilara, 2011), which is a group of a single-chain proteins containing 199 amino acids. α_{s1}-CN has been stated to demonstrate anti-oxidant and radical scavenging properties (Kitts, 2005). Compared to other casein molecules, α_{s1}-CN has the highest charge (Chandan & Kilara, 2011). This casein fraction exists as a monomer at low ionic strength, however, it is able to undergo self-association (pH dependent) upon an increase in ionic strength, in which self-association decreases with an increase in pH and vice-versa (Rollema, 1992).

2.3.1.2. α_{s2}-caseins (α_{s2}-CN)

The structure of α_{s2}-CN is made up of 207 amino acids and the molecular weight of it is around 25.4 kDa. There are several genetic variations of α_{s2}-CN containing between 10 and 13 SerP units. α_{s2}-CN contains two cysteine residues unlike β-CN and α_{s1}-CN (Chandan & Kilara, 2011). Proteolytic fragments of α_{s2}-CN have been reported to display antibacterial activity. α_{s2}-CN is the most hydrophilic, Ca^{2+} sensitive casein that has 10 to 13 mol phosphates/mol, where the phosphate residues are found in three main phosphate centre clusters. This casein fraction has also been reported to contain 10 proline residues, which are located at the N-terminal, half of the protein away from the phosphate centers. Instead of large aggregates, α_{s2}-CN are only able to form dimers and may have some intrachain disulphide bonding. This inability of α_{s2}-CN to undergo aggregation has been attributed to the presence of alternative negative and positive charged areas in its structure (Jenness et al., 1988).

2.3.1.3. β-caseins (β-CN)

β-CN is the second most plentiful protein and integral in maintaining casein micelle structure. The primary structure of β-CN is made up of 209 amino acids with an approximate molecular weight of 24 kDa and is the most hydrophobic casein fraction. There are six recognized genetic variations containing between 0 and 5 SerP units. These SerP units are located between residue 1 to 43 making the N-terminus the most hydrophilic part of the protein chain (Chandan & Kilara, 2011). The primary structure of β-CN is illustrated in detail in Figure 2.6.

Similar to α_{s1}-CN, β-CN has very few secondary structures caused by the incidence of the large number of proline residues with ~35 proline residues (Chandan & Kilara, 2011). β-CN association depend on temperature and ionic strength, with an increase in association being observed with increased temperature and ionic strength. The relationship between temperature and association has been attributed to the hydrophobic interactions within β-CN. In contrast, the repulsion between the charged N-terminals in the polymer leads to both micellar formation and ionic strength interactions (Rollema, 1992). The fragments of β-CN and β-CN itself has been involved in several biological functions. The casoparan peptide has been stated to activate macrophage phagocytosis and peroxide release. Casohypotensin and casoparan (Figure 2.6) may be involved in bradykinin regulation. β-CNs are also a source of casomorphin peptides which exhibit opioid activity; binding to opioid receptors (Tiruppathi et al., 1990).

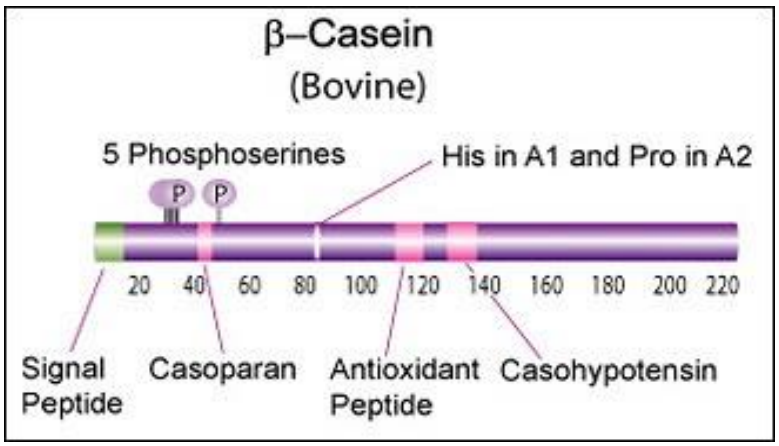

Figure 2. 6. Detailed schematic features of the primary structure of β-CN (Jenness et al., 1988).

2.3.1.3.1. The genetic variants of β-CN

β-CN is polymorphic in nature, with a number of variants being genetically identified. Approximately 13 genetic variants are well recognized, namely, A1, A2, A3, B, C, D, E, F, H1, H2, I, and G. However, the A4 genetic variant is not well recognized yet. In Table 2.2 below, the amino acid sequences of β-CN variants are presented (Farrell et al., 2002). The genetic variants contain similar amino structure, but they differ in several positions. Amongst these variants, A1 and A2 have been identified to be the most common variants in dairy cattle (Farrell et al., 2002; Nguyen et al., 2018).

Table 2. 2. Explanatory table of the amino acid sequences of β-CN variants (Farrell et al., 2002).

Beta-casein variants	Change in amino acid sequence													
	18	25	35	36	37	67	72	88	93	106	117	122	137	138
A2	Ser-P	Arg	Ser-P	Glu	Glu	Pro	Glu	Leu	Gln	His	Gln	Ser	Leu	Pro
A1						His								
A3										Gln				
B						His						Arg		
C			Ser		Lys	His								
D	Lys													
E				Lys										
F						His								Leu
G						His						Leu		
H1		Cys						Ile						
H2							Glu		Leu					Glu
I									Leu					

2.3.1.3.1.1. A1, and A2 β-CN

Bovine A1 β-CN variant is different to not only bovine A2 β-CN variant, but also to other mammalian β-CNs. Those variants are only different at amino acid on position 67, with histidine for A1 and proline for A2 milk, which could result in altered secondary structures (Caroli et al., 2016; Nguyen et al., 2018; Raynes et al., 2015). The possession of the amino acid difference between A1 and A2 variants is highlighted in Figure 2.7.

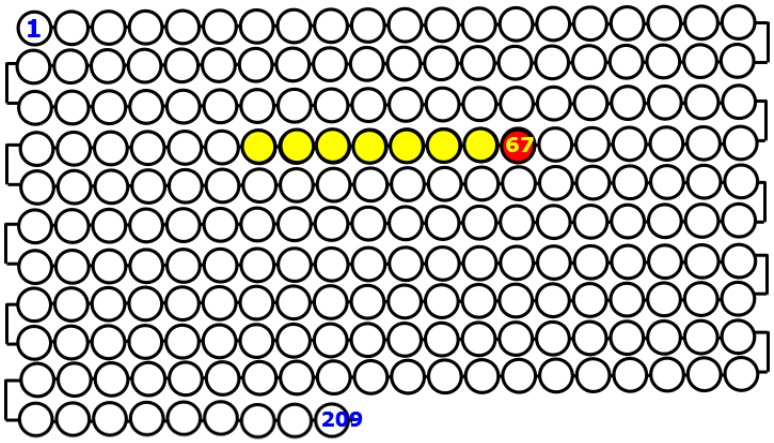

In A1-βCN the amino acid in position **67** is **Histidine**

In A2-βCN the amino acid in position **67** is **Proline**

Figure 2. 7. Schematic representation of the positions of the diverse amino acids in A1 and A2 β-CN chains in bovine milk.

As mentioned before, A2 is the original β-CN in bovine milk, with A1 being a result of mutation (Miluchova et al., 2013; Woodford, 2007). As a result of the incidence of histidine at amino acid position 67, digestion of A1 β-CN milk liberates a seven amino acid bioactive peptide named beta-casomorphin 7 (BCM-7) in small intestine, whereas proline in A2 milk at position 67 inhibits splitting at this particular site and generates peptide BCM-9 (Miluchova et al., 2013). Figure 2.8 shows the formation of BCM-7 during the digestion process of milk.

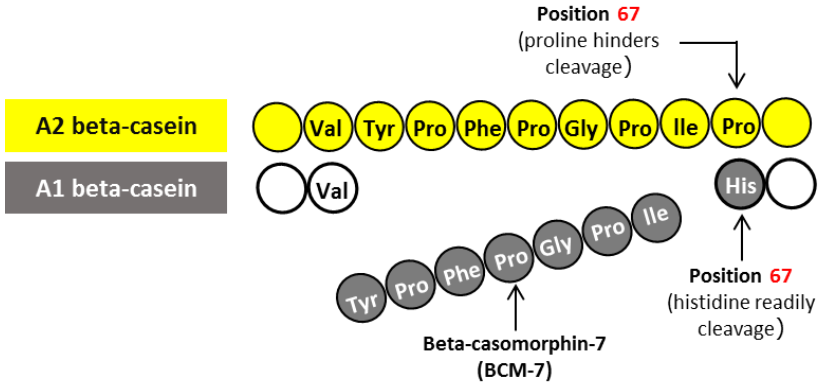

Figure 2. 8. Schematic representation of the differences between the amino acid structure in A2 β-CN and A1 β-CN, and the formation of BCM-7 during the digestion process of milk (Pal et al., 2015).

Because of this variation in the amino acid composition, many researchers believe that upon enzymatic digestion, bovine β-CN A1-5P releases the bioactive opioid peptide BCM-7. Digestion of bovine β-CN A2-5P, on the other hand, releases BCM-7 at a very low rate or does not release it at all (Miluchova et al., 2013; Nguyen et al., 2018). This exogenous opioid can bind μ-opioid receptors present in cells in the human body. A number of scientists believe that BCM7 is connected with milk intolerance and many illnesses, including a range of auto-immune disease, autism, heart disease and Type 1 diabetes (Miluchova et al., 2013). However, these claims are very controversial and additional scientific research is necessary.

2.3.1.4. κ -caseins (κ-CN)

κ-CN contains 169 amino acids with a molecular weight value of 19 kDa and contains both glycosylated and phosphorylated residues. It has the ability to be as a dimer up to a decamer with the smaller units linked via disulphide bridges. κ-CN is also regarded to be calcium insensitive unlike the other caseins and is able to surround the micelles and keep them intact (Chandan & Kilara, 2011). This is due to its role as a functional interface between the aqueous

milk serum and the hydrophobic calcium-sensitive caseins (Creamer et al., 1998). It usually contains one SerP unit, however, up to three phosphoserines have been identified in generic variants of κ-CN (Chandan & Kilara, 2011).

κ-CN is readily cleaved into the insoluble cationic para-κ-CN, which along with water soluble fragments and the hydrophobic caseinomacropeptide are released during clotting of milk (Creamer et al., 1998). It is the only casein in cow's milk with a carbohydrate (complex oligosaccharides made up of galactose, galactosamine and sialic acid) in its primary chain which can be esterified to Thr, making it the only known glycoprotein in the casein complex (Augustin et al., 2011). In addition, κ-CN is regarded as being partially amphiphilic due to the N-terminal being partially hydrophilic and the C-terminal being hydrophobic (Jenness et al., 1988). The attachment of oligosaccharides does enhance its hydrophilic capabilities (Augustin et al., 2011).

2.3.2. Whey proteins

Whey proteins, also known as serum proteins, account for approximately 20% of the total protein in bovine milk (Phadungath, 2005). They are defined as the soluble proteins remaining in milk serum upon precipitation and subsequent removal of casein (Phadungath, 2005; Jenness et al., 1988). They are considered to be a good source of high concentration of amino acids in postprandial plasma as they undergo rapid digestion (Haug et al., 2007). Whey proteins also exhibit foam stabilizing properties via the formation of a rigid film at the air-water interface. In addition, they have been known to enhance fat loss, protein synthesis and hormonal response (Chandan & Kilara, 2011). Whey proteins are mostly globular proteins, highly hydrophobic, with densely folded peptide chains. They are also heat sensitive and will denature and become insoluble when milk is heated (Phadungath, 2005).

The main fractions of whey proteins are β-lactoglobulin (β-lg), α-lactalbumin (α-lac), bovine serum albumin (BSA) and immunoglobulins (Igs). Bovine β-lg, α-lac and BSA are identified by their different primary sequences, and Igs by their micro-heterogeneity (Jenness et al., 1988). The presence of hydrogen bonds and crosslink interactions with calcium and phosphate makes whey proteins hydrophilic. In addition to being heat sensitive, whey proteins are also less sensitive to calcium (Phadungath, 2005), and have well developed secondary, tertiary and quaternary structures, making them different from casein proteins (Chandan & Kilara, 2011).

2.3.2.1. β-lactoglobulin (β-lg)

β-lg represents approximately 50% of total whey proteins and 10% of the total proteins in milk. β-lg has a molecular weight of ~18 kDa and comprises 180 amino acids containing two disulphide bonds and a thiol group (Jenness et al., 1988). However, 18 of these amino acids (monomers) make up the signal peptide residue which is removed post secretion (Creamer et al., 2011). The presence of the thiol group allows for β-lg to link to the surface of casein micelles under heat treatment (Jenness et al., 1988).

β-lg is a globular protein made of 10-15% of α-helical, 43% of β-sheet and 47% of random coil structures (Inagaki et al., 2017). It exists as either a monomer or a dimer under equilibrium conditions in bovine milk, however, its association is dependent on factors such as; temperature, protein concentration, pH and ionic conditions (Chandan & Kilara, 2011). In particular, β-lg is pH sensitive and undergoes conformational changes at various pH ranges. At milk's pH ranging from 5.5 to 7.5, it exists as a dimer via hydrophobic interactions, whereas it disassociates to exist as a monomer at a pH of less than 3.5 and above 7.5. However, it can also exist as an octamer within a pH ranging from 3.5 to 5.5 (Jenness et al., 1988).

There are five overall genetic variants of β-lg, with variant A and B being the dominant ones in bovine milk. β-lg is able to bind to a variety of small hydrophobic ligands, including retinol and fatty acids. This is essential in its biological role of protecting and transporting of retinol (vitamin A) along with being able to stimulate lipase activity via binding of fatty acids. β-lg is also known to exhibit antiviral, anti-carcinogenic, and immunodulatory properties (Chandan & Kilara, 2011).

2.3.2.2. α-lactalbumin (α-lac)

α-lac is an essential protein making up about 25% of total whey proteins (Jenness, 1988). It is a spherical, glycosylated, compactly folded metalloprotein with a molecular weight of approximately of 14 kDa (Chandan & Kilara, 2011). It is initially made up of 142 amino acids but, the first 19 amino acids make up the signal peptide residue, hence cleaves to form the 123 residues protein (Brew, 2013). α-lac is a quaternary protein made up of an α-helix domain and β-sheet domain. The α-helix domain is made up of only amino acids and is bound by two disulphide bridges. β-sheet domain is also bound by two disulphide bonds; however, the domain is also connected by a calcium binding loop, which enhances its structural stability.

However, this stability is pH sensitive as lowering of pH below 4 leads to displacement of calcium, resulting in the unfolding of the protein structure and increasing susceptibility to heat denaturation (Walstra et al., 2006).

2.4. Casein micelles

Milk's role as a source of nutrients to newborn is facilitated by the milk proteins' ability to form large colloidal particles. The native casein micelle has been identified as an association colloid in fresh milk, demonstrating exceptional stability with κ-CN being responsible for its initial formation (Ahmad et al., 2009). Approximately 80% to 90% of the casein component in milk exists as casein micelles (Augustin et al., 2011). The casein micelles are greatly hydrated with around 3.4 g water/g of dry matter (Augustin et al., 2011), with around 15% of the water being bound to the protein (de Kruif & Holt, 2003), and the remainder found within the casein micelle. Dry casein micelles consist of approximately 94% of caseins (α_{s1}-CN, α_{s2}-CN, β-CN and κ-CN) and 6% of organic constituents which are mostly composed of colloidal calcium phosphate (Ahmad et al., 2009). Casein micelles occur as highly porous, solvated, spherical and micellar aggregates of sizes ranging from 50 to 600 nm in diameter (de Kruif & Holt, 2003). A typical casein micelle contains approximately 104 individual casein molecules (Augustin et al., 2011; Fox et al., 1998). The total number of casein micelles in 1 mL of milk ranges between 10^4 to 10^6 tightly packed micelles (Fox et al., 1998; Huppertz et al., 2018).

The stability and structure of casein micelles associations are due to electrostatic interactions, hydrophobic, hydrogen bonding and linkages via calcium phosphate (Ahmad et al., 2009). The degree of association amongst casein micelles is dependent on temperature, pH and pressure (de Kruif & Holt, 2003). Decrease in pH, addition of calcium chelatants (EDTA), cooling, high pressure treatment, and alkalinization are known to disrupt casein micelle (de Kruif & Holt, 2003). Studies indicate that alkalinization can lead to changes such as, reduced turbidity of milk, casein micelle gelation and enhanced transparency (Augustin et al., 2011). An improvement in casein concentrations and decline in concentration of ionic calcium and inorganic phosphate from the aqueous phase, have also been reported. These changes in the micelle are not immediate but are dependent on slow diffusion processes (de Kruif & Holt, 2003). Casein micelle's ability to scatter light contributes to milk's white color, and their subsequent disruption could lead to milk losing its whiteness (Fox et al., 1998).

2.4.1. Structure of casein micelles

Because of the importance of casein and casein micelles in the uses of milk and dairy products, the structure and nature of casein micelles have been studied extensively. Whilst there seems to be a consensus regarding the generic structure of casein micelle, its precise structure is still debatable. This is due to the size and complex structure of casein micelle along with its genetic variation and sensitivity to lactation stages (Phadungath, 2005). A number of models for the structure of casein micelles have been proposed. The three major models, which have been used to approximate casein micelle structure, are the *Sub-micelle* model, the *Nano-cluster* model, and the *Dual Binding* model (Horne, 2011). Of these three, the *Dual Binding* and the *Sub-micelle* models will be discussed in the following sections.

2.4.1.1. Dual-binding model

The *Dual Binding* model was proposed by Horne and is based on the primary structures of caseins existing as block polymers (Horne, 1998). This model suggests that proteins in casein micelles are subject to two types of bonding, hydrophobic attractions and electrostatic repulsions. Hydrophobic attractions are integral in casein micelle formation, whilst electrostatic repulsions can limit the growth of polymer chains (Phadungath, 2005). Interactions between hydrophobic regions of casein micelles allows self-association to occur, which in turn allows for polymerisation to take place.

This polymerization leads to an increase in negatively charged phosphoseryl clusters, resulting in a buildup of electrostatic repulsion hence limiting casein micelle growth. The linkage between SerP rich clusters of α_{s1}-, α_{s2}- and β-CNs to colloidal calcium phosphate nanoclusters (CCP) is known to enhance casein micelle association (Horne, 2002). Calcium in CCP being cationic is able to bond to SerP residues, which in turn reduces electrostatic repulsion (Horne, 1998). This allows hydrophobic interactions to still dominate resulting in further casein molecules association. The dual binding model of the casein micelle is shown in Figure 2.9.

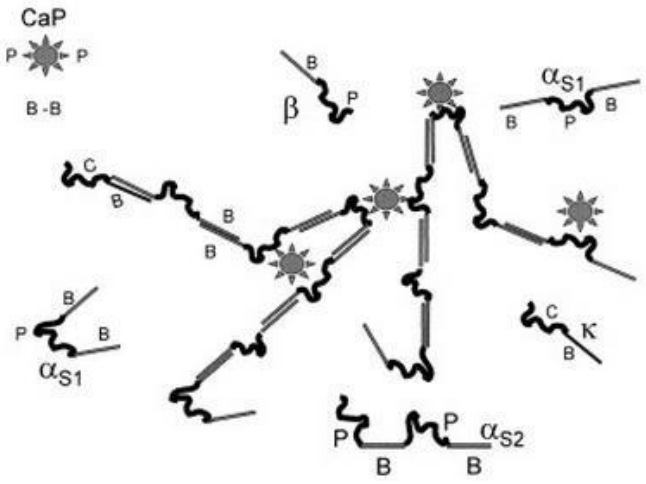

Figure 2. 9. Schematic diagram of dual binding model of casein micelles. Individual caseins α_{s1}-CN, α_{s2}-CN, β-CN and κ-CN are shown as monomers. B represents hydrophobic regions and P represents the hydrophilic regions (Horne, 2003).

Phosphate clusters provide charge stabilization for monomers to bind to each other (Ehssein et al., 2004). Molecules of κ-CN limit further growth of structure (Horne, 2002). However, addition of excess calcium could result in the precipitation of casein micelles, as a result of variations in ionic charge of casein micelles. This is minimized by equilibration with calcium and phosphate ions in solution. Both hydrophobic and electrostatic interactions are also pressure sensitive, with an increase in pressure resulting in the dissociation and unfolding of casein micelles which is irreversible (Chandan & Kilara, 2011).

2.4.1.2. Sub-micelle or subunit model

The first sub-micelle model was proposed by Morr in 1967 who stated that α_{S1}-CN, β-CN and κ-CN monomers formed small uniform sub-micelles. This model was based on the results obtained by studying the influence of urea and oxalate treatment on the casein micelle disruption using sedimentation velocity. It was further suggested that they were stabilized by hydrophobic bonding and calcium caseinate bridges, with aggregation of sub-micelles facilitated by CCP bridges (Rollema, 1992). A second sub-micelle model was proposed by Slattery and Evard in 1973, where experimental results were based on the influence of calcium on the sedimentation and behaviour of particles formed in caseins (Slattery & Evard, 1973). It was proposed that the hydrophobic regions of caseins undergo aggregation in an aqueous environment, forming subunits of 15 to 20 sub-micelles of various composition (Horne, 2011).

Sub-units were either made up of α_{S1}-CN and β CNs, or α_{S1}-CN, β-CN and κ-CNs. It was further suggested that sub-micelles rich in κ-CNs formed the hydrophilic surface of the micelle, which helped stabilize the subunits, with sub-micelles poor in κ-CN being formed in the micellar core where hydrophobic regions dominate (Horne, 2011; Phadungath, 2005). Figure 2.10 below illustrates this model.

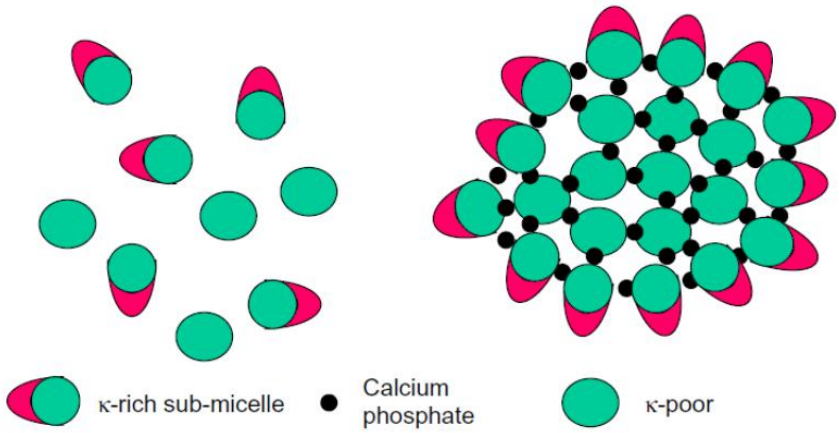

Figure 2. 10. Schematic diagram of the structure of casein micelle based on the sub-micelle model (Horne, 2006).

The most commonly accepted model in the sub-micelle category was proposed by Walstra (2006). This model suggests that casein micelles are made up of sub-micelles with varied composition, with each sub-micelle made up of 20 to 25 casein molecules. These subunits are spherical in shape, sizes ranging from 12 to 15 nm in diameter (Phadungath, 2005; Walstra et al., 2006). The sub-micelles are bound together by hydrophobic interactions between proteins and via calcium phosphate linkages. The casein micelle is made up of two major subunits (sub-micelles), one consists of α_{s1}-CN, α_{s2}-CN and β-CN, hydrophobic regions found in the center of the sub-micelle, and the other α_{S1}-CN, α_{S2}-CN and κ-CN (Jenness et al., 1988), which are more hydrophilic due to the presence of sugar residues in κ-CN (Phadungath, 2005). The κ-CN is found on the external part of the micelle, with the hydrophilic C-terminal extending outside the micelle's surface as a hairy layer, stabilizing the whole structure and alleviating aggregation through steric and electrostatic repulsion (Phadungath, 2005; Walstra et al., 2006). As a result, micelles are usually stable and not prone to flocculation.

2.5. Caseinate

Caseinates are the water-soluble derivatives of acid caseins, which are formed after their reaction with alkali. The preparation of the caseinate is done by the reaction of either freshly precipitated acid casein curd or dry acid casein with dilute alkali solutions, including potassium hydroxide (KOH) (Nagasawa et al., 2015), Sodium hydroxide (NaOH), Calcium hydroxide ($Ca(OH)_2$), Magnesium hydroxide ($Mg(OH)_2$), and Ammonium hydroxide (NH_4OH) (Walstra et al., 2006). The aim of this reaction is to dissolve and convert fractions of casein to appropriate salt form at the pH level close to neutral pH between 6 to 7. The equation representing the neutralization of acid casein with alkali is presented below:

$$\underbrace{{}^{+}H_3N\text{-}R\text{-}COO^{-} + OH^{-}}_{\text{(pH 4.6) Acid casein } \textit{Insoluble} \text{ particles}} \rightarrow \underbrace{H_2N\text{-}R\text{-}COO^{-} + H_2O}_{\text{(pH 6.6) Caseinate } \textit{soluble} \text{ particles (solution or colloid dispersion)}} \quad (2.1)$$

R in the equation represents casein protein (Carr & Golding, 2016).

Manufactured through a spray drying process, caseinates supply all the essential amino acids and have excellent functional characteristics and nutritional properties. These properties make caseinates an outstanding ingredient for a variety of food, nutritional and beverage applications. The physicochemical properties of caseinates determine their functional properties (Chandan, 1997). Since all casein components possess particular primary structure, they all demonstrate an amphiphilic character.

It is preferred to use the fresh acid casein curd over dried casein as a raw material. The flavor of caseinates yielded from the fresh acid casein is blander. Another important point is that, since the preparation of caseinates from dry casein requires prior drying, dry processing, packaging and storage of casein, this will inevitably lead to additional production costs. Nevertheless, in countries that do not produce their own casein, buyers often prefer to buy casein and make their own caseinates (Badem & Uçar, 2017). The schematic process of producing caseinates is shown in Figure 2.11. It should be noted that initial reagents, rennet casein and acid casein are insoluble in water.

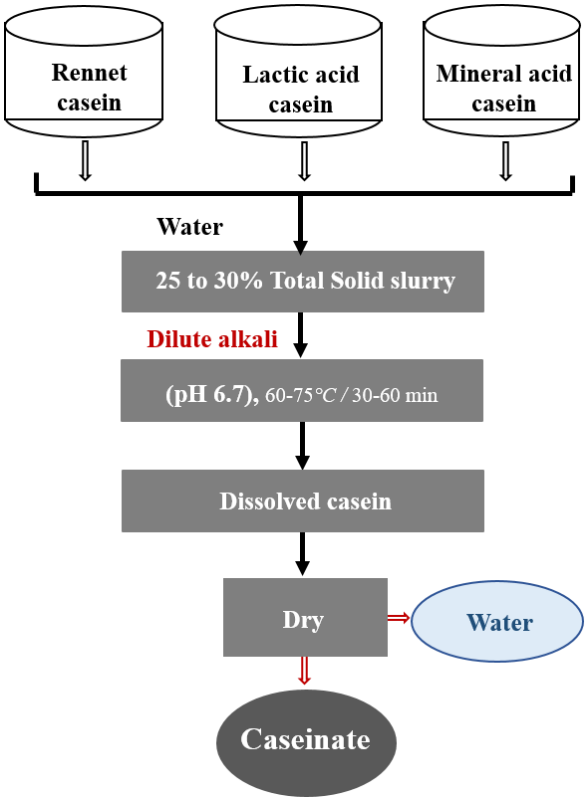

Figure 2. 11. Schematic representation of the manufacture process of caseinates (Badem & Uçar, 2017).

To obtain a caseinate solution with a low lactose content (< 0.2% dry basis) and a low viscosity, it is important to ensure that casein has a low content of calcium (< 0.15% dry basis). It is also vital to control the characteristics of the curd in order to ensure rapid dissolution (Sarode et al., 2016). The most commonly used form of casein in the food industry is SC, which is used as a protein source, as well as for its functional and nutritional properties in a great number of processed food products. SC has the best flavor, color and nutritional value. Calcium caseinate is another common caseinate that finds its application not only as a food ingredient, but also in pharmaceutical preparations. This caseinate functions both as a supplier of calcium and as a supplier of protein. Depending on the end use, the specifications of calcium caseinate may vary significantly. These specifications frequently include a calcium content limitation to 1.0-1.5% (Sarode et al., 2016). The physicochemical characteristics of calcium caseinate differ from that of SC and potassium caseinate, which have good solubility in water and are almost flavorless (Walstra et al., 2006). A combination of a high temperature and a high pH level during caseinate manufacture results in the formation of lysinoalanine (Tsakali et al., 2010).

The ability to melt and the very high heat stability of calcium caseinate make it hard to be replaced in many food applications. The formation of a protein matrix affects the demand for casein for use in a number of food applications, for example, in the production of cheese analogs such as “mozzarella” cheese and processed cheese. Calcium caseinate undergoes similar thermomelting process to that of processed cheese (Sarode et al., 2016). The production of calcium caseinate is carried out similarly to that of SC with the exception of a few differences. When heated at a pH below 6, calcium caseinate solution destabilizes. Another important factor is that calcium caseinate dissolves more slowly that its SC counterpart. However, the complete dissolution of casein in ammonium can be used to accelerate the reaction between $Ca(OH)_2$ and casein (Badem & Uçar, 2017).

2.5.1. Sodium caseinate (SC)

SC is used in a wide range of applications due to its water absorption, long-lasting and strong electrostatic and steric stabilization mechanism in emulsions (Ye, 2008). Due to the ability of SC to absorb significant amounts of water, it can be used in many food applications for the following purposes: modification of the texture of baked and dough products; increasing the consistency of solutions, for example soups; and acting as the matrix former in cheese products (Sarode et al., 2016). SC is a good film-former and, as such, is used in several foaming and whipping applications, as well as in fat/water and oil/water emulsions (Khwaldia, 2004; Sarode et al., 2016). The excellent surfactant property of caseinate makes it an excellent ingredient for use in the production of cake mixes, whipped toppings and ice cream (Khwaldia et al., 2004). However, it should be noted that even though SC produces higher foam overruns, the resulting foams are less stable than that of whey protein concentrates or egg white.

β-CN and α_{s1}-CN provide colloidal stability if the emulsion is prepared with SC at neutral pH. SC is known for its high solubility in water. SC also demonstrates stability in alcohol solutions, which is a very important factor for the preparation of cream liqueur (Permyakov & Berliner, 2000). Table 2.3 shows the percentages of the total compositions of caseinates generated by different methods. It is found that the protein content in SC is higher than the protein in other types of caseinate, with the moisture content in SC being lower than in other caseinates. Moreover, the sodium content of SC at a pH between 6.5 and 7.0 is around 1.2% to 1.4% (Sarode et al., 2016).

Table 2. 3. Typical composition of caseinates manufactured by diverse methods (all the values are presented on a dry basis) (Sarode et al., 2016).

Compounds	Acid	Rennet	Sodium	Calcium
Protein	96.4	90.2	95.0	94.8
Ash	2.0	8.0	3.7	4.0
Lactose	0.1	0.1	0.1	0.1
Fat	1.5	0.9	1.1	1.1
Calcium	-	3.0	0.1	1.3-1.6
pH	4.9	7.5	6.5-6.9	6.8-7.0

The process to produce SC commercially consists of several steps, which are the preparation of a casein suspension, solubilization of casein using NaOH and drying the obtained SC. Nevertheless, the transformation of acid casein to SC is accompanied by certain difficulties. The major difficulty is that the solid content for spray drying is limited to 20% due to very high viscosity of the solution of SC of moderate concentration. Another one is that the dissolution of casein aggregates on the addition of alkali is hindered by the formation of a viscous, jelly-like and relatively impervious coating on the aggregate surface (Sarode et al., 2016). The SC manufacturing process is designed in a way that minimizes the adverse effect of viscosity on the process capacity. Since the viscosity adversely affects throughout of the process, the caseinate manufacturing process must be designed in such a way to minimize this impact.

There are several significant factors that should be considered to minimize the effect of SC viscosity. The temperature throughout processing must be maximized in order to reduce viscosity. The correlation between the temperature of casein solution and viscosity decreases logarithmically with increases in temperature (Carr & Golding, 2016). To achieve a balance between minimizing the plasticization of the unreacted curd and reducing viscosity, the first addition of alkali occurs at a relatively moderate temperature of about 40°C. Following by the slurry containing both unreacted and reacted curd is heated at temperature between 60 to 75°C and then pumped into the reaction vessel. The pH level of SC is another significant factor that must be considered. In order to minimize the impact of viscosity, the pH level of the aqueous phase should be maintained at pH value of 6.7. A substantial increase in the apparent viscosity can be observed at pH higher or lower than 6.7. Generally, temperature and pH values can

cause a limitation on the solid content for spray drying process. To overcome this issue, precise control of temperature and pH during conversion is required (Permyakov & Berliner, 2000). Particle size, total solids concentration and air incorporation are also important factors that should be considered. The reduction in the size of particles of the feed curd is necessary for two reasons. It is important to minimize the diffusion distance from unreacted curd in the center to alkali and to maximise the surface area available for conversion (Permyakov & Berliner, 2000). This can be done by passing the mixture of water and casein through a colloid mill before adding alkali (Sarode et al., 2016). Moreover, the incorporation of air during the dissolving process of SC solutions must be minimized to prevent a significant increase in viscosity caused by air bubbles (Carr & Golding, 2016).

2.6. Factors influencing the physicochemical properties of milk

Milk processing requires milk systems to be subjected to various environmental conditions such as pH changes, heat and pressure, and addition of chelatants, which can influence casein micelle stability (Gaucheron, 2005). These conditions and methods can significantly influence the techno-functionalities and the structure of both casein molecules and casein micelles (Broyard & Gaucheron, 2015). Gaining further understanding of the induced changes to protein is important in the manufacture of dairy products and ingredients. Figure 2.12 presents the diverse physicochemical conditions that influence casein molecules. The following sections will be focused on acidification, alkalinization, heat treatment, and high-pressure treatments, and their effects on bovine casein.

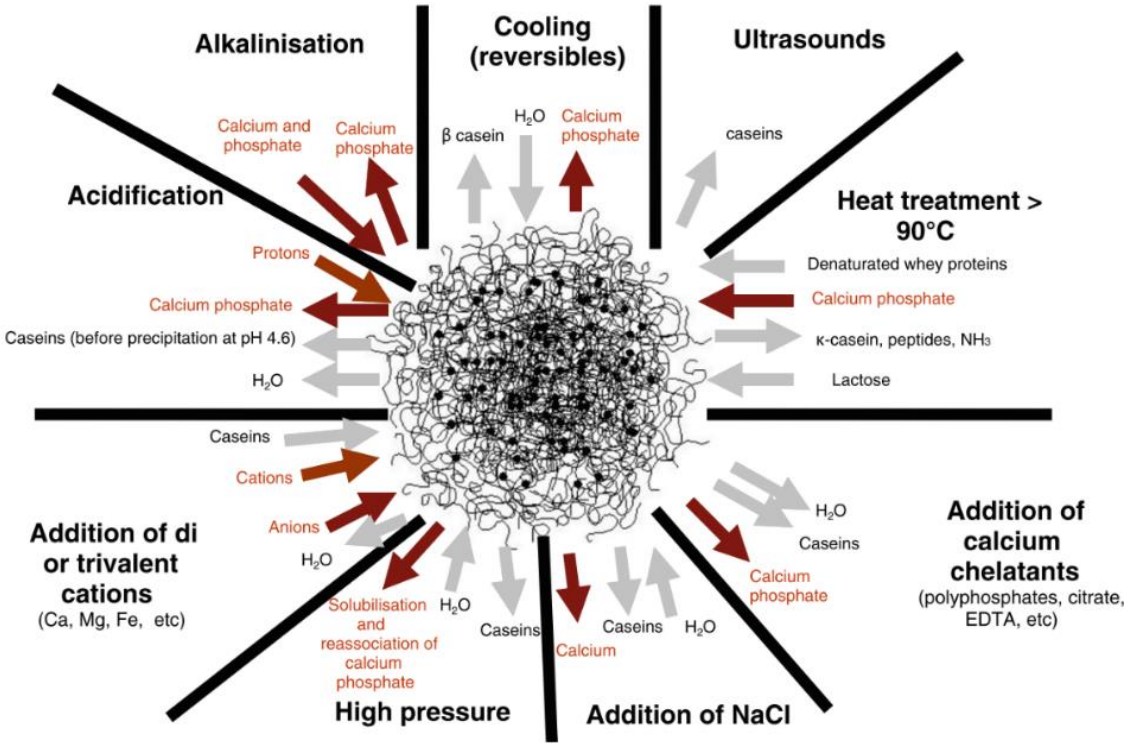

Figure 2. 12. Schematic representation of the exchanges of minerals, water and casein molecules as a function of various physicochemical conditions (Broyard & Gaucheron, 2015).

2.6.1. Acidification

Acidification of milk is a common step in acid milk gelation and is the basis to produce fermented milk products such as cheese and yoghurt. Acidification of milk can be done by using bacterial cultures, whereby lactose is fermented to lactic acid (Lucey et al., 1998) or using an acidifying agent, such as glucono-δ-lactone (GDL), which is hydrolyzed to gluconic acid, resulting in a reduction of pH (Badem & Uçar, 2017; Lucey et al., 1998). At normal milk pH (pH 6.7). Most proteins have a net negative charge value resulting in long range electrostatic repulsion and short-range hydration repulsion between protein molecules, which in turn stabilize casein micelles (Philippe et al., 2003). Milk acidification influences the stability of the casein micelles and the protective κ-CN hairy layer on the surface of the micelles (Dalgleish & Corredig, 2012). When pH decreases towards the isoelectric point of the casein protein (pH ~ 4.6), the disruption of the κ-CN layer on the surface of the micelles occurs, resulting in steric and electrostatic stabilization being compromised prompting casein micelles to undergo aggregation (Dalgleish et al., 2004; Donato et al., 2007; Liu & Guo, 2008). This phenomenon leads to protein clusters becoming denser, forming a more compact structure prior to gelling (Liu & Guo, 2008).

Upon acidification, as the pH decreases, surface charges of casein micelles are titrated and the inorganic CCP nanoclusters affiliated with the phosphoserine amino acids in the interior of the micelles gradually dissolves into the aqueous phase until fully dissolved (Dalgleish & Law, 1989; Lee & Lucey, 2010). It was reported that there were no changes occurred on the size of casein micelles at the pH ranged from 6.7 to 6.0 (Lee & Lucey, 2010). Acidifying the milk to reach pH 6.0 causes the neutralisation of the negative charge on the caseins by the H^+ in the acid, which leads to decrease the electrostatic repulsion among the charged groups as well as solubilisation of a little amount of CCP into the liquid phase. Even though several caseins are separated from the casein micelles into the serum due to H^+ in the acid neutralising the charges, the full dissociation of casein micelle will not occur.

Decreasing the pH from 6 to 5 causes a shrinkage in the protective κ-CN layer on the surface of micelles because of the decrease in the negative charge on the surface. When the pH reaches the isoelectronic point of casein 4.6, the electrostatic repulsion among casein micelles can be screened completely due to the drop of the zeta potential value of to zero (Lee and Lucey, 2010). This will increase the interaction between the casein-casein particles. Consequently, an acid milk gel will be formed consisting of a three-dimensional protein gel network spreading throughout the liquid phase (Bonanomi et al., 2004; Horne, 1998).

Milk gels made with different types of acidifying agents differ in their rheological properties, due to their respective acidification rates. For example, it was found that the rate of acidification of milk gels using different solutions is different, allowing for different final pHs, depending on temperature, concentration of GDL, or the protein type. GDL undergoes rapid hydrolysis to gluconic acid resulting in the isoelectronic pH 4.6 of casein to be reached faster and then remains stable, thus allowing for prolonged ageing at the isoelectric point. This allows for continuous fusion and rearrangement of the casein particles. In contrast, acidification via the use of bacteria culture is a longer process, where there is a slight drop in pH to begin with, followed by a more rapid and steady decrease during fermentation. Acidification rate is better controlled with the use of GDL as the final pH of the GDL induced milk gels is proportional to the initial quantity of GDL added. However, bacterial cultures acidify milk by lowering pH below 4.0 until the bacteria is inhibited by the low pH (Lucey et al., 1998). Because of the low reproducibility of the bacterial fermentation, a lot of studies have been considered utilising GDL as an acidifying agent.

The physical and rheological properties of acid gels made with GDL are different from those obtained by fermentation. This can be explained by the different degrees of cluster and particle rearrangements, different acidification rates during the critical stage of aggregation of the casein particles, and the physicochemical changes occurring in casein micelles. Bacteria used as starter for the acidification can continue to produce acid even at very low pH (lower than pH 4.1). In practice, to prevent the product to become too acidic, bacterially acidified gels are cooled when the necessary acidity is achieved (Lucey, 2016).

GDL, is a natural ingredient that could be found in many different types of foods such as honey, fermented food and fruit juices. GDL has been used frequently as a food additive to prevent the growth of bacteria or to achieve slow acidification when required (Søltoft-Jensen & Hansen, 2005). Scientifically, GDL has been used in many studies to understand the network structure and the properties of acid milk gels. The equilibrium reaction below represents the hydrolysis behaviour of GDL with the aqueous medium (de Kruif, 1998).

$$GDL + H_2O \leftrightarrow GH \leftrightarrow G^- + H^+ \quad (2.1)$$

where *GH* is gluconic acid that is created when the GDL mixes with water. G^- is gluconate ion and H^+ is proton. Dropping the pH of milk to the isoelectric point of caseins pH 4.6, the forward reaction is preferred to create $G^-$and H^+, as a result of the low concentration of *GH*. So, H^+ will be created, when a certain amount of GDL is added to milk, leading the protein to be aggregated and to gelation (de Kruif, 1998; de Kruif, 1999).

2.6.2. Alkalisation

Increasing the pH of milk to above 6.7 causes many alterations in the physicochemical properties of casein micelles, e.g., disruption and destabilisation of casein micelles. Alkalising the milk cause the dissociation of carboxyl groups, precipitation of calcium phosphates, and the ionisation of phosphoserine residues (Horne, 1999). In addition, alkalisation leads to the alteration in ionisation of proteins which increases overall negative charges and electrostatic repulsion amongst neighboring proteins leading to micellar disassociation (Ahmad et al., 2009; Hemar et al., 2000; Lam et al., 2018; Madadlou et al., 2009).

The particle size of the casein micelles changes significantly with changing the pH of the milk (Ahmad et al., 2009; Hemar et al., 2000; Lam et al., 2018; Madadlou et al., 2009). Due to the increasing electrostatic repulsions between the negatively charged casein molecules when the pH of the milk raises to approximately pH 8, an increase in the particle size of the casein micelles is observed (Lam et al., 2018, Madadlou et al., 2009). Altering the pH of milk from 6.35 to 8 also decrease turbidity of casein solution. Turbidity has been found to be an extremely sensitive and non-invasive way of monitor changes to casein micelles (Huppertz et al., 2006). This has been attributed to the disruption of casein micelles. As pH increases, there is an increase in anionic charge of casein micelles. These high negative charges strengthen electrostatic repulsive forces amongst protein molecules resulting in a looser bulkier casein micelle (Liu & Guo, 2008).

It was reported that the extent of decreasing turbidity of skim bovine milk at alkaline pH from 8 to 11 increased with an increase in pH (Vaia et al., 2006). Huppertz et al. (2006) similarly reported that with an increase in milk pH to 10, turbidity decreased to a value close to that of milk serum, suggesting complete disintegration of casein micelles (Huppertz et al., 2006). In addition, it was reported that the particle size of the casein micelles decreased significantly, at pH >8, due to the disruption of micelles to a smaller size (Ahmad et al., 2009; Lam et al., 2018). In addition to particle size, the viscosity of the milk is also affected significantly with the change in pH. Increasing the pH of milk also increases its viscosity (Ahmad et al, 2009; Lam et al., 2018).

2.6.3. Heat treatment

Different methods of heat treatment have different purposes and are applied depending on the manufactured product. The main objective of pasteurisation is to reduce the number of non-pathogenic microorganisms that may cause spoilage and to eliminate pathogens. Fore-warming, also called pre-heating, is the technique that is used before the sterilisation to increase the milk's heat stability. Sterilisation provides long-term shelf-stability of milk, thought prolonged storage might be accompanied by undesirable changes in milk, such as flavour change and gelation (Fox et al., 2015). Table 2.4 shows some heat treatment techniques used on dairy products.

Table 2. 4. Examples of typical heat treatment techniques utilised in the dairy industry (Fox et al., 2015).

Techniques	Conditions
Thermization	e.g., 65^{o}C x 15 s
Low Temperature, Long Time (LTLT)	63^{o}C x 30 min
High Temperature, Short Time (HTST)	72^{o}C x 15s
Fore-warming for sterilisation	e.g., 90^{o}C x 2-10 min, 120^{o}C x 2 min
Ultra- High Temperature (UHT)	130- 140^{o}C x 3-5 s
In-container	110- 115^{o}C x 10-20 min

Unlike whey proteins, the caseins are not susceptible to thermal denaturation. For example, SC maybe safely heated at the temperature of 140°C for more than one hour without any visible changes to its physicochemical properties. Pasteurisation has either little effect on the casein micelles or no effect at all. However, substantial changes might be observed under severe heat treatments, including aggregation, dephosphorylation and cleavage of peptide bonds, which occurs because of the formation of 12% Trichloroacetic Acid (TCA) soluble peptides. It is possible that aggregation is the result of the formation of inter-molecular isopeptide bonds or inter-molecular disulphide bonds (Treweek et al., 2011).

High-temperature heat treatment causes denaturation of the whey proteins, which leads to sulphydryl–disulphide interactions between whey proteins with the casein micelles; between β-lg and κ-CN. Recent studies have shown that even though neither α_{s1}-CN nor α_{s2}-CN can exchange disulphide bridges, both these caseins inhibit large scale heat-induced aggregation of globular proteins, including whey proteins (Voswinkel & Kulozik, 2011). Such sulphydryl–disulphide interactions of caseins with whey proteins can significantly affect the properties of micelles, including rennet coagulation properties and heat stability. High-temperature heat treatment may cause Maillard browning, dissociation of κ-CN from the micelles, a decrease in pH level, which together will eventually lead to coagulation (Fox & Brodkorb, 2008).

The excellent heat stability of caseins makes it possible to produce heat sterilised dairy products without any significant changes in their physical properties. For non-concentrated milk, the

heat stability in almost all cases is good enough to withstand all the usual methods of heat treatment. Although it should be noted that rare defect might be encountered, which is known as the “Utrecht phenomenon”. This defect causes milk to coagulate on High-Temperature Short Time (HTST) pasteurization. The reason for the "Utrecht phenomenon" is the poor heat stability of the milk, related to very high concentration of Ca^{2+} and low concentration of citrate (Fox et al., 2015).

The study on the effect of temperature on solubility of bovine casein properties carried out by Post et al. (2012) indicated that the solvency of different types of casein is dependent on the temperature. It was stated that the solubility of the β-CN tends to increase, when the temperature of the solvent decreases. However, they suggested that the level of solubility of the β-CN is highly influenced by the pH of the solvent (Post et al., 2012). Vincent et al. (2016) reported that temperature above 75^{o}C tends to maintain all types of casein in a denatured state. Fundamentally, it was pointed out that temperature played a key role in determining the mass transfer kinetics and the conformation of the β-CN and all casein in general (Vincent et al., 2016). Further research studied on the effects of temperature on β-CN indicated that the protein started dissociating when subjected to temperatures below 4^{o}C. It has been observed that at 0^{o}C, the aggregation of the β-CN protein stopped completely. Moreover, the subjection of the protein to temperatures below 0^{o}C leaded to its precipitation. It was stated that temperature played a key role in determining the level of demicellization and micellisation of the β-CN proteins. Researchers pointed out that temperature was one of the defining factors on the level of concentration of proteins in the micelles of the β-CN proteins present in bovine milk (Faizullin et al., 2017).

Raikos, (2010) suggested that heat treatment of milk was essential for the improvement of the organoleptic properties of dairy products through the manipulation of the functionalities of the proteins available in milk. However, the author showed that heat treatment of β-CN proteins essentially inhibited heat-induced aggregation of all other proteins available in the bovine milk. Furthermore, he suggested that the effect of heat treatment of the casein proteins inadvertently lead to either α_{s1}-CN or β-CN proteins competing with κ-CN for the interaction with the whey proteins that are denatured by temperature.

As mentioned, heat treatment is a key factor that influences the casein prosperities; it can also disturb the digestion process of casein and specifically the β-CN in the human body (Ye et al., 2017). They postulated that the heat treatment of bovine β-CN and casein proteins, in general, tends to decrease their digestibility in the stomach. The researchers argue that the denaturation of the β-CN proteins results in the formation of some crosslinks such as lanthionine and lysinoalanine that inhibit the digestion of caseins proteins. In short, the authors attributed the limitation experienced in the digestion of heat-treated β-CN proteins to their heat-induced denaturation which inhibits the hydrolysis of the proteins in the stomach (Ye et al., 2017).

From a health viewpoint, it was reported that heat treatment essentially reduced the clinical allergenicity of bovine milk. A significant improvement on the enzymatic digestion was observed as a result of the heat treatment of β-lg. It was suggested that coupling the heat treatment with the enzymatic digestion decline the production of β-lg and α-CN to histamine release. In essence, the researchers pointed out that heat treatment of bovine milk played a key role in elevating the enzymatic digestion of the proteins by taking advantages of both optimal temperature and time. The heat treatment of the casein micelles and the heightened heat-induced susceptibility to enzymatic digestions effectively disrupts the B cells epitomes, thus reducing the allergenicity of bovine milk (Morisawa et al., 2009).

2.6.4. High pressure (HP) treatment

HP technique has some unique advantages in processing milk and dairy products. Pressure is able to kill microorganisms without changing the nutritional value of the dairy products significantly. In many cases, HP treatment has important unusual influence on the individual ingredients of milk. Generally, this treatment has an ability to change the appearance, raise the pH, decrease the turbidity of milk, minimize the rennet aggregation time and improve cheese yield (Huppertz et al., 2018).

Focusing on milk proteins, HP causes whey proteins to denature as well as disrupting the structure of casein micelles even though casein molecules are resistant to pressure more than the whey proteins (Huppertz et al., 2002). HP treatment is known to alter casein micelle sizes with a reported increase in micelle size by 30% at low pressures. Increase in micelle size could be attributed to the interactions between casein micelles and denatured whey proteins or the aggregation of casein micelles themselves (Huppertz et al., 2004). However, HP treatment at~

230 MPa produced a particle size reduction that leads to some changes in the physicochemical properties of milk such as the colour and the viscosity. The increase in the viscosity of treated milk is a consequence of improving the whey proteins water-binding capacity. Increasing the water-binding capacity of whey protein can be beneficial in manufacturing yoghurts. It is reported that the quality of the acid milk gel (yoghurt) prepared using HP treated milk is improved in terms of the gel texture, viscosity, and its syneresis resistance (Johnston et al., 1994).

In one of the earliest investigations on the effects of HP on whey proteins, the amount of non-casein nitrogen in milk serum was shown to decrease with increasing pressure, suggesting denaturation and insolubilisation of whey proteins (Johnston et al., 1994). Denaturation of individual whey proteins in milk is commonly determined by measuring their level in the pH 4.6 soluble fraction of milk and expressing the level of denaturation relative to control samples. Treatment of untreated milk collected directly from the farm at up to 100 MPa does not denature β-lg (Scollard et al., 2000; Lopez-Fandiño et al., 1996). Application of higher pressures results in considerable denaturation of β-lg, reaching 70% to 80% after treatment at 400 MPa (Garcia-Risco et al., 2000; Huppertz et al., 2002; Lopez-Fandiño et al., 1996; López-Fandiño & Olano, 1999). While denaturation of β-lg and its subsequent interaction with casein micelles in milk treated at >100 MPa has been reported, the exact nature of these interactions is yet to be understood (Huppertz et al., 2004).

The sensitivity of casein micelles to pressure alterations limits their applications hence reducing these sensitivities is vital to expanding their application in dairy foods. It is found that enzymes present in milk are quite stable under HP. Although, exposing milk to HP can change the stability of mineral in the milk (Huppertz et al., 2002). The influence on the minerals can be differed into the impacts on the distribution between the diffusible and colloidal phases, and the impacts on ionisation. It was stated that applying 400 MPa on a high temperature treated or pasteurised milk causes an increase in the level of calcium distribution which points to the effect of HP on increasing the solubilisation of native and heat- precipitated CPP (Sigh et al., 2019). That agrees with the finding of the disruption of casein micelles under the HP causes by the enhancement of the solubilisation of CPP, electrostatic interactions and the disruption of hydrophobic interactions which contribute to increase in the light transmittance of treated milk (Huppertz et al., 2004). It was noticed that the concentrations of magnesium, calcium and phosphorus were improved when the pressure increased up to 300 MPa (Sigh et al., 2019).

However, dissociation of the casein and minerals from the micelles at 300 MPa can cause a fast aggregation of para-casein micelles (Needs et al., 2000). As the rise in the pressure continued to 400 MPa, the concentration of the soluble minerals decreased (Sigh et al., 2019).

2.7. Summary

The information on milk with a focus on proteins, specifically on caseins, was presented in this literature review. The influence of some treatments on the physicochemical of the casein micelle in the milk such as changing the pH, heating and pressure treatments, were discussed. Some information found in this chapter could be repeated in the upcoming chapters. Other information derived from the literature search, not given in this chapter, will be reported in the introductions to the working chapters.

Chapter 3.

Materials and Methods

3.1. Materials

3.1.1. Raw Materials

Raw regular A1A2 and A2 cow's milks were collected from Fresha Valley Processors Farm in (Waipu, Northland, New Zealand). Two different batches of milk were collected from each type of milk. Table 3.1 shows the dates the milks were collected for each type of fresh milk. Milks were skimmed and freeze-dried in the laboratory for further works. These milks were used for preparing the SCs investigated in ***Chapter 4***.

Table 3. 1. Information of fresh milk collection.

Samples	Day/ date	Season
First batch of fresh A2 milk (A2_B1)	**Monday the 7th of November, 2016**	**Spring**
Second batch of fresh A2 milk (A2_B2)	**Monday the 14th of November, 2016**	**Spring**
First batch of fresh A1A2 milk (A1A2_B1)	**Monday the 14th of November, 2016**	**Spring**
Second batch of fresh A1A2 milk (A1A2_B1)	**Monday the 12th of December, 2016**	**Summer**

In addition, three different types of spray dried low-heat skim milk powders were used over in the experiments reported in ***chapter 5*** and ***chapter 6***. Two of them were regular A1A2 and one was A2 milk powder. The two A1A2 low-heat skim milk powder were from Westland Milk Products (Hokitika, New Zealand), and Fonterra Ltd (Auckland, New Zealand). A2 low-heat skim milk powder was obtained from Synlait Milk Ltd. (Rakaia, New Zealand). The table below presents the composition (w/w %) obtained from the material data sheet of the spray dried milks used in this research.

Table 3. 2. Composition of A1A2 (Westland and Fonterra milks) and A2 milk powder.

Content	Westland Milk	Fonterra Milk	A2 Milk
Protein	33.5%	32.9%	40.6%
Minerals	7.8%	7.9%	7.8%
Lactose	53.8%	54.5%	44.2%
Fat	1.3%	0.9%	0.7%
Moisture	3.7%	3.8%	6.7%

3.1.2. Minor chemicals

Most chemicals used in this study were of analytical grade and they were purchased from Sigma Aldrich, Auckland, New Zealand, and Sigma Aldrich, St. Louis, Missouri, United States. The chemicals will be illustrating in the material section of each working chapter.

3.2. Methods

3.2.1. Solutions and samples preparation methods

3.2.1.1. Preparation of Imidazole-HCl (pH 7.0) Buffer

Pre-prepared 250 mL of 0.2 M imidazole and 115 mL of 0.2 M of hydrochloric acid preparation (HCL) solutions were needed to prepare 1 L of imidazole-HCl buffer. 250 mL of 0.2 M Imidazole solution was prepared by dissolving 3.405 ± 0.001 g (w/w) of imidazole powder into Milli-Q water containing 0.02% sodium azide. 115 mL of 0.2 M HCl (Mw = 36.46 g/mol) was added to the imidazole solution and stirred for a short time using a magnetic stirrer. After that, the pH of the mixture was checked and adjusted to pH 7.0 ± 0.01 if it required. MilliQ water containing 0.02% (w/w) sodium azide was added to the buffer to reach a final volume of 1 L.

3.2.1.2. Skimming the untreated milk

Once collected, 0.02% (w/w) sodium azide was added to the fresh regular A1A2 and A2 milks. The method of skimming the fresh milk was adapted from Jensen and Pitas (1976). Milks were skimmed by centrifugation at 5,000 x *g* for 20 min at 5 ^{o}C in a Sorvall Lynx 4000 Centrifuge (Thermo Fisher Scientific, North Carolina, USA) using a Fiberlite fixed angle rotor (F12-6x500 LEX, Thermo Fisher Scientific, North Carolina, USA). After centrifugation, the milk fat present at the top layer of the sample was carefully discarded.

3.2.1.3. Preparation of sodium caseinate (SC)

The preparation method of SC was modified from Lucey et al. (2000). SC was obtained from the skimmed regular A1A2 and A2 milks obtained from Fresha Valley. Processors Farm. Skimmed milks were acidified using 2 M HCl to achieve pH 4.60 ± 0.01 at room temperature. Acidified milks were left for 2 h to ensure that the acidification and isolation of casein proteins is complete. The sample was poured into a cheesecloth to discard the serum, and the retained curd was washed many times with Milli-Q water until the running water was clean. The washed curd was dewatered by leaving it hanging into the cheesecloth for 10 min until all the water was removed. Curd was placed in a large beaker and mixed in a proportion of 1:3 (v/v) with

Milli-Q water containing 0.02% sodium azide. 2 M NaOH was used to increase the pH of the mixture to reach a pH range between 6.80 ± 0.01 and 7.00 ± 0.01 to resolubilise the curd. The sample was stirred at room temperature for 48 h using a magnetic stirrer to ensure full hydration and solubilisation of the protein. SC solutions were divided into small portions and transferred to 50 mL centrifuge tubes, frozen at -80 °C in an ultra-low temperature upright freezer and lyophilised using a FreeZone Plus 12 freeze dryer (Labconco Corporation, Missouri, USA) at -83 °C for 72 h under a constant pressure of 0.008 mBar. The steps involved in the SC preparation are shows in Figure 3.1 below.

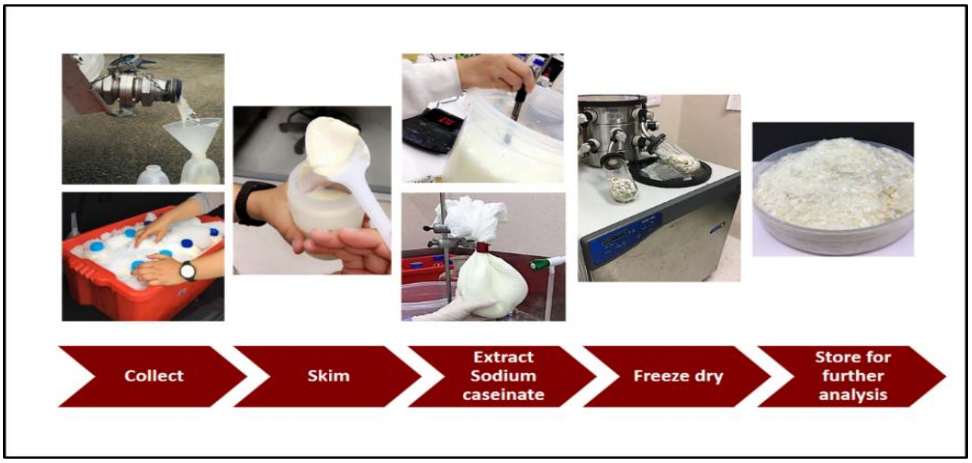

Figure 3. 1. Schematic representation of the steps involved in the preparation of SC.

Freeze dried SC were sent to the Nutrition Laboratory of Massey University (School of food and Advanced Technology, Massey University, Palmerston North, New Zealand) for chemical composition (Table 3.3).

Table 3. 3. Composition of the SCs obtained from two different batches (B1 and B2) of A1A2 and A2 milks.

Samples	Protein (%)	Fat (%)	Lactose g/100g	Moisture (%)	Ash (%)
A1A2_B1	84.3	1.2	0.1	11.4	3.6
A1A2_B2	82.8	1.1	0.1	11.4	7.9
A2_B1	78.2	1.5	0.1	12.6	4.0
A2_B2	84.0	1.9	<0.1	11.7	3.8

3.2.1.4 Reconstitution of SC samples

Freeze dried SCs were reconstituted into a 0.2 M imidazole-0.2 M HCl Buffer, pH 7, to create stock samples with different concentrations based on the requirements of each experiment in ***chapter 4***. A magnetic stirrer was used to stir the mixture gently at room temperature for 2 h to prepare low concentration (≤ 10% (w/w)) samples, and for 24 h to prepare the samples with concentration > 10% (w/w).

3.2.1.5 Reconstitution of milk samples

Spray dried skim milk powders were reconstituted in Milli-Q water containing 0.02% sodium azide to obtain stock milk solutions with different concentrations based on the requirement of each experiment in ***chapter 5*** and ***chapter 6***. A magnetic stirrer was used to stir the mixture gently for 2 h at room temperature to ensure the full dispersion of the milk powder. Milk solutions were stored 24 h in the fridge at 4 ^{o}C to ensure full hydration. Before use in experiments, the reconstituted milks were left at room temperature at least 2 h for equilibration.

3.2.1.6 Preparation of acid milk gels

Acid milk gels were prepared using pre-heated and un-heated methods. Heating of milk was carried out using a water bath set at 85 ^{o}C for 30 min. Regular A1A2 and A2 skim milk powders were used to prepare milk samples with different total solid concentrations such as 5%, 10%, 15%, and 20% (w/w). Gels were obtained by a slow acidification process by the addition of Glucono-δ-lactone (GDL) (Sigma-Aldrich Co., Auckland, New Zealand) to reach pH 4.30 ± 0.01. This pH is obtained by averaging the pH of several commercial yoghurts sold in New Zealand. The amount of GDL required for each concentration was calculated using standard curves obtained by varying the amount of GDL added to the milk samples and measuring the resulting pH. It was found that 0.83%, 1.7%, 2.24%, and 2.7% (w/w) of GDL were required for 5%, 10%, 15%, and 20% (w/w) of milk samples respectively to reach the target pH 4.3. Note that GDL was mixed with the milk sample using a magnetic stirrer constantly for 5 min.

3.2.1.7 Preparation of milk samples used in the high pressure experiments

The three different types of low-heat skim milks (Westland, Fonterra, and A2 milks in Table 3.2) were reconstituted to prepared 500 g of 15% (w/w) stock milk solutions. Milk powders were used in the experiment of investigating the effect of pressures using the turbidity method

to ensure that batch consistency by avoiding the differences in the contents in fresh milks. Acidification (Table 3.4) has been done by using 0.1 M of HCl while alkalisation (Table 3.5) was performed using 0.1 M NaOH. The final concentration of each sample (24 g) was 10% (w/w). The table 3.4 below shows the formulation used to obtain the different samples.

Table 3. 4. Different amounts of stock milk solution (15%), NaOH, and Milli-Q water (containing 0.02% sodium azide) used to obtain milk samples (10%) with different acidic pHs.

Sample	Milk 15% (g)	HCl 0.1M (g)	Milli-Q water (g)	Total weight (g)	pH
1	16.0	0.0	8.0	24.0	6.7
2	16.0	0.6	7.4	24.0	6.5
3	16.0	1.6	6.4	24.0	6.3
4	16.0	2.5	5.5	24.0	6.0
5	16.0	3.0	5.0	24.0	5.7
6	16.0	3.5	4.5	24.0	5.5

Table 3. 5. Different amounts of stock milk solution (15%), NaOH, and MilliQ water (containing 0.02% sodium azide) used to obtain milk samples (10%) with different alkaline pHs.

Number	Milk 15% (g)	NaOH 0.,1M (g)	MilliQ Water (g)	Total weight (g)	pH
1	16	0.00	8.00	24	6.70
2	16	0.38	7.62	24	6.75
3	16	0.48	7.52	24	6.80
4	16	0.96	7.04	24	7.00
5	16	1.46	6.54	24	7.25
6	16	1.92	6.08	24	7.50
7	16	2.34	5.66	24	7.75
8	16	2.70	5.30	24	8.00
9	16	3.06	4.94	24	8.25
10	16	3.36	4.64	24	8.50
11	16	3.66	4.34	24	8.75
12	16	3.94	4.06	24	9.00
13	16	4.42	3.58	24	9.25
14	16	4.84	3.16	24	9.50
15	16	5.34	2.66	24	9.75
16	16	5.76	2.24	24	10.00
17	16	6.36	1.64	24	10.25
18	16	7.20	0.80	24	10.50

3.2.2. Physical methods

3.2.2.1. Rheological measurements

The viscosities of the extracted SC samples in ***chapter 4*** were measured by using both a capillary viscometer and a rheometer. An Anton-Paar Physica MCR 301 stress-controlled rheometer (Anton-Paar, Austria) (Figure 3.2 (A)) was used. A cup and bob (Couette) (the inner diameter of the cup is 27.5 mm and the diameter of the bob is 26.5 mm; giving a gap between the cup and the bob of 1.0 mm) was chosen as the measuring geometry (Figures 3.2 (B) (D)). The dimensions schematically are illustrated in Figures 3.2 (C). The cup was filled with

approximately 25 mL of the samples before it is mounted to the rheometer. After initializing the instrument, the sample was poured into the cup geometry and a low viscosity silicon oil was used to cover the surface of the sample to avoid evaporation. Three types of measurements (frequency sweep, time sweep, and strain sweep) were employed to determine the dynamic (oscillatory) rheological behaviour of the samples.

3.2.2.1.1. Frequency sweep

Most of the measurements are carried out at a constant temperature of 25 °C. However, in some cases the temperature is varied. The frequency sweep measurement consists in applying a constant strain of 1% (within the linear viscoelastic region, LVR) and by varying the frequency from 0.01 to 100 Hz. The elastic (storage) modulus G' and the loss (viscous) modulus G'' are recorded. The behaviour of G' and G'' as a function the frequency allows characterising the rheological behaviour (i.e. liquid, gel, etc) of the sample. LVR correspond to the range of strains where the values of G' and G'' does not change.

3.2.2.1.2. Time sweep

The time sweep measurement is performed at the end of the *frequency sweep.* The temperature is kept constant (in most of the experiments it was set at 25 °C). In this experiment both the strain (1%) and the frequency (0.1 Hz) were kept constant. G' and G'' are recorded as a function of time. This experiment allows monitoring the changes in the viscoelastic properties of the samples with time.

3.2.2.1.3. Strain sweep

A strain sweep is a large deformation experiment where the strain is varied from 0.1% to 10000% at a constant frequency (0.1 Hz) and constant temperature (25 °C). G' and G'' are recorded as a function of the strain. The strain sweep allows to determine the LVR region, but also allows to determine the strain at which the sample start to yield (or flow), defined as the strain at which $G' = G''$.

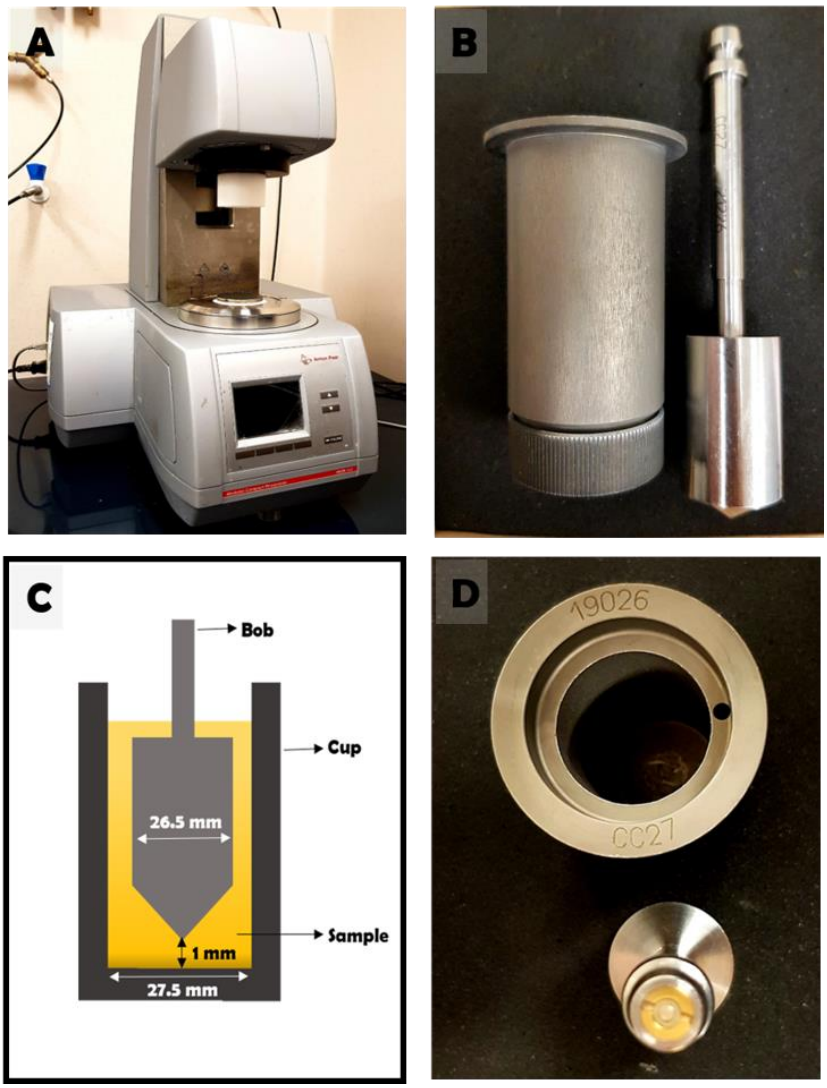

Figure 3. 2. (A) Anton-Paar Physica MCR 301 stress-controlled rheometer used. (B) The side view of the cup (left) and bob (right) geometry. (C) Schematic of the coaxial cylinders measuring system of the geometry. (D) The top view of the cup (up) and bob (down) geometry.

3.2.2.2. Viscosity measurements

While the frequency, time, and strain sweeps are dynamic oscillatory measurements, the rheometer was also used to measure the viscosity of the samples. In this case the shear rate is varied, typically from 0.1 to 1000 s^{-1}, and the viscosity is recorded. Note that when the viscosity of the sample is very high, such as in the case of acid milk gels or in the case of high concentration SC, a Cone-Plate (CP50-2) geometry is used (Figure 3.3). The diameter of the truncated cone 50 mm and its angle is 2°.

In the case of acid milk gels (yoghurts), the viscosity was measured by first applying an increasing shear rate from 0.1 to 1000 s^{-1} then a decreasing shear rate from 1000 to 0.1 s^{-1}. This allow to investigate the time-dependent behaviour of these samples. For a time-independent sample the viscosities measured at the increasing strain and decreasing counterpart should be the same. Note at that before each dynamic and viscosity measurement a waiting time of at least 3 min is applied to ensure that temperature of the sample reaches equilibrium.

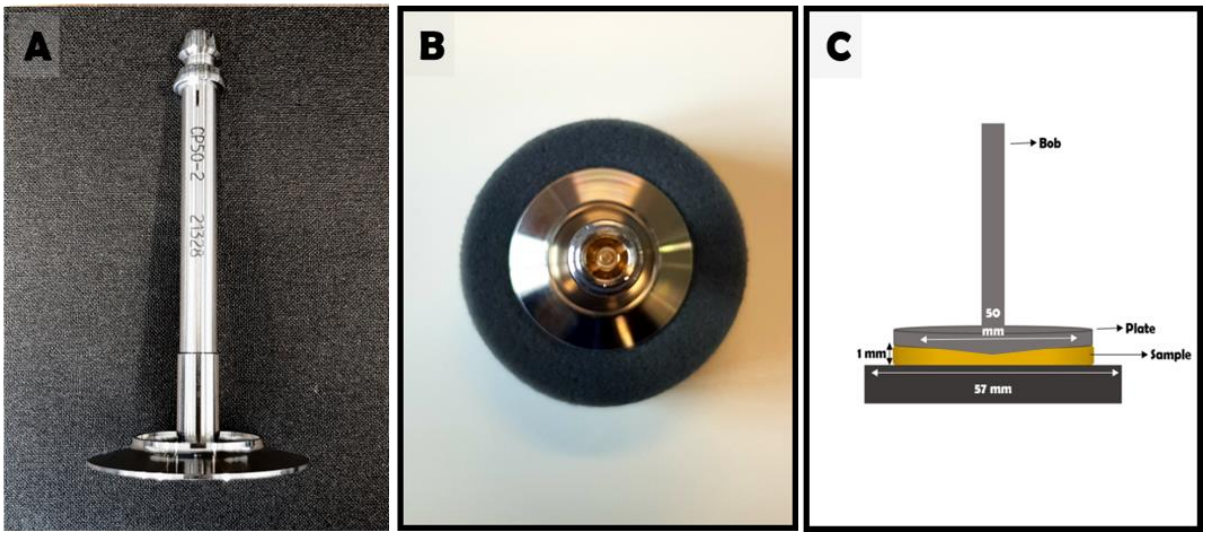

Figure 3. 3. (A) The side view of the Cone-Plate CP50-2 geometry. (B) The top view of the Cone-Plate CP50-2 geometry. (C) The coaxial cylinders measuring system of the geometry.

3.2.2.3. Capillary viscometry

The capillary viscosity meter used in this thesis is depicted in Figure 3.4. It consists of an SI Analytics Ubbelohde Glass capillary viscometer (diameter of 0.78 ± 0.01 mm and a viscometer constant K = 0.2898 mm^2/s^2) (Schott, SI Analytics, Mainz, Germany) connected with the viscosity measuring unit, Visco-clock (Schott, SI Analytics, Mainz, Germany). The two parts were both placed vertically in a water bath (FRB5D, Bibby Scientific Ltd., UK) with a constant temperature maintained by a temperature controller (Modelled SD07R-20-A12E, PolyScience, Niles, USA) at 25 ^oC.

Using this technique required the sample to move from upper to lower measurement mark of the measurement bulb of the viscometer to calculate the flow time of the sample. Milli-Q water was used as a reference in this experiment and its flow time was measured. Using the calculated

flow time of each sample (t sample) and the flow time of the Milli-Q water (t water), the densities of samples (ρsample) and water (ρwater), and the viscosity of water (ηwater = 0.891 mPa·s at 25 °C), the viscosity of the sample (ηsample) can be calculated using (Rao, 2007):

$$\eta\text{sample} = \eta\text{water}\ \frac{\rho\text{water}}{\rho\text{sample}} \times \frac{t\text{sample}}{t\text{water}} \qquad (3.1)$$

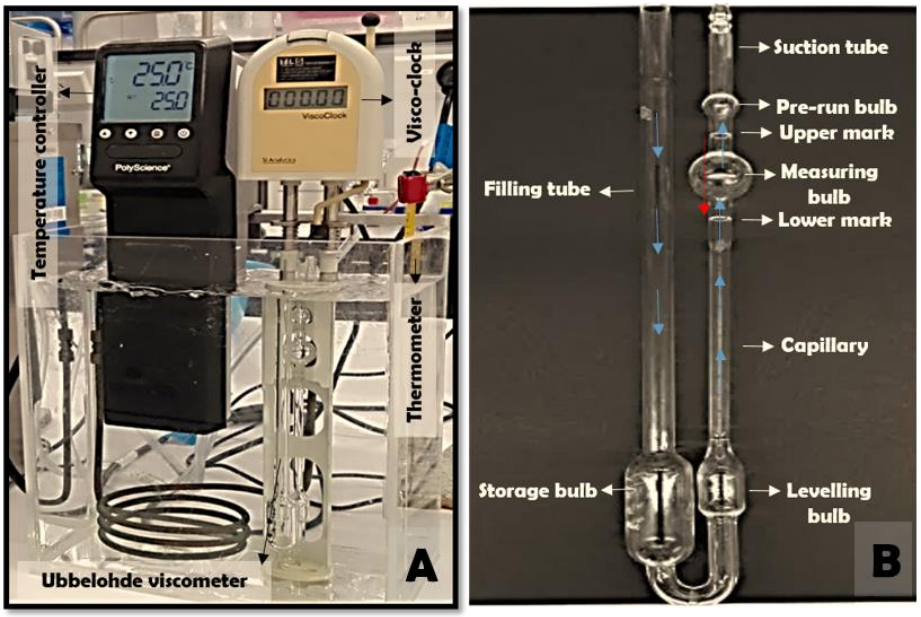

Figure 3. 4. (A) Capillary viscometry experimental setup (A) Ubbelohde viscometer (filling tube and suction tube).

3.2.2.4. Particle sizing measurements

Two different instruments were used to measure the particle size of different samples. In ***chapter 4,*** a Malvern ZSP Nano Zetasizer (Malvern Instruments, Worcestershire, UK) was used to measure SCs solutions and latex particles coated with SCs. This instrument is based on the dynamic light scattering method. In ***chapter 6***, the particle size of the acid milk gels was measured using Malvern Mastersizer 2000 (Malvern Instruments, Malvern, UK), a static light scattering based instrument.

3.2.2.4.1. Dynamic light scattering (DLS)

DLS is performed on a Malvern ZSP Nano Zetasizer (Malvern Instruments, Worcestershire, UK) fitted with a 5 mW 633 nm helium-neon laser. The duration of the measurement was set

by the instrument (typically in the order of a few second per measurement). During the measurement, the measurement position number was maintained at 4.65 mm, meaning that the volume of the sample probed is at the center of the sample cuvette (10 mm pathlength). The count rate of the measurements was between 150 to 500 kcps which is correspond to a laser intensity high enough to give accurate measurements, but low enough to avoid multiple scattering effects. The measurements are performed by diluting 10 µL of the sample into the sample cuvette containing 1.5 mL of Milli-Q water. The measurements were performed at 25 ^{o}C and each sample was measured 10 times.

3.2.2.4.2. Static light scattering (SLS)

The diameter of the particles in acid milk gels were determined by laser light scattering using a Mastersizer 2000 (Malvern Instruments, Malvern, UK), with a He/Ne laser (633 nm) and an electroluminescent diode (466 nm), fitted with a dispersing unit Hydro 2000 SM. The refractive index of 1.33 for water and a refractive index of 1.5 for the particles were used. Malvern software was used to calculate the Sauter volume/surface diameter D[3,2] from the size distribution of the particles. Measurements were performed at room temperature 10 time for each sample.

3.2.2.5. Diffusing Wave Spectroscopy (DWS) and Multi Speckle Diffusing Wave Spectroscopy (MSDWS)

DWS and MSDWS were coupled (Figure 3.5) to measure the dynamic behaviour of the acid milk gels because these samples are very turbid and have very slow dynamics (high viscosity). The DWS instrument is based on the equipment previously described by Hemar et al. (2004). Both DWS and MSDWS measurements were carried out simultaneously in the backscattering geometry. Two different type of acid milk gels were measured by this technique are stirred and unstirred gels. The measurement of stirred gels and commercial yoghurts were performed in Auckland while the unstirred gels were measured in the Institute Physical and Chemistry Materials of Strasbourg (IPCMS) in France (Figure 3.6).

The DWS setup in Auckland uses a 35 mW high power He-Ne laser (HNL150L) (Thorlabs, Newton, NJ, USA) functioning at wavelength λ = 633 nm and delivering 35 mV to measure the sample. The laser beam was extended to approximately 8 mm on the surface of the cuvette using a beam expander (BE03M-A, Thorlabs Inc., New Jersey, and USA). Approximately 4

mL of the stirred acid milk gel sample was contained in a standard disposable cuvette. A single-mode optical fibre (Thorlabs, Newton, NJ, USA) connected with GRIN lense (F230FC-B, Thorlabs, Newton, NJ, USA) was used to collect the light scattered from the sample. A PMT-120-OP/B photomultiplier detector (Bridgewater, NJ, USA) was connected to the other side of the optic fibre to obtain the intensity autocorrelation function.

For the MSDWS system a Basler ace acA1300–200 um CCD camera was used as the detection system. The scattered light is detected by the camera running at 200 frames/s. The images were transferred to a computer running at 2.2 GHz using a National Instrument data acquisition board IMAQ-1409. More detail on the experimental setup as well as the way the autocorrelation functions is calculated from the images is given in ***chapter 5***.

Both DWS and MSDWS were performed simultaneously allowing probing a dynamic of the sample from 10^{-9} s up to hours.

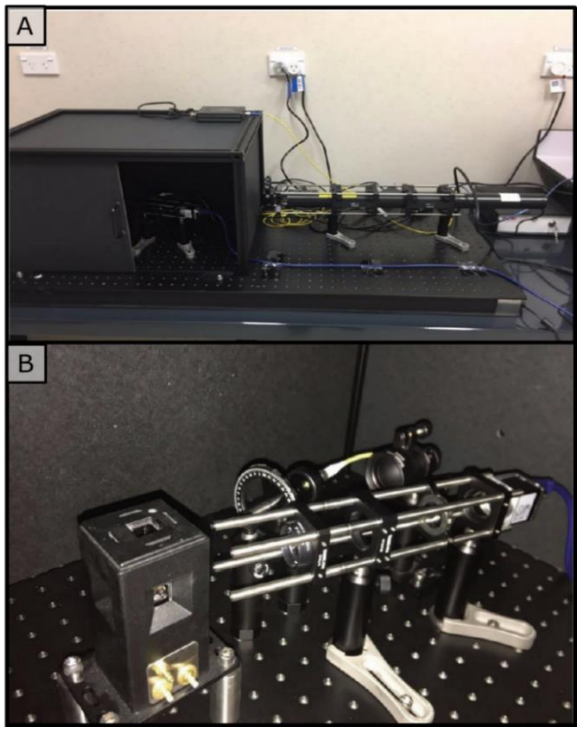

Figure 3. 5. (A) The covered DWS and MSDWS setup used at the University of Auckland, Auckland, New Zealand. (B) DWS and MSDWS detection systems.

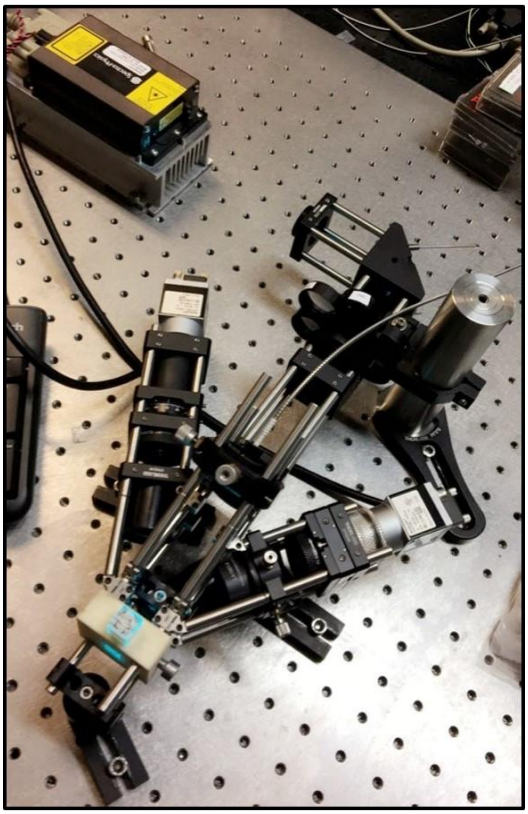

Figure 3. 6. The DWS and MSDWS setup used at Institute Physical and Chemistry Materials De Strasbourg (IPCMS), Strasbourg, France.

3.2.2.6. High pressure treatments

3.2.2.6.1. Pressure treatment using High Pressure Food Processing System (HPP)

Avure 2 L High Pressure Food Processing System (QFP 2 L-700, Avure Technologies, Ohio, USA), was used for treating milks at different pressures (Figure 3.7). The pressure medium of this instrument is distilled water. Two thermocouples were attached to the HHP chamber to record the change in the temperature during the HHP cycle. Milk samples were filled into Beckman Polyallomer centrifuge tubes (Beckman Instruments, Inc., USA) and heat sealed carefully before the high-pressure treatment. Three centrifuge tubes were prepared for each pressure and each tube was filled with around 2 mL of milk sample.

Samples were held at a maximum pressure level of 100, 200, 400, and 600 MPa for 30 min pressurisation duration. It takes less than 2 min to increase the total pressure and less than 2 sec to depress it instantaneously to ambient pressure at the end of the treatment. Treatment was

conducted at room temperature (approximately 25 ^{o}C). Temperature was monitored and recorded during the treatment and it never exceeded more than 27^{o}C.

Figure 3. 7. Schematic representation of the Avure 2L High Pressure Food Processing System.

3.2.2.6.2. Pressure treatment using a diamond anvil cell (DAC)

The utilised diamond anvil cell (DAC) (easylab, UK), with hole diameter of 0.5 mm and gasket thickness of 0.2 mm, was filled with small amount of milk sample. Micron sized ruby balls were added to the milk sample to serve as internal pressure sensor. The pressure generated by tightened the four cap screws gradually can exceed 1 GPa. A Lab RAM HR Evolution Raman system (Horiba scientific, France) was used with an accuracy of ± 10 MPa to measure the pressure from the shift of the ruby fluorescence (Piermarini et al., 1975).

This high pressure system was used to monitor *in-situ* the change in milk using small angle X-ray scattering (SAXS). The DAC was inserted into the beamline as soon as the applied pressure was achieved. Three SAXS patterns were recorded at each pressure and each pattern takes around 4 min. After completing the measurement at highest pressure the reversible effects of HHP on the milk samples were measured by unscrewing the DAC until the pressure released to ambient pressure.

The *in-situ* SAXS experiments were performed at the Shanghai Synchrotron Radiation Facility (Shanghai, China) using the BL19U2 BioSAXS beamline of National Centre for Protein Science Shanghai (NCPSS). The range of the *q* utilised was between 0.003 and 0.17 $Å^{-1}$. Using the equation below the *q* value has been calculated where the λ is the X-ray wavelength =1 $Å^{-1}$ and 2θ is the scattering angle.

$$q = \frac{4\pi \sin\theta}{\lambda} \quad (3.2)$$

The detector used to collect the scattered X-ray of each sample is a Pilatus 1M detector (DECTRIS Ltd.). Using the BioXTAS RAW software version 1.2.3, the collected SAXS scattered intensities were reduced, normalised and averaged (Nielsen et al., 2009). Please note that the same beamline is used to investigate SC solutions. The only difference is that instead of the DAC, a quartz capillary with an internal diameter of 1.5 mm was used.

3.2.2.6.3. High pressure system with an optical spectroscopic cell

A high-pressure system with optical cell for spectroscopy (Model 765.0570, SITEC-Sieber Engineering AG, Maur (Zurich, SWITZERLAND) in Figure 3.8 was used for treating the milk samples with various pressures. The unit is designed for a maximum operating pressure of 700 MPa and a maximum temperature of 200 °C. The pressure medium used of this instrument is Milli-Q water. In Figure 3.8, the red arrows represent the direction of water in the tubes and the yellow arrows represent the two places where pressure is applied. Approximately 3 mL of milk sample is injected through the blind plug to fill the optical cell equipped with a separation piston, which avoid the sample to be contaminated by the pressurising liquid. Once the blind plug was closed tightly, the valve number (V3) has to be close to hold the pressure to avoid pressure release. Then, by rotating the hand lever pump (P1) the pressure can be increased as required. A pressure gauge (manometer) is used to read the pressure applied to the sample.

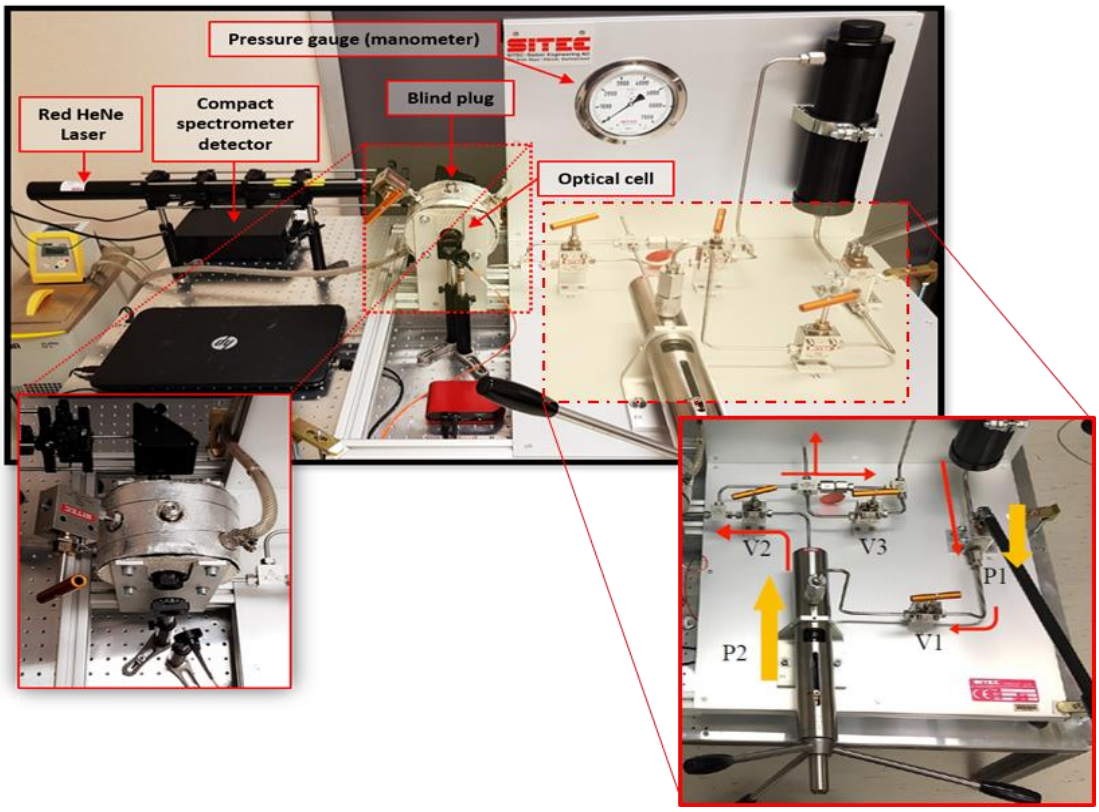

Figure 3. 8. Schematic representation of the light scattered method connected to a laboratory High-pressure system with optical cell for spectroscopy (Model 765.0570, SITEC-Sieber Engineering AG, Maur (Zurich), Switzerland).

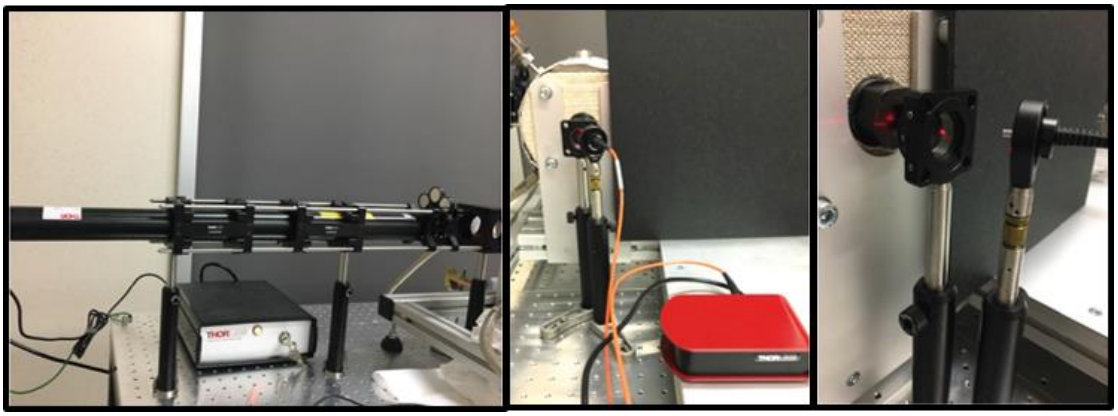

Figure 3. 9. Schematic representation of the Red Helium Neon Laser system and compact spectrometer detector.

Changes in the sample due to the application of the pressure is obtained by measuring the change in the turbidity of the sample. The measuring system consists of a red HeNe Laser system (HNL 210l) as a light source and a compact spectrometer detector (THORLABS, CCS200/ M) as the detector (Figure 3.9). Thorlabs OSA Software was used to record the results of each measurement. The transmitted light is collected by a multimode optical fibre. Details on this system is also given in ***chapter 6***.

3.2.3. Chemical methods

3.2.3.1. Sodium dodecyl sulfate-polyacrylamide gel electrophoresis (SDS-PAGE)

SDS-PAGE is a method that is commonly used to identify the proteins contained in a sample. This identification occurred by separating the proteins based on their molecular weight utilising the electrophoresis in the polyacrylamide gels. Mixing the sample with sodium dodecyl sulphate (SDS) is causes the proteins to be denature by breaking down their noncovalent bonds and developing negative charge complexes. The molecular weight of the protein is also an important factor in the their movement down in the gels (García-Descalzo et al., 2012). SDS-PAGE was used under reducing conditions with on a Mini-PROTEAN tetra cell (Bio-Rad Technologies, Inc., California, USA) to determine the type of proteins. The Mini-PROTEAN tetra cell was connecting to a PowerPac basic power supply (Bio-Rad Technologies, Inc., California, USA). Some reagents are required for running SDS-PAGE including a running buffer, a resolving gel (12%), a stacking gel (4%), a staining and destaining solutions. A Laemmli buffer is a sample buffer and the electrophoresis are a running buffer that used at pH 8.30.

Based on the Laemmli (1970) the compositions of each reagent are listed below:

1. 12% resolving gel

- 33% (v/v) double deionised water
- 12% (v/v) premixed acrylamide: bis-acrylamide solution
- 0.375 M Tris-HCl (pH 8.80)
- 0.01% (w/v) sodium dodecyl sulphate
- 0.01% (w/v) ammonium persulfate
- 0.0004% (v/v) tetramethylethylenediamine

2. 4% stacking gel

- 56% (v/v) dd- water
- 4% (v/v) premixed acrylamide: bis-acrylamide solution
- 0.125 M Tris-HCl (pH 6.80)
- 0.01% (w/v) sodium dodecyl sulphate
- 0.005% (w/v) ammonium persulfate
- 0.001% (v/v) tetramethylethylenediamine

3. Running buffer

- 25 mM Tris
- 192 mM glycine
- 0.1% (w/v) sodium dodecyl sulphate

4. 4% stacking gel

- 56% (v/v) dd- water
- 4% (v/v) premixed acrylamide: bis-acrylamide solution
- 0.125 M Tris-HCl (pH 6.80)
- 0.01% (w/v) sodium dodecyl sulphate
- 0.005% (w/v) ammonium persulfate
- 0.001% (v/v) tetramethylethylenediamine

5. Sample buffer

- 62.5 mM Tris-HCl (pH 6.80)
- 2% (w/v) sodium dodecyl sulphate
- 5% (v/v) 2-mercaptoethanol
- 0.01% (w/v) bromophenol blue
- 25% (v/v) glycerol

6. Staining solution

- 40% (v/v) methanol
- 10% (v/v) glacial acetic acid
- 0.1% (w/v) Coomassie brilliant blue R-250

7. Destaining solution

- 50% (v/v) dd- water
- 40% (v/v) methanol
- 10% (v/v) glacial acetic acid

3.2.3.1.1. Preparation of sodium dodecyl sulphate polyacrylamide gels

The ingredients of 12% resolving gel and 4% stacking gel solutions were mixed to prepare the gel solutions. Firstly, 12% resolving gel solution was mixed and vortexed for 10 s; the solution of 12% resolving gel is then loaded into the cassette up to 2 cm below the top of the cassette. This space is needed for the following placement of stacking gel and comb. A little amount of 2-Propanol (Isopropanol) was added on the surface of the resolving gel to prevent the creation of the air bubbles. Resolving gel was left for at least 35 min to set and polymerise. Following this, the resolving gel surface was dried by getting rid of the isopropanol. In this stage the ingredients of stacking gel solution were mixed by vortexing for 10 s, and the mixture was placed on the top of the polymerised resolving gel. 10 wells comb was positioned on the top of the loaded stacking gel solution then it left for another 35 to 40 min at least to set. The comb was removed directly before loading the samples and running SDS-PAGE.

3.2.3.1.2. Instrumentation and characterisation

Milk sample was diluted in a ratio of 1:1.9:0.1 (v: v: v) with the mixture of laemmli buffer and 2-mercaptoethanol and vortex for short times. 10 µL of the mixture was further mixed with 70 µL of laemmli buffer. This mixture was heated in a water bath for 5 min at 100 ^{o}C. After cooling down to room temperature, the treated sample is then loaded into the wells of the SDS-PAGE gel after it cooled down at room temperature. SDS-PAGE gel run at a stable voltage of 110V for around 4 h. By the end of the experiment SDS-PAGE gel was staining for 24 h using the staining solution followed by the destining the gel using the prepared destaining solution for few hours.

3.2.3.2. Determination of β-CN Gens Fractions Using Liquid Chromatography Coupled with Tandem Mass Spectrometry (LC− MS/MS)

LC-MS/MS, QSTAR-XL Quadrupole Time-of-Flight mass spectrometer (Applied Biosystems, Foster City, CA, USA) was used to identify the type of β-CN gens fractions present in the A1A2 and A2 milks. Investigating the specific gen fraction of β-CN using LCMS/MS required

running first an SDS-PAGE for each type of milk.

3.2.3.2.1. Digestion the β-CN gel band

The method used for digesting the β-CN band in the polyacrylamide gel of each type of milks (A1A2 and A2 milk) was modified from to the method of Albright et al. (2009) and Shevchenko et al. (1996). This method has been carried out by following 5 main steps.

1. **Rinsing and dicing the gel**

   Gel is washed many times to ensure that all the solutions were completely removed. The targeted gel band is cut and placed into an Eppendorf tube. The gel band is diced to small cubes with dimensions of ~0.5-1.0 mm utilizing a scalpel and the wall of the tube. A 200 µL of 50 mM ammonium bicarbonate is added and overtax for 30 s.

2. **Destaining the gel pieces**

   A 200 µL of 50% acetonitrile containing 50 mM of 50% ammonium bicarbonate is added to the gel and vortexed for 30 s. The mixture is placed into a heater/shaker block for 10 min or longer if required. Heat is set to 56 ^{o}C and shaking at 1400 rpm. The gel is checked to determine if the blue Coomassie stain has been removed completely from the gel pieces.

3. **First dehydration and reduction the gel pieces**

   Liquid is removed completely from the gel pieces then a 200 µL of 100% acetonitrile is added and vortexed for 30 sec. Once the gel pieces become white and hard, acetonitrile is removed, and the gel pieces are dried by placing the tube with the lids open into the heater block at 56 ^{o}C with no shaking. Once the pieces are completely dry, a 50 µL of 10 mM DTT in 50 mm ammonium bicarbonate is added to re-swell and submerge the gel pieces. The tube is placed back into the heater block at 56 ^{o}C for 1 h with no shaking.

4. **Alkylation**

   The liquid in the tube is removed and a 50 µL of 50 mM iodoacetamide in 50 mM ammonium bicarbonate is added into the tube. The tube is then stored into a dark

place for 30 min up to a maximum of 1 h at room temperature.

5. **Second dehydration and digestion step**

A 200 µL of acetonitrile is added after removing the previous liquid form the tube and the mixture is vortex for 30 sec. The gel pieces become opaque and "clumpy" to begin with, before finally becoming hard and shrunken as before. The liquid is removed, and the tube is placed in the heater block at 56 ^{o}C without shaking with the lids open, but with the clear rectangular cover balanced on them to keep the dust out. Once the sample is completely dry, 20-50 µL of freshly prepared 12.5 ng/µL trypsin in 50 mM ammonium bicarbonate is added to the dried gel pieces. Few minutes later the gel pieces are checked if they are still submerged or not. If not, a small volume of 50 mM ammonium bicarbonate is added to just cover the gel pieces with a smooth meniscus of liquid. The mixture is then incubated at 37 ^{o}C for 24 h.

3.2.3.2.2. LC− MS/MS instrumentation and characterisation

The chromatographic separation of A1 and A2 was achieved by injecting a 10 µL aliquot prepared as per the previous Section onto a C_{18} PepMap trap cartridge (LC Packings, Amsterdam, Netherlands) for desalting. The peptides content in the sample will be isolated on a 0.3x100 mm, 3.5 µm particle size, Zorbax 300 SB C_{18} Stablebond column (Agilent Technologies, Santa Clara, CA, USA). The mobile phase constituted of (A): 0.1% formic acid in Milli-Q water and (B): 0.1% formic acid in acetonitrile at a flow rate of 6 µL/min. The elution programme used is presented in Table (3.6) below:

Table 3. 6. elution conations for LC-MS/MS.

Time (min)	A	B
0.0-0.1	80 %	20 %
0.1-24	40 %	60 %
24-26	3 %	97 %
26-30.5	80 %	20 %
30.5-35	80 %	20 %

The column eluate is ionised in the electrospray source of a QSTAR-XL Quadrupole Time-of-Flight mass spectrometer (TOF-MS, Applied Biosystems, Foster City, CA, USA). A TOF-MS scan from 400-1200 *m/z* is performed, followed by five Product Ion Scans 100-1200 *m/z* for confirmation of peptide identity. The table below (3.7) shows the five product ions used in the identification.

Table 3. 7. Parameters for peptide identification by LC− MS/MS.

β-CN	Peptide Sequences	Charge	Product ion (m/z)	Collision Energy (V)
A1	AQTQSLVYPFPGPIHN	2+	884.95	48
	IHPFAQTQSLVYPFPGPIHN	3+	755.06	41
A2	IHPFAQTQSLVYPFPGPIPN	2+	1112.08	60
	IHPFAQTQSLVYPFPGPIPN	3+	741.70	41
	AQTQSLVYPFPGPIPN	2+	864.95	47

Retention times for peak integrations were based on positive identifications of the expected peptide forms from the MS/MS data (Product Ion Scans).

Chapter 4.

Are dilute sodium caseinate solutions made from A1A2 and A2 milks different? Comparison between their viscosity, size, structure, and interfacial properties

4.1. Introduction

Sodium caseinate (SC) is a widely used dairy ingredient due to its functional and nutritional properties, particularly for its emulsification capability. It is obtained by the coagulation of milk by acidification (pH 4.6) to obtain a casein curd, discarding the serum phase (mainly whey protein, lactose and mineral), resolubilising the curd by mixing it with water and bringing the pH to neutral using sodium hydroxide, then drying (Mulvihill, 1992; Southward, 1989; Augustin et al., 2011). SC contains the different casein proteins, namely a_{S1}-CN, a_{S2}-CN, β-CN and κ-CN, in a proportion similar to that existing in the starting skimmed milk, with a weight fraction of approximately 0.4:0.1:0.4:0.1, for α_{S1}-, α_{S2}-, β- and κ-CN respectively (Fox & McSweeney, 2003). Of interest here, β-CN which account for 40% of the caseins, is an intrinsically disordered protein which is highly amphiphilic due to a hydrophilic N-terminal, and hydrophobic C-terminal, and central regions (Darewicz & Dziuba, 2007).

Recently, A2 milk, which contains only the A2 β-CN variant, has gained a lot of interest due to health claims. It has been suggested that A2 milk reduces the risk of cardiovascular disease and type 1 diabetes (Bell, Grochoski, Clarke, 2006) due to the absence of the β-casomorphin-7, an opioid peptide normally produced during the digestion of A1 β-CN. The difference between A1 β-CN and A2 β-CN is the substitution of the histidine in the A1 β-CN by the proline in A2 β-CN at the amino acid position 67 of the protein (Farrell et al., 2004). From a physicochemical viewpoint, it has been shown that A2 β-CN had a lower hydrophobicity and formed smaller micelles compared to A1 β-CN (Raynes et al., 2015). It has been also reported that A2 β-CN imparted poor rennet coagulation properties to milk (Jensen et al., 2012). Recently Nguyen et al., (2018) reported that acid milk gels made from A2 milk had a lower elastic modulus, a higher porosity and a thinner protein strands compared to the gels obtained with A1 milk. They also reported that A2 milk has a lower foam formation capability than A1 milk.

In this study, we investigate whether the physicochemical behaviour of SCs obtained from A1A2 and A2 milks such as the viscosity, particle size, the structures, and the adsorption behaviour to polystyrene spheres are different. Here we refer to A1A2 milk, the most commercially available milk, which contains both A1 and the A2 β-CN variants. To compare between these two types of SCs some of their important physicochemical properties are investigated. The SC solution concentration was varied between 0.01 and 10 wt%. Their

viscosity was determined using a capillary viscometer, and their particle size was determined by dynamic light scattering. The structure of the SCs was also probed using small angle x-ray scattering (SAXS). Because SC is extensively used as a surface-active agent, its adsorption behaviour to polystyrene spheres was also investigated. We believe that this study is the first to investigate the differences between SCs made from these two different types of milks.

4.2. Materials and methods

4.2.1. Materials

Imidazole, hydrochloric acid (HCl), sodium hydroxide (NaOH), and sodium azide were of analytical grade and purchased from Sigma Aldrich, Auckland, New Zealand and Sigma Aldrich, St. Louis, Missouri, United States. MilliQ water was used in all sample preparation.

4.2.2. Preparation of sodium caseinates (SCs)

Fresh milks were collected from Fresha Valley Processors Farm in Waipu, Northland, New Zealand. Two different batches of each type of milk were collected on 3 different days. 0.02% (w/w) sodium azide was added to the chilled fresh milks (~4 °C) after the collection to prevent microbial growth. Milks were skimmed in the laboratory at the University of Auckland in Auckland, New Zealand, following the method stated by Zhang et al., (2012). The skimming process was performed by centrifuging the milks at 5,000 x *g* for 20 min at 5^{o}C in a Sorvall Lynx 4000 centrifuge (Thermo Fisher Scientific, North Carolina, USA) using a Fiberlite fixed angle rotor (F12-6x500 LEX, Thermo Fisher Scientific, North Carolina, USA).

SCs used in this work were prepared from the skimmed milks following the method of Lucey et al. (2000) with some modifications. Skimmed milks were acidified using 2 M HCl to pH 4.60 ± 0.01 at room temperature. Acidified milks (5 L) were left for 2 h to ensure that the whey phase is separated from the micellar (protein) phase which formed a curd. After discarding the whey phase, the curd was gently poured into a cheesecloth. The curd inside the cheesecloth was washed several times with Milli-Q water until the water run clear. The curd was suspended in the cheesecloth to dewater for at least 10 min. The curd was transferred into a large beaker and mixed with 3 volumes of Milli-Q water containing 0.02% sodium azide. 2 M NaOH was used to increase the pH of the mixture to a pH range between 6.80 ± 0.01 to 7.00 ± 0.01. The mixture was stirred at room temperature for 48 h using a magnetic stirrer bar to ensure full hydration and solubilisation of the curd. The mixtures were divided into small portions (<25

mL) and transferred to 50 mL centrifuge tubes, frozen at -80 °C in an ultra-low temperature upright freezer and lyophilised using a FreeZone Plus 12 freeze dryer (Labconco Corporation, Missouri, USA) at -83 °C for 72 h under a constant pressure of 0.008 mbar. Dried SCs were stored at -80 °C until for further use. The composition of the SCs extracted from the different type of milks were determined at the Nutrition Laboratory of Massey University (School of food and Advanced Technology, Massey University, Palmerston North, New Zealand) using a rapid Max N EXCEED, Elementar, Donaustraze 7, 63452 Hanau, Germany. Table 4.1 below shows the composition of the different batches of SC. SDS-PAGE showed that the SCs did not contain whey proteins (Appendix 1).

The SC will be named A1A2-B1 and A1A2-B2 when obtained from A1A2 milk batch 1 and batch 2, respectively. The same denomination, A2-B1 and A2-B2 is used for SCs obtained from A2 milk batch 1 and A2 milk batch 2.

Table 4. 1. Chemical composition (wt%) of the A1A2 and A2 SCs.

Samples	Protein (%)	Fat (%)	Lactose (%)	Moisture (%)	Ash (%)
A1A2-B1	84.3	1.2	0.1	11.4	3.6
A1A2-B2	82.8	1.1	0.1	11.4	7.9
A2-B1	78.2	1.5	0.1	12.6	4
A2-B2	84	1.9	<0.1	11.7	3.8

4.2.3. Sample preparation

SCs powders were reconstituted in a 0.2 M Imidazole-0.2 M HCl Buffer containing 0.02% sodium azide, pH 7.0 to create stock sample solutions (10 wt%). The stock solutions were gently stirred using a magnetic stirrer for 2 h then left overnight in the fridge to ensure full hydration. The desired SC solutions were prepared by diluting the stock SC solution with the required amount of buffer.

4.2.4. Viscosity measurements

SI Analytics Ubbelohde Glass capillary viscometer (diameter of 0.78 ± 0.01 mm and a viscometer constant K = 0.2898 mm^2/s^2) (Schott, SI Analytics, Mainz, Germany) connected

with the time measuring unit, Visco-clock (Schott, SI Analytics, Mainz, Germany) was used to measure the viscosity of SCs samples with concentrations of 0, 0.1, 0.2, 0.4, 0.6, 0.8, 1, 2, 4, 6, 8, and 10 wt%. The viscometer containing the sample was kept at a constant temperature of 25 ^{o}C using a water bath (FRB5D, Bibby Scientific Ltd., UK) and a temperature controller (Modelled SD07R-20-A12E, PolyScience, Niles, USA).

Milli-Q water was used as the reference liquid. Using the equation below (Rao, 2007) the viscosities of the SC samples (ηsample) were calculated.

$$\eta\text{sample} = \eta\text{water}\ \frac{\rho\text{water}}{\rho\text{sample}} \times \frac{t\text{sample}}{t\text{water}} \qquad (4.1)$$

where the flow time of the sample is *t*sample, the flow time of the Milli-Q water is *t*water, the density of the samples is ρsample and the density of water is ρwater. The viscosity of water (ηwater) is 0.891 mPa·s at 25 ^{o}C. Viscosity measurements were performed at least 3 times on duplicated samples, resulting in 6 values for each SC sample.

4.2.5. Particle size measurements

4.2.5.1. SC solutions

The particle size measurements were performed using dynamic light scattering (DLS) on a Malvern ZSP Nano Zetasizer (Malvern Instruments, Worcestershire, UK) fitted with a 5 mW 633 nm helium-neon. Refractive indices of 1.5 and 1.33 were chosen for the SC and water, respectively. Samples (with concentrations of 0, 0.1, 0.2, 0.4, 0.6, 0.8, 1, 2, 4, 6, 8, and 10% (w/w)) were held in transparent polymethyl methacrylate (PMMA) cuvettes. Each sample was measured 10 times on duplicated samples at a constant temperature of 25 ^{o}C.

4.2.5.2. Determination of the adsorbed SC layer on the polystyrene spheres surface

To measure the size of the adsorbed layer, the samples were prepared as follow. SC solutions (1.5 mL) at concentrations of 0, 0.0005, 0.001, 0.0015, 0.002, 0.004, 0.006, 0.008, 0.01, 0.02, 0.04, 0.06, 0.08, and 0.1% (w/w) were held in the PMMA cuvettes. To the cuvettes 10 µL of polystyrene particles (nominal diameter from the manufacturer of 100 nm) suspension (Polysciences, Inc., USA) were added. The mixture was left for 24 h at room temperature to allow protein adsorption to occur. Same refractive indices as for particle sizing above were

used. The measurements were performed at 25 ^{o}C, and each sample was measured at least 10 times, with each sample duplicated.

4.2.6. Small-angle X-ray (SAXS) scattering

4.2.6.1. SAXS experiments

The total solid concentrations for the SCs samples used in this measurement are 0.1, 0.2, 0.4, 0.6, 0.8, 1, 2, 4, 6, 8, 10% (w/w). Small amount of samples were filled into a 1.5 mm capillary tube and placed into the instrument. Measurements were performed at the Shanghai Synchrotron Radiation Facility (Shanghai, China) on the BL19U2 BioSAXS beamline of The National Centre for Protein Science Shanghai (NCPSS). The range of the q utilised was between 0.0103-0.199 Å^{-1}, and the scattered X-ray was collected by a Pilatus 1 M detector (DECTRIS Ltd.). Samples were measured at room temperature (~25 ^{o}C). The measured data were normalized, background-subtracted, and averaged using BioXTAS RAW software version 1.2.3.

4.2.6.2. SAXS analysis

Synchrotron small angle X-ray scattering analysis occurred by fitting the SAXS scattering data of SC samples at various concentrations were performed using the Modelling II tool macro embedded in the commercially available Igor pro software (v 8.0, Wavemetrics, USA).

The general SAXS scattering intensity from protein solutions can be expressed as:

$$I(q) = N(\Delta\rho)^2 \int N(r)[V(r)F(q,r)]^2 S(q,r)dr + Bkg \qquad (4.2)$$

Where N is the total protein particles per unit volume in the solution, $\Delta\rho$ is the X-ray scattering contrast between the scattering objects and solvents, $N(r)$ is the particle size distribution, $V(r)$ is the volume of the scatter, $F(q,r)$ is the form factor which depicts the particle shape, and $S(q,r)$ is the structure factor describing the particle-particle interactions and time averaged distribution of protein particles in the solution. Bkg represents the scattering background from the solvent (Zhang, et al., 2012). The scattering data were fitted with two structural levels (Smialowska et al., 2017). The first level (low-q) was modelled with a spherical form (F(q)) (the aspect ratio is set to 1) with a radius r, which is given in the following (Pedersen, 1997):

$$F(q,r) = \frac{3[\sin(qr) - Qr\cos(qr)]}{(qr)^3} \tag{4.3}$$

The protein particle size in the first level is assumed to follow a log-normal distribution, given by:

$$N\,(r) = \frac{1}{\sqrt{2\pi}\sigma r}\exp\left\{-\frac{1}{2}\left[\frac{ln\left(\frac{r}{r_0}\right)}{\sigma}\right]^2\right\} \tag{4.4}$$

where r_0 is the mean particle size and σ is the standard deviation (spread) of the size distribution. σ is fixed to 0.3 throughout the fitting process. In the second level (high-q), the unified fit was employed to account for the scattering from the smaller protein inhomogeneities within the SC. The unified fit equation is expressed as (Beaucage, 1996; Beaucage, 1995):

$$I(q) = \sum_{i=1}^{n} \mathrm{G_i}\exp\left(\frac{-q^2R_{\mathrm{gi}}^2}{3}\right) + \mathrm{B_i}\exp\left(\frac{-q^2R_{\mathrm{g(i+1)}}^2}{3}\right)\left[\frac{(\mathrm{erf}\left(\frac{qR_{\mathrm{gi}}}{\sqrt{6}}\right))^3}{q}\right]^{\mathrm{P}_i} \tag{4.5}$$

where n is the number of structural levels observed, G is the exponential Guinier pre-factor, R_{g} is the radius of gyration. B and P are the pre-factor and the exponent of the power-law function, respectively.

When the concentration of SC is [3]1vwt%, a structure factor $S(q,r)$ is required to fit the scattering profiles. In these cases, a hard spheres structure factor with a monodisperse size distribution is employed (Ingham, et al., 2016; Pedersen, 1994):

$$S(q,R_{HS}) = \frac{1}{1 + 24\eta\frac{G(2qR_{HS})}{2qR_{HS}}} \tag{4.6}$$

There are two important parameters that can be obtained from the structure factor: the hard sphere radius R_{HS} that typically refers to the hard limit of the minimum distance between two particles, and the volume fraction or interaction strength η.

Under diluted conditions (concentration of SC < 1 wt%), the interactions can be neglected and $S(q,r)\equiv 1$.

4.2.7. Statistical analysis

The mean comparison of the resulting parameters obtained from the SAXS fits were conducted through analysis of variance (ANOVA) test using the Origin 2018 software package (OriginLab, USA). The significance was set at $P < 0.05$

4.3. Results and Discussion

4.3.1 Viscosity and particle size measurements

The viscosity of the SC solutions as a function of concentration is shown in Figure 4.1. At concentrations lower than 1 wt%, the viscosity increases slightly. Typically, the viscosity increases from ~0.93cP at 0.1% to ~1.03 cP at 1% SC (see inset Figure 4.1). However, when the SC is further increased (>1 wt%) the viscosity increases markedly to nearly the double the value at 4% SC and to reach ~20 cP at 10 wt%. This behaviour is expected for a dispersion of particles where the viscosity is expected to increase with concentration. Clearly, from the viscosity measurements, it could be seen that within experimental errors, the viscosity does not depend on the milk genotype. SC obtained from A1A2 and A2 milk show similar values of viscosity and similar viscosity behaviour.

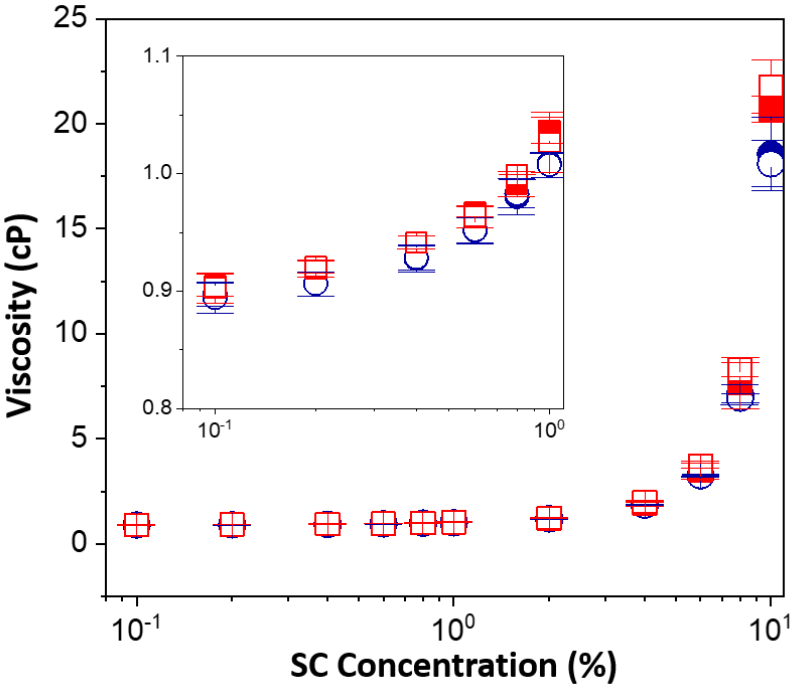

Figure 4. 1. Viscosity as a function of concentration for SC solutions obtained from A1A2 milks (●, ○) and A2 milks (■,□). Solid symbols and open symbols correspond to first and second batch, respectively. Error bars correspond to standard deviations. Inset is the data replotted for concentrations varying between 0.1 and 1 wt%.

In addition to viscosity, the particle size of the SC was also measured using dynamic light scattering. Figure 4.2 shows the intensity particle size average (z-average) as a function of the SC concentration. Similarly, to viscosity, when the concentration of SC is ≤ 1 wt%, the particle size is constant with an average size diameter of ~75 nm. When the concentration is further increased the particle, size increases exponentially with SC concentration; up to ~3000 nm when SC concentration is 10 wt%.

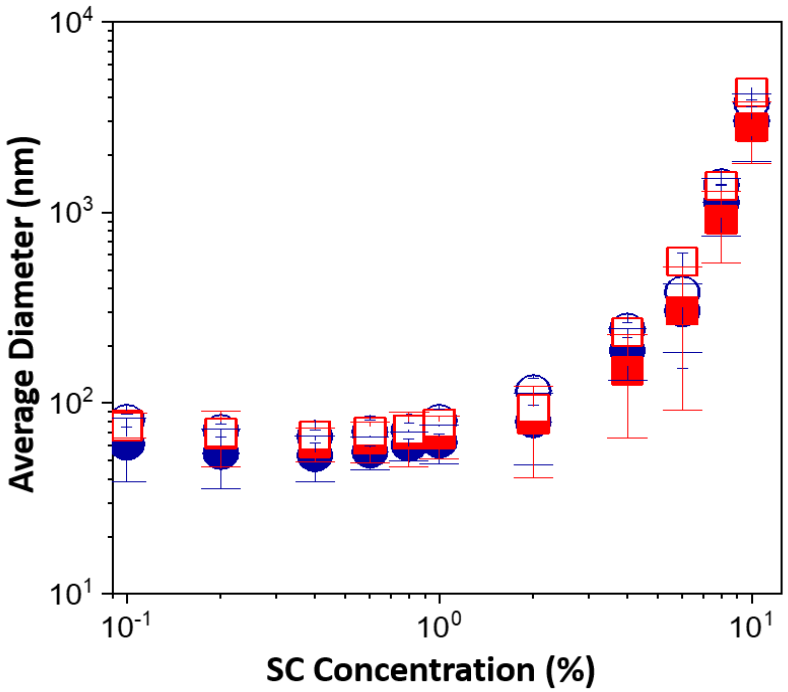

Figure 4. 2. Intensity average diameter as a function of concentration for SC solution obtained from A1A2 milks (●, ○) and A2 milks (■,□). Solid symbols and open symbols correspond to first and second batch, respectively. Error bars correspond to standard deviations.

This increase in particle size is due to two reasons. Firstly, the particle size as measured by dynamic light scattering is calculated based on the viscosity of the continuous phase (here water). However, as seen in Figure 4.1 for SC concentration ≥1% the viscosity increases markedly. It is not straightforward to replace the viscosity of water by that of SC to correct for the particle size, since the SC particle still mainly diffuses in the continuous phase. A second possibility is that when the SC concentration is high, SC particles interact to form larger aggregates. Even if the number of these aggregate is small, because the average diameter is calculated based on the intensity scattered, their contribution to the average size is expected to be noticeable. This has been previously reported for SC by Chu et al., (1995), Nash et al., (2002), and HadjSadok et al., (2008). In fact, the intensity size distributions (Figure 4.3) show clearly that the distributions are not monomodal but multimodal for SC made from both A1A2 and A2 milks. In general, there are two main peaks around 10 nm and 150 nm, however peaks at size >1000 nm can be also observed. However, as discussed before it is likely that the dominant size is around 10 nm (as indicated larger particle scatter more than smaller ones).

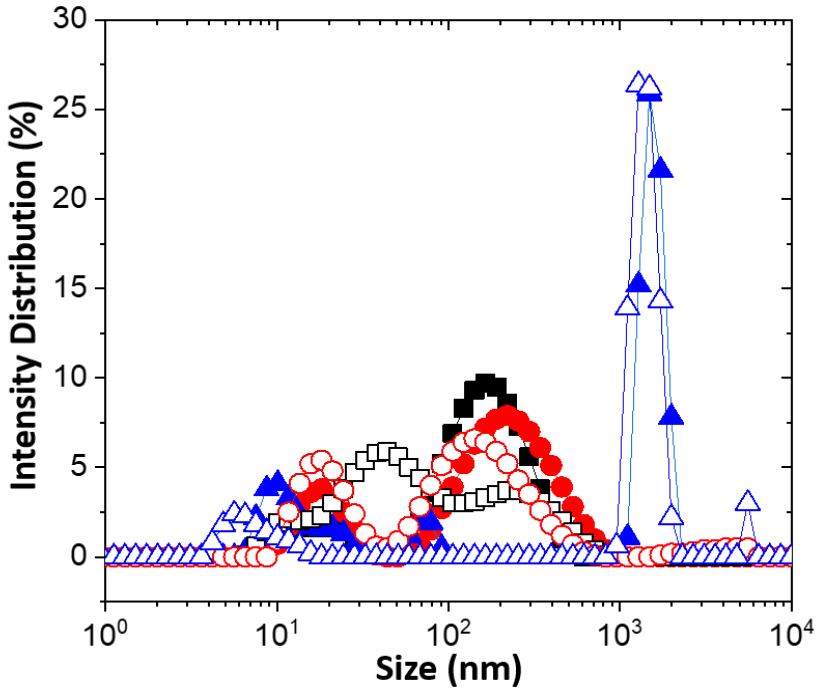

Figure 4. 3. Intensity size distribution for CS solution at concentration of 0.1% (■,□), 1% (●,○), and 10% (▲,△). Solid symbols are SC obtained from A2-B1 milk and open symbols are for SC obtained from A1A2-B2 milk.

4.3.2. SAXS investigation

Synchrotron SAXS was employed to probe the fine structure of different SC at a concentration in a range of 0.1-10.0 wt%. The scattering intensity I(q) are plotted versus the scattering wavevector, q for all the samples in Figure 4.4. The scattering curves were vertically shifted to avoid overlap. All the samples exhibit two main structural regions which are identified as high-q, 0.05< q (Å^{-1}) < 0.02, and low-q, 0.01 < q (Å^{-1}) < 0.05. The low-q regime is fitted by the spherical particles with a log-normal distribution, while the high-q regime is modelled by the unified fit model. Therefore, the total fit consists of two structural levels, and is presented as a solid black line in Figure 4.4.

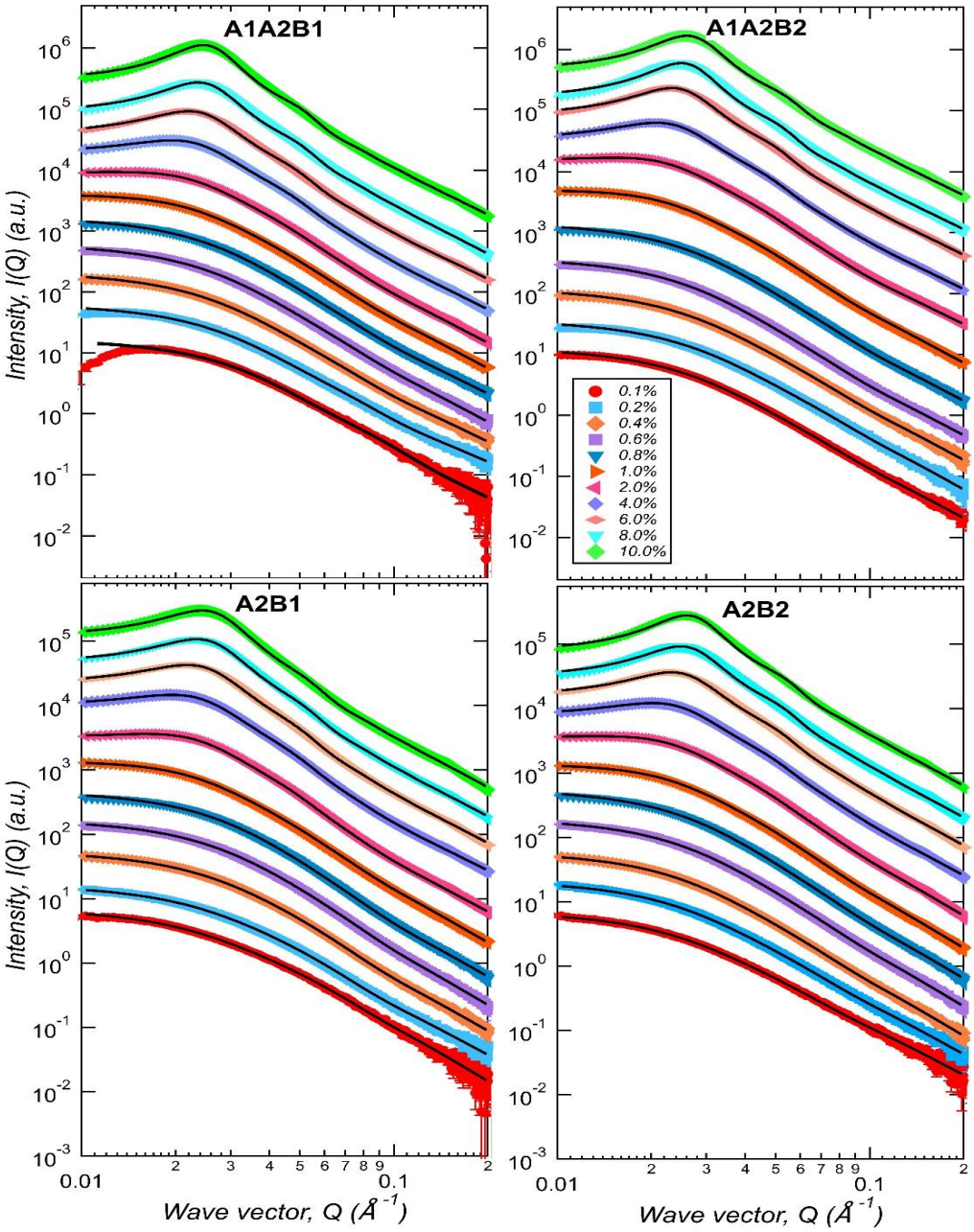

Figure 4. 4. SAXS curves of the different sodium caseinates at different concentrations. The scattering profiles are vertically shifted for clarity. The model fits are demonstrated as a solid black line in each plot.

At any given concentrations, all four SC samples exhibit a similar SAXS scattering profile through visual inspection. For instance, at the concentrations below 2 wt%, the scattering patterns show a Guinier plateau at low-*q* followed by an intensity decay at high-*q*. However, for the samples above 2 wt%, the low-*q* Guinier plateau features transitions to a peak. Also, this peak feature becomes more pronounced and shifts to a higher *q* with increasing concentration of SC. This peak is attributed to an appearance of a structure factor due to

protein-protein interactions and roughly represents a nearest neighbour distance of approximately 2 $\pi/q_{m.}$ (Goldenberg & Argyle, 2014; Pitkowski et al., 2008). For example, the peak position q_m moves from 0.026 to 0.03 $Å^{-1}$ when the concentration increases from 2 to 10 wt%, and accordingly the nearest neighbour distance decreases from 242 to 209 Å. The protein-protein distance of ~ 200 Å is an indicative of the close packing behaviours of SC in solutions. Similar findings were also observed in other SAXS studies on SC systems. For instance, Pitkowski, et al. (2008) found that a faint SAXS peak centered at q_m~0.03 $Å^{-1}$ appears at the concentration, c=12 % w/v. The decreased distance between the nearest protein particles with increasing the protein concentrations was also found in myoglobin (Goldenberg & Argyle, 2014) and bovine serum albumin (BSA) (Zhang, et al., 2007).

The deconvoluted profiles for each individual level of the overall fit is demonstrated in Figure 4.5, and the variation of the fitting parameters as a function of concentration are summarized in Tables 4.2-4.5. For all the samples, level 1 mean radius, R represents the overall size of SC particles in a range of 60 to 80 Å. These values agree well with previous reports on the SAXS and SANS study of SC. For instance, the R_g of SC in D_2O is determined as ~65 Å by SANS (Stothart & Cebula, 1982). In another study, by assuming SC to exhibits a core-shell structure, Kumosinski et al., (1988) employed SAXS to determine its shell and core sizes as ~ 88 Å and 38 Å, respectively. The results are fairly comparable with the size obtained by dynamic light scattering (Diameter~ 100 Å). The small deviations could be due to a broad size distribution of samples and different assumptions that are made to calculate particle sizes from these two different techniques. In addition, it can be observed that the sizes tend to decrease at higher concentrations. It may arise from the compression of its loose and flexible outside layers or shells when the SC approach the close packing (Kumosinski, et al., 1988).

The volume fraction η and hard spheres diameter 2 R_{HS} defined by the structure factor are plotted versus the concentration (w/v, g/mL) in Figure 4.6. The SC concentration in w/v is calculated from w/w using a density of 1.384 g/mL. All the SC samples saw that the volume fractions η increases linearly with protein concentration up to 6 w/v%. At the meantime, the 2 R_{HS} that indicates the distance between two protein particles shows a linear decrease with increasing concentrations, suggesting the SC particles become more closely packed. Similar trend was also observed in myoglobin solutions (Goldenberg & Argyle, 2014). Linear fits to the η-c data of all four samples yield a swelling ratio S (=η/c) of 3.5-4.1 cm^3/g, which is in the range of that reported in the published literature (S~ 4.0-4.5 cm^3/g) (Farrer & Lips, 1999;

Pitkowski, et al., 2008). A previous study suggest that the value *S* would be reduced if the SCs are not perfect spheres and exhibit some irregular non-spherical structures. In this case, the simplified hard sphere structure factor cannot sufficiently depict the protein-protein interactions particularly at very high concentrations (Kumosinski, et al., 1988). This is also manifested in η-*c* plots deviating from the straight line once the concentration reaches 8 and 10 wt% (Figure 4.6), consistent with a previous SAXS study of myoglobin at high concentrations (Goldenberg & Argyle, 2014).

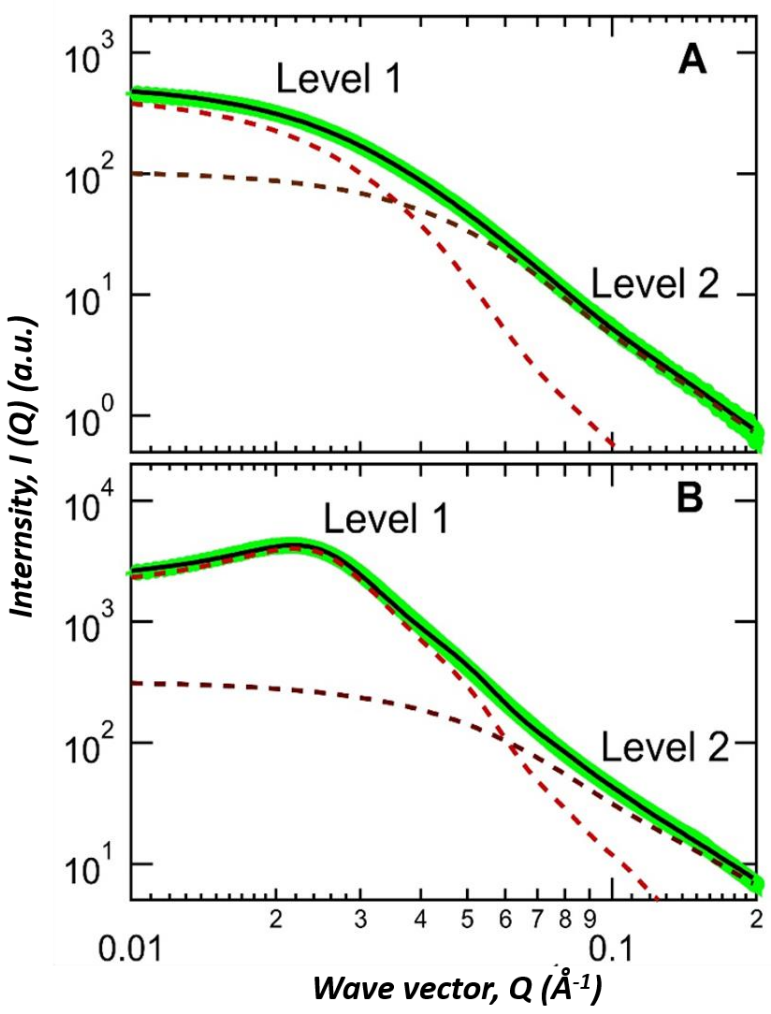

Figure 4. 5. SAXS data of A2B1 type SC of 0.6 wt% (A) and 6 wt% (B). The overall fits to the experimental SAXS data are demonstrated as solid black lines and individual levels are depicted as brown and dark red dashed lines for levels 1 and 2, respectively.

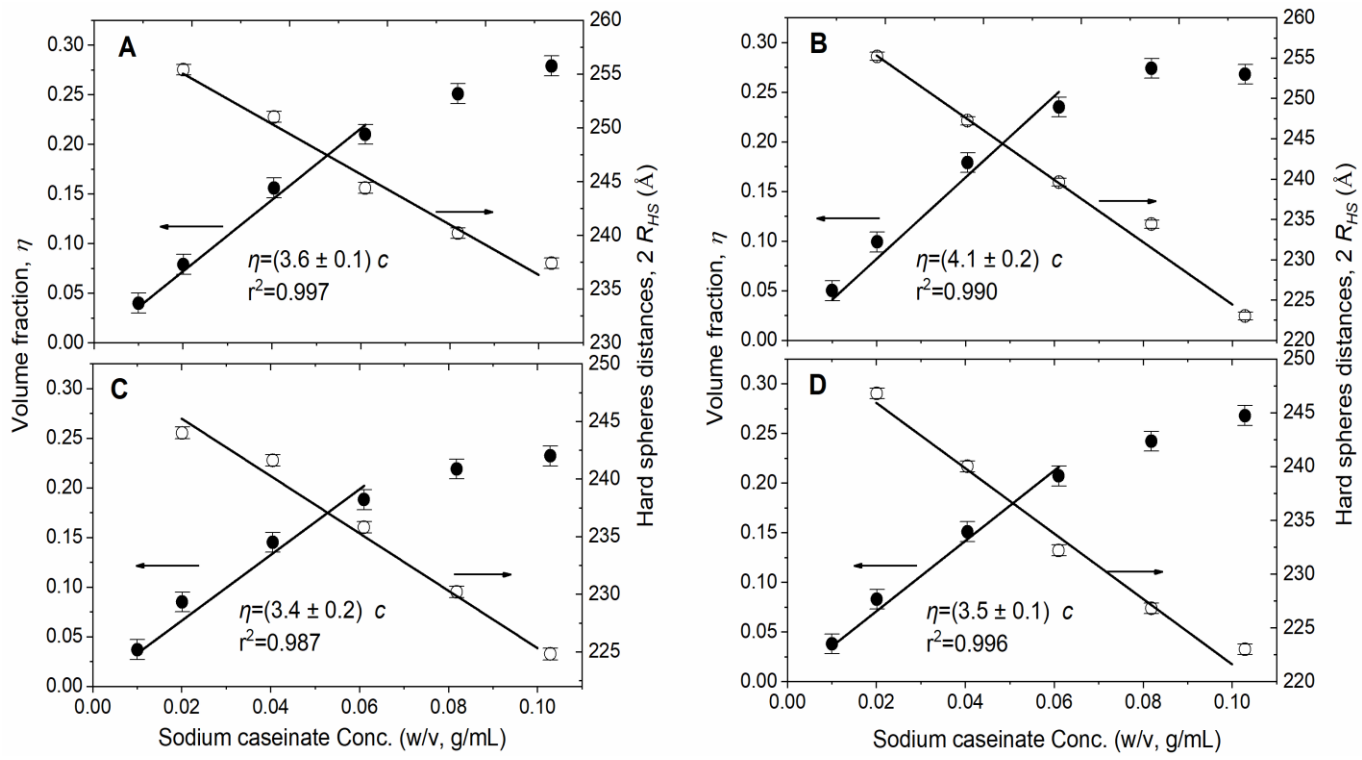

Figure 4. 6. Fit parameters of (A) A1A2-B1, (B) A1A2-B2, (C) A2-B1, and (D) A2-B2 type of SCs defining the hard spheres structure factor, r the hard spheres radius, and η the volume fraction occupied by the protein hard spheres. The lines represent least-square fits to the data (excluding the value for η at 8 and 10 w/w% SC).

A unified fit was required to model the high-*q* regime, since the single structural level is not able to fit the scattering curves over the whole *q* range. Conventionally, the high *q* shoulder feature in the milk has been attributed to the scattering of colloidal calcium phosphate (CCP) nanocluster (Shukla et al., 2009). However, the CCP is solubilized due to acidification during the preparation of SCs; therefore, the faint shoulder likely arises from 'protein inhomogeneities' or unevenly located dense protein regions that was firstly proposed by De Kruif (2014). Recently, resonant soft X-ray scattering measurements on milks support the existence of protein inhomogeneities in the casein micelles (Ingham, et al., 2015). The high-*q* R_g lies in between 25 and 41 Å for all the samples (Tables 4.2-4.5), which is in line with the values found in SC with various degree of cold solubility (Smialowska, et al., 2017) as well as in milk systems (Ingham, et al., 2016; Li, et al., 2018). In SC, this characteristic size is suggested to arise from the dense protein regions that formed by caseins through weak interactions such as van der Waals forces and/or the caseinate monomers in solution (Smialowska, et al., 2017). Moreover, all the samples exhibit a power-law decay in the high *q*

region. The power law exponent of 2.4-2.8 has been identified for all the samples (Tables 4.2-4.5), and it may reflect weakly segregated network such as percolation cluster or diffusion limited aggregates, randomly branched gaussian chains (2.28), or mass fractals (< 3.0), among others (Beaucage, 1996; Hammouda, 2010). The differences in the high-q power law exponent that characterizes the small-scale structure probably suggest a variation of polymer conformations and packing behaviour existing among different SC samples. However, given the high-q power law exponent is very sensitive to the solvent background subtraction, we will not over interpret the exponent to reach unambiguous conclusions.

Finally, the statistical analysis (ANOVA test) was conducted on the fitting parameters of the mean radius R, hard spheres radius R_{HS}, and volume fraction η from the level 1; and the R_g from the level 2. The results revealed that there are no significant structural differences among different types of SC at each concentration.

Table 4. 2. SAXS model fit structural parameters of A1A2B1 type SC at different concentrations (w/w%).

Conc. (w/w%)	**Level-1 size distribution**		**Level-1 structure factor**		**Level-2 unified fit**		
	Fraction	**Mean radius** R **(Å)**	**Hard spheres radius** R_{HS} **(Å)**	**Hard spheres volume fraction** η	**Scalar** G **(cm^{-1})**	**Size** R_g **(Å)**	**Exponent** P
0.1	0.5 (0.05)	60.1 (0.5) ^{d}	-	-	5.9 (0.3)	26.6 (0.5) ^{a}	2.4 (0.1) ^{a}
0.2	0.9 (0.05)	66.8 (0.5) ^{a}	-	-	21.0 (1.0)	32.9 (0.5) ^{ab}	2.4 (0.1) ^{a}
0.4	2.0 (0.1)	70.8 (0.5) ^{b}	-	-	59.8 (1.0)	36.8 (0.5) ^{b}	2.4 (0.1) ^{a}
0.6	3.2 (0.1)	71.2 (0.5) ^{b}	-	-	93.7 (3.0)	37.7 (0.5) ^{b}	2.6 (0.1) ^{a}
0.8	5.1 (0.1)	70.2 (0.5) ^{b}	-	-	118.1 (5.0)	36.9 (0.5) ^{b}	2.4 (0.1) ^{a}
1.0	5.6 (0.1)	73.5 (0.5) ^{bc}	127.2 (0.5) ^{b}	0.040 (0.01) ^{e}	205.4 (5.0)	41.0 (0.5) ^{c}	2.6 (0.1) ^{a}
2.0	12.5 (1.0)	70.4 (0.5) ^{b}	127.7 (0.5) ^{b}	0.079 (0.01) ^{d}	291.6 (5.0)	39.1 (0.5) ^{c}	2.5 (0.1) ^{a}
4.0	35.0 (2.0)	66.7 (0.5) ^{a}	125.5 (0.5) ^{ab}	0.156 (0.01) ^{c}	331.1 (5.0)	34.7 (0.5) ^{b}	2.4 (0.1) ^{a}
6.0	58.1 (2.0)	66.0 (0.5) ^{a}	122.2 (0.5) ^{a}	0.210 (0.01) ^{b}	323.2 (5.0)	31.5 (0.5) ^{a}	2.3 (0.1) ^{a}
8.0	78.6 (5.0)	66.1 (0.5) ^{a}	120.1 (0.5) ^{a}	0.251 (0.01) ^{ab}	335.3 (5.0)	29.4 (1.0) ^{a}	2.5 (0.1) ^{a}
10.0	96.6 (5.0)	66.9 (0.5) ^{a}	118.7 (0.5) ^{a}	0.279 (0.01) ^{a}	357.3 (5.0)	28.2 (1.0) ^{a}	2.5 (0.1) ^{a}

Numbers in parentheses represent σ error bars (or 68.3% confidence levels).

Different letters in the same column represent significant difference according to Turkey test ($P < 0.05$).

Table 4. 3. SAXS model fit structural parameters of A1A2B2 type SC at different concentrations (w/w%).

Conc. (w/w%)	**Level-1 size distribution**		**Level-1 structure factor**		**Level-2 unified fit**		
	Fraction	**Mean radius** R **(Å)**	**Hard spheres radius** R_{HS} **(Å)**	**Hard spheres volume fraction** η	**Scalar** G **(cm^{-1})**	**Size** R_g **(Å)**	**Exponent** P
0.1	1.2 (0.05)	70.1 (0.5) [c]	-	-	42.4 (0.5)	36.7 (0.5) [c]	2.7 (0.1) [a]
0.2	0.9 (0.05)	68.7 (0.5) [c]	-	-	29.5 (1.0)	35.3 (0.5) [c]	2.8 (0.1) [a]
0.4	1.4 (0.1)	70.6 (0.5) [c]	-	-	50.3 (1.0)	37.0 (0.5) [c]	2.7 (0.1) [a]
0.6	3.7 (0.1)	70.6 (0.5) [c]	-	-	108.3 (3.0)	37.6 (0.5) [c]	2.6 (0.1) [a]
0.8	5.0 (0.5)	69.6 (0.5) [c]	-	-	125.4 (3.0)	36.8 (0.5) [c]	2.6 (0.1) [a]
1.0	5.8 (0.5)	73.3 (0.5) [d]	126.1 (0.5) [d]	0.050 (0.01) [e]	230.0 (5.0)	41.0 (0.5) [c]	2.4 (0.1) [a]
2.0	15.1 (0.5)	69.2 (0.5) [c]	127.6 (0.5) [d]	0.099 (0.01) [d]	314.3 (5.0)	38.1 (0.5) [c]	2.4 (0.1) [a]
4.0	38.4 (2.0)	65.2 (0.5) [b]	123.6 (0.5) [c]	0.179 (0.01) [c]	331.2 (5.0)	33.8 (0.5) [b]	2.4 (0.1) [a]
6.0	63.1 (2.0)	64.1 (0.5) [b]	119.8 (0.5) [b]	0.235 (0.01) [b]	306.9 (5.0)	30.0 (1.0) [b]	2.4 (0.1) [a]
8.0	83.1 (2.0)	64.4 (0.5) [b]	117.2 (0.5) [b]	0.274 (0.01) [a]	309.1 (5.0)	27.7 (1.0) [a]	2.4 (0.1) [a]
10.0	91.4 (3.0)	60.2 (0.5) [a]	111.5 (0.5) [a]	0.268 (0.01) [a]	312.5 (5.0)	25.2 (2.0) [a]	2.6 (0.1) [a]

Numbers in parentheses represent σ error bars (or 68.3% confidence levels).

Different letters in the same column represent significant difference according to Turkey test ($P < 0.05$).

Table 4. 4. SAXS model fit structural parameters of A2B1 type SC at different concentrations (w/w%).

Conc. (w/w%)	**Level-1 size distribution**		**Level-1 structure factor**		**Level-2 unified fit**		
	Fraction	**Mean radius** ***R* (*Å*)**	**Hard spheres radius R_{HS} (*Å*)**	**Hard spheres volume fraction η**	**Scalar** ***G* (cm^{-1})**	**Size** **R_g (*Å*)**	**Exponent** ***P***
0.1	0.2 (0.05)	77.3 (0.5) ^{c}	-	-	19.3 (0.5)	39.0 (0.5) ^{bc}	2.8 (0.1) ^{a}
0.2	0.6 (0.05)	74.3 (0.5) ^{b}	-	-	45.1 (1.0)	39.9 (0.5) ^{bc}	2.6 (0.1) ^{a}
0.4	1.6 (0.1)	70.5 (0.5) ^{b}	-	-	82.0 (2.0)	39.2 (0.5) ^{b}	2.7 (0.1) ^{a}
0.6	2.8 (0.1)	68.2 (0.5) ^{a}	-	-	105.9 (5.0)	38.1 (0.5) ^{b}	2.8 (0.1) ^{a}
0.8	4.4 (0.2)	66.6 (0.5) ^{a}	-	-	122.0 (3.0)	37.0 (0.5) ^{b}	2.6 (0.1) ^{a}
1.0	5.0 (0.5)	72.8 (0.5) ^{b}	122.6 (0.5) ^{b}	0.037 (0.01) ^{e}	208.6 (5.0)	40.3 (0.5) ^{c}	2.7 (0.1) ^{a}
2.0	18.1 (0.5)	67.4 (0.5) ^{a}	122.0 (0.5) ^{b}	0.085 (0.01) ^{d}	326.2 (5.0)	38.4 (1.0) ^{b}	2.4 (0.1) ^{a}
4.0	35.3 (0.5)	66.1 (1.0) ^{a}	120.8 (0.5) ^{ab}	0.145 (0.01) ^{c}	317.1 (5.0)	35.0 (0.5) ^{b}	2.4 (0.1) ^{a}
6.0	56.4 (2.0)	66.0 (0.5) ^{a}	117.9 (0.5) ^{a}	0.188 (0.01) ^{b}	322.2 (5.0)	32.5 (0.5) ^{ab}	2.4 (0.1) ^{a}
8.0	75.2 (2.0)	66.0 (1.0) ^{a}	115.1 (0.5) ^{a}	0.219 (0.01) ^{a}	336.0 (5.0)	30.7 (1.0) ^{a}	2.4 (0.1) ^{a}
10.0	88.6 (4.0)	65.9 (0.5) ^{a}	112.4 (0.5) ^{a}	0.232 (0.01) ^{a}	329.8 (5.0)	28.9 (1.0) ^{a}	2.6 (0.1) ^{a}

Numbers in parentheses represent σ error bars (or 68.3% confidence levels),

Different letters in the same column represent significant difference according to Turkey test ($P < 0.05$),

Table 4. 5. SAXS model fit structural parameters of A2B2 type SC at different concentrations (w/w%).

Conc. *(w/w%)*	**Level-1 size distribution**		**Level-1 structure factor**		**Level-2 unified fit**		
	Fraction	**Mean radius** ***R* (*Å*)**	**Hard spheres radius R_{HS} (*Å*)**	**Hard spheres volume fraction η**	**Scalar** ***G* (cm^{-1})**	**Size** ***R_g* (*Å*)**	**Exponent** ***P***
0.1	0.3 (0.1)	74.9 (0.5) ^{c}	-	-	17.0 (0.5)	39.1 (0.5) ^{c}	2.5 (0.1) ^{a}
0.2	0.7 (0.1)	75.0 (0.5) ^{c}	-	-	45.1 (0.5)	39.3 (0.5) ^{c}	2.6 (0.1) ^{a}
0.4	1.6 (0.1)	73.9 (0.5) ^{c}	-	-	75.2 (0.5)	39.3 (0.5) ^{c}	2.8 (0.1) ^{a}
0.6	2.9 (0.1)	72.1 (0.5) ^{c}	-	-	109.7 (2.0)	38.6 (0.5) ^{c}	2.8 (0.1) ^{a}
0.8	4.7 (0.1)	70.0 (0.5) ^{bc}	-	-	133.8 (2.0)	37.5 (0.5) ^{c}	2.8 (0.1) ^{a}
1.0	4.9 (0.1)	73.3 (0.5) ^{c}	121.8 (0.5) ^{bc}	0.038 (0.01) ^{e}	218.9 (2.0)	40.9 (0.5) ^{c}	2.8 (0.1) ^{a}
2.0	12.8 (0.2)	68.7 (0.5) ^{b}	123.4 (0.5) ^{c}	0.083 (0.01) ^{d}	325.5 (2.0)	38.5 (0.5) ^{c}	2.8 (0.1) ^{a}
4.0	31.8 (0.5)	62.8 (0.5) ^{a}	120.0 (0.5) ^{a}	0.151 (0.01) ^{c}	310.1 (2.0)	32.7 (0.5) ^{b}	2.5 (0.1) ^{a}
6.0	55.3 (0.5)	60.9 (0.5) ^{a}	116.1 (0.5) ^{b}	0.207 (0.01) ^{b}	298.6 (4.0)	29.0 (0.5) ^{b}	2.6 (0.1) ^{a}
8.0	73.9 (0.5)	60.3 (0.5) ^{a}	113.4 (0.5) ^{a}	0.242 (0.01) ^{a}	305.2 (4.0)	26.9 (1.0) ^{a}	2.6 (0.1) ^{a}
10.0	91.6 (2.0)	60.2 (0.5) ^{a}	111.5 (0.5) ^{a}	0.268 (0.01) ^{a}	305.3 (4.0)	24.9 (1.5) ^{a}	2.7 (0.1) ^{a}

Numbers in parentheses represent σ error bars (or 68.3% confidence levels).

Different letters in the same column represent significant difference according to Turkey test ($P < 0.05$).

4.3.3. Adsorption of SCs onto latex particles

As an example, the particle size distributions of latex spheres alone and in the presence of SCs are shown in Figure 4.6. It can be seen that both the latex suspension and their mixtures with the SCs, for the concentrations of 0.02 and 0.1% SCs shown here, are monomodal. The latex suspension alone sows a peak at ~70 nm. When SCs is added the main peak shifted to ~80 nm. It can be also seen that the shift in the particle size distributions is the same for both SCs concentration and is independent of the β-CN phenotype; i.e. the same shift is observed in the case of A1A2 and A2 milks.

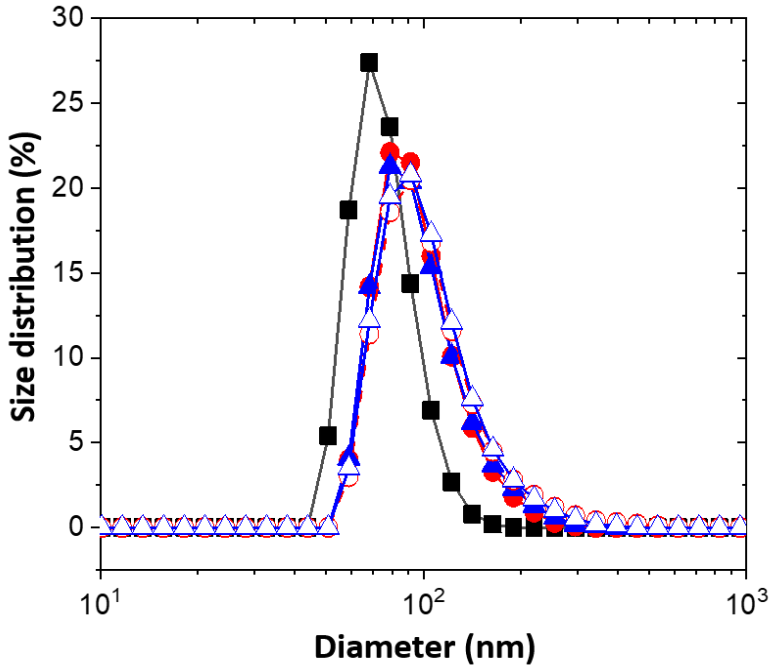

Figure 4. 7. Example of number particle size distribution of latex spheres alone (■, □), and in the presence of 0.02% (●,○) and 0.1 % (▲,△) SCs. Solid Symbols are for A1A2-B1 and open symbols are for A2-B1.

In order to compare between the SCs adsorption for different milks, the number-average particle size diameter D_N is plotted as a function of the concentration of added SCs. D_N of the latex spheres alone was 78±1 nm. In the presence of very small amount of SCs (0.004%) the diameter increases markedly. This increase in particle size is due to bridging flocculation, which is known to occur when the concentration of large molecular weight surface active agent is small and thus can adsorb to more than one particle surface. Dickinson et al., (1997) reported

that when the amount of SC is lower than half of the required amount for total surface coverage, oil-in-water emulsions undergoes bridging-flocculation. Increasing the concentration of SCs from 0.004 to 0.01% increases slightly the particle diameter up to ~100 nm. Further increase in SCs concentration from 0.01% to 0.1% does not result in an increase in the particle size which remains constant at ~100 nm. Note that the change in the diameter of the particles is also independent of the milk phenotype.

Since the increase in the size at the plateau (~100 nm) and the size of the bare particles (~78 nm), the SC layer adsorbed at the polystyrene particles is ~11 (=(100-80)/2) nm. This value is same as the value obtained by Dalgleish (1992) for the adsorption of β-CN to latex spheres and to the adsorption of a mixture of β-CN and α_{s2}-CN (11.1 nm).

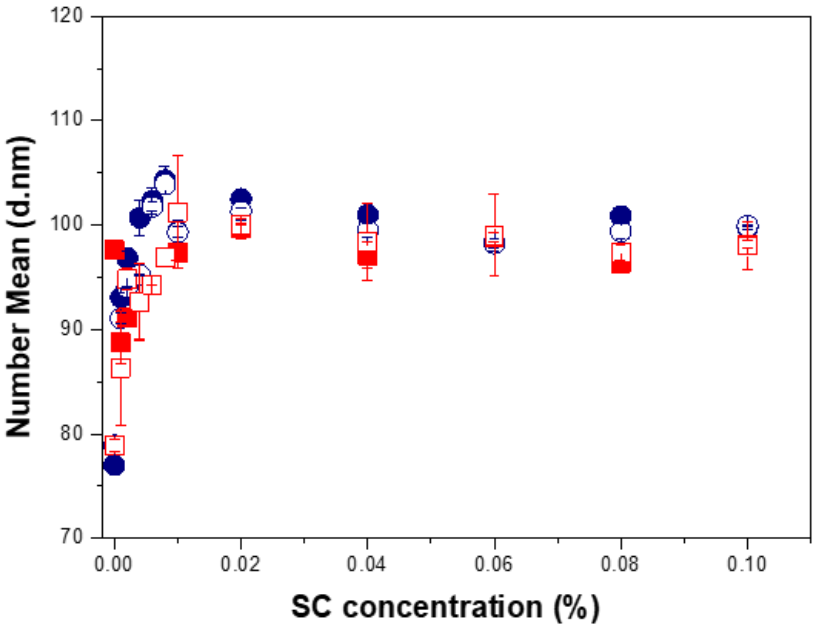

Figure 4. 8. Diameter of the latex particles mixed with SCs as a function of SCs concentration. Symbols represent: A1A2-B1 (■), A1A2-B2 (□), A2-B1 (●), A2-B2 (○) milks. Bars represent standard deviations.

From this experiment a full surface coverage value *G* (=amount of adsorbed SCs / total area of the particles) can be estimated. The total surface area the polystyrene particles is given by:

$$s = 6\,\emptyset\,V_p/D_N \qquad (4.7)$$

where $\emptyset$ (=2.5%) is the volume fraction of the particles as provided by the manufacturer, V_p (=10mL) is their volume, and D_N(=78 nm) their diameter. Since 0.02% of SCs present in 1.5 mL water, is the concentration at which the measured diameter does not longer change, this yields a value of G=15.6 mg/m^2. This result is in very good agreement with Yang & Schoemaker (1990) which reported a G value of ~15 mg/m^2 for SC adsorbed to polystyrene particles (the value is obtained visually from Figure 1 in their manuscript). It is important to note that their method used for the determination of G relied on measuring the difference of the protein concentration in the solution before and after adsorption on the latex particles; the amount of protein in solution being determined by centrifuging the polystyrene particle-SC mixtures.

4.4. Summary

In this work SC derived from A1A2 milks and A2 milks have been investigated for their viscosity and adsorption to polystyrene surfaces behaviours, as well by particle size and SAXS measurements. The results showed that SC viscosity, as expected, increases with SC concentration. Particle size measurements also showed that the size increases with the SC concentration. This is attributed to the increase in viscosity and to the presence of larger aggregates at high SC concentration, likely due to hydrophobic interaction between the SC particles. SAXS showed that the size of SC particles has a mean radius around 7 nm. This size is much smaller than that obtained by dynamic light scattering even at low SC concentrations (approximately 35 nm); and this is also likely due to the large contribution of the larger aggregate as indicated above.

An important finding of this work is that the results obtained in this work indicate that there are no noticeable differences between the behaviour structural and interfacial properties of SC obtained from A2 and A1A2 milk. This is likely due to the fact that although there are differences between A1 β-CN and A2 β-CN the difference in the amounts found in these SC maybe not large enough to impart differences on the behaviour of the SCs. Using Liquid chromatography coupled with mass spectrometry, the amount of A1 β-CN found in the A1A2 milks used in these studies very low (less than 10%) (Appendix 2). Thus, we argue that from a physicochemical viewpoint there is no advantage in the use of A2 SC compared to A1A2 SC. However, it will be worth investigating further if the physicochemical behaviour of SC obtained from A1 milk and A2 milks are different.

Chapter 5.

Application of DWS-MSDWS to model skim milk set gels and commercial stirred yoghurts

5.1. Introduction

Diffusing-wave spectroscopy (DWS) and multiple speckle diffusing-wave spectroscopy (MSDWS) have attracted a lot of interest in the last few years for their adequacy in the study of turbid media. However, DWS suffers from two drawbacks: firstly, it is not suitable for the study of non-ergodic systems such as gels, although this can be solved by the use of the double-cell method (Scheffold et al., 2001a) or by moving the sample and spatially average the autocorrelation functions (Xue et al., 1992). The *double-cell* method is easy to implement and consist in placing in the front of the cell containing the non-ergodic sample (gel) another cell containing an ergodic sample, such as a suspension of solid particles. The measured autocorrelation function is ergodic and is the product of the correlation function of the gel and that of the suspension. This allow inferring an ergodic autocorrelation function for the gel sample. However, this method is limited since the obtained autocorrelation function has the same correlation time as the suspension, and thus the longer correlation times of the gel cannot be probed. The second method consisting in rotating or translating the sample also has limitations as implementing this method require setting up mechanical devices which can affect the measurement by introducing vibrations which can affect the autocorrelation function, and might also affect the integrity of the gel, especially weal milk gels. Another limitation of DWS is due to the use of commercial correlator which, while very effective in measuring fast dynamics especially when used in a cross-correlation mode, do not allow monitoring samples with very slow dynamics (typically with a relaxation time >10 s). MSDWS solves these two problems as it uses a CCD-camera as the detection system. This allow obtaining the correlation function using images containing several speckles, and thus allowing probing non-ergodic and slow dynamics materials. The only limit of MSDWS is at short time, where the limiting time is defined by the number of images per second that can be collected.

The formation of a milk gel is an important step in the manufacture of yoghurts and cheeses. The casein micelles in milk are stabilized by electrostatic and steric repulsion associated with the presence of a hairy layer made of κ-CN at the surface of the micelles (Tuinier & De Kruif, 2002). While acidification neutralizes the electrostatic charges, the addition of rennet in cheese making result in the cleavage of the κ-CN. These effects result in the interaction between the casein micelles which aggregate to form a colloidal protein gel entrapping the milk serum. These gels are very weak and are also prone to syneresis, the diffusion of the serum phase out of the gel. DWS has been extensively used to study milk-based gel obtained by acidification

(Grygorczyk et al., 2013; Famelart et al., 2013; Ion-Titapiccolo et al., 2013; Titapiccolo et al., 2011; Cucheval et al., 2009; Alexander et al., 2008; Donato et al., 2007; Alexander & Dalgleish, 2005; Dalgleish et al., 2004; Vasbinder et al., 2001) or by the addition of rennet (Han et al., 2016; Sandra & Corredig, 2013; Zhao & Corredig, 2016; Sandra et al., 2012; Titapiccoloet al., 2010; Hemar et al., 2004). Most of these studies investigate the early stage of gelation, where the transition from liquid to gel can be accurately determined.

While DWS has been extensively used to investigate milk gels, to the best of our knowledge only few studies were reported on the use MSDWS to investigate milk gels. We believe that the first study is a preliminary work investigating the acid gelation of skim milks (Hemar et al., 2004). This study demonstrated that the two relaxations times are observed in the autocorrelation function. The fast relaxation time (~ms), which was independent of the protein concentration, was assigned to the dynamics of the protein particle within the gel strand. The slow relaxation time (>1 s), which increases with the protein concentration, describes the overall dynamic of the gel. Recently a commercially available MSDWS equipment was used to investigate milk gelation. The MSDWS setup used is commercially available and provides an elasticity index (EI) extracted from the mean-square displacement obtained from the analysis of the measured auto-correlation function at very short times (<0.1 s). It was shown that this instrument is able to monitor milk gelation and the associated syneresis (Rohart et al., 2016). This instrument was also used to investigate the effect of extracellular polysaccharides (EPS) produced by *Streptococcus thermophiles* on the characteristics of acidified milks (Surber et al., 2019), and to monitor the fermentation of milk containing two types of resistant starch (He et al., 2019). Here we use a combination of DWS and MSDWS to study commercially available stirred yoghurts, and model set acid milk gels made from heated and non-heated A1A2 and A2 milks with a milk solid concentration varying from 5 to 20%. A purpose builtequipment is used, and the analysis of the autocorrelation functions differs from that used by the commercial instrument. The limitations and advantages of the DWS-MSDWS to study these systems are discussed.

5.2. Materials and Methods

5.2.1. Materials and sample preparation

Low-heat skim A2 milk powder containing 40.6% protein, 7.8% ash, 44.2% lactose, 0.7% fat, was sourced from Synlait Milk Ltd. (Rakaia, New Zealand). Low-heat skim A1A2 milk powder

containing 32.9% protein, 7.9% ash, 54.5% lactose, 0.9% fat was obtained from Fonterra Ltd (Auckland, New Zealand). Glucono-δ-lactone (GDL), and sodium azide were purchased from Sigma-Aldrich (Missouri, USA).

Nine commercial stirred yoghurts were purchased from supermarkets in the Auckland area (New Zealand). Their compositions are provided in Table 5.1 below, and their pH ranges between from ~4.1 to ~4.52, with an average of 4.29 ± 0.14.

Table 5. 1. Composition of the different commercial yoghurts (%) and their pHs.

Brands	Protein	fat	Carbohydrate	pH at 25 °C
Biofarm	3.60	4.40	3.80	4.19
De Winkel	5.60	1.40	0.80	4.40
Gopala	3.30	2.60	4.50	4.52
Greek lite	5.00	4.50	7.10	4.12
Greek natural	4.60	7.50	6.30	4.26
Naturalea	3.60	3.10	3.90	4.10
Symbio	4.70	1.00	2.80	4.34
The Collective	5.20	5.70	5.20	4.30
Yoplus	4.60	3.10	4.70	4.35

Model set yoghurts were prepared by dissolving the A2 and A1A2 milk powders at different concentrations in MilliQ water containing 0.02% sodium azide under magnetic stirring for 2 h followed by overnight storage at 4^{o}C to ensure full hydration. These reconstituted milks were either non-heat treated (unheated milks) or heated to 85 ^{o}C for 30 min (heated milks) in a water bath after equilibration to room temperature. Appropriate amounts of GDL were added to these milks to achieve a pH of 4.30±0.01 after incubation at 30 ^{o}C for 24 h. A long gelation time was chosen due to the fast dynamic of the acid milk gels occurring during the early stage of gelation. Consequently, 24 h was chosen to ensure that milk gels were well set, and their dynamic were longer than measuring time. These set acidified milk gels were made in a 10 mm path length PMMA (polymethylmethacrylate) cuvettes; the cuvettes were sealed to avoid evaporation.

5.2.2. DWS and MSDWS experimental setups

DWS and MSDWS measurements were performed with two purpose-built setups. The experiments were performed at room temperature. At the ICPMS (The University of Strasbourg, France) the equipment was used on model acidified milk gels. In this setup the illumination source is a 50 mW 488 nm solid-state laser (Spectra Physics), whose intensity is controlled by a series of grey filter. The beam is expanded to a diameter of 8 mm by a focal Galilean telescope and the sample is illuminated close to its normal. The thickness of the sample, 1 cm, is ~100 times larger than the photon scattering mean free path, ensuring that the speckle dynamics does not depend on the sample thickness. The backscattered light is collected at ~30° along two arms. For DWS, light is collected by a single mode optical fiber and detected by an ALV/SO-SIPD photomultiplier (ALV, Hessen, Germany). The correlation function is then computed with a purpose-built FPGA correlator (Gamari et al. 2014). Along the MSDWS arm, the light is focused onto a diaphragm of varying diameter, allowing to control the spatial coherence of the speckle pattern. The speckle size is chosen ~10 pixels^2 in order to optimize the signal-to-noise ratio. A CMOS camera Basler acA1300-200µm (1280 × 1024 4.8 µm pixels) placed behind the diaphragm collects the diffused light. The exposure time is 1 ms so that the full dynamic of the camera is used. A series of MSDWS correlation functions are computed. A reference image I_p (t_{ref}) is acquired and the correlation function g_2 is defined as:

$$g_{2,t_{ref}}(t) = \frac{\langle I_p(t_{ref}) I_p(t_{ref}+t)\rangle_p}{\langle I_p(t_{ref})\rangle_p \langle I_p(t_{ref}+t)\rangle_p} \quad (5.1)$$

Where averaging is performed over pixels *p*.

A similar DWS-MSDWS setup was also built at the University of Auckland, with few differences, to study the commercial yoghurts. The DWS setup relies on a correlator (flex99oem-12) and two photomultipliers (PMT120-OP) purchased from Correlator.com Ltd (Hong Kong). The measurements were also carried out in the back-scattering geometry but in a cross-correlation mode using a bifurcated single optical fiber from Ozoptics (Ontario, Canada). A 25 mW HeNe laser (Thorlabs, USA) with a wavelength of 632 nm was the light source. The MSDWS setup is the same as the one described above. The MSDWS measurements were performed for up to 10^4 s.

5.2.3. Particle size and viscosity measurements

Particle size and viscosity measurements were performed on the commercial stirred yoghurts. A Malvern Mastersizer 2000 (Malvern Instruments, Malvern, UK) was employed to measure the size using a refractive index of 1.5 and 1.33 for the protein particle aggregate and water, respectively. The measurements were performed at room temperature on duplicate samples, and the size value is averaged on 10 measurements. The viscosity was obtained using an Anton-Paar Physica MCR 301 stress-controlled rheometer (Anton-Paar, Austria) fitted with a cone (50 mm diameter, 2° angle) and plate geometry. The viscosity was obtained by varying the shear rate from 0.1 to 1000 s^{-1}. All measurements were performed in duplicate at a constant temperature of 25°C.

5.3. Results and Discussion

Figure 5.1 shows some examples of the autocorrelation function $g_1(t)$ obtained by DWS-MSDWS measurements performed on model set acid milk gels. It can be seen that $g_1(t)$ exhibits two well separated decay times with a fast one τ_{fast} at around the millisecond and the slower relaxation time τ_{slow} at longer time (>100s). This behaviour is characteristic of complex fluids that exhibit viscoelastic responses that depend on frequency (Hemar et al., 2003). At short times, the local viscosity of the diffusing objects is measured while the terminal viscosity corresponding to the relaxation of network of aggregated protein particles, that is acidified casein micelles.

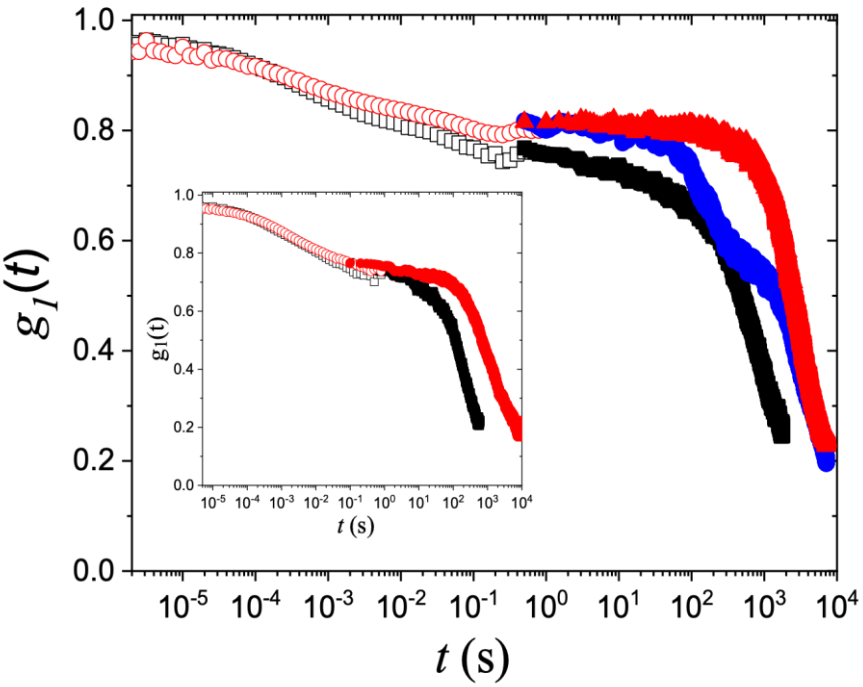

Figure 5. 1. Example of DWS (open symbols) and MSDWS (solid symbols) autocorrelation functions for model acid milk gels made using unheated (black symbols) milk and heated (red and blue symbols) A1A2 milks. Inset: DWS-MSDWS of unheated milk gels made with milks with a concentration of 10% (black symbols) and 20% (red symbols).

Interestingly, for all the measured samples, the value of τ_{fast} is equal to 0.6-2.0 ms. The origin of this decay mode may be attributed to the self-diffusion of the protein particles in the serum phase. Under this hypothesis, the radius (R) of the particle can be estimated using:

$$R = \frac{k_B T\, q_0^2}{6\,\pi\,\eta}\tau \qquad (5.2)$$

Where η (≈1 mP.a) is the viscosity of the serum phase which mainly contains water, k_B is the Boltzmann constant, T (=298 K) is the absolute temperature at which the measurements where performed, q_0 = (2π/λ, and λ=488 nm) is the wave vector, and τ is the relaxation time.

Using equation (5.2), for a relaxation time $\tau = \tau_{fast}$ =2 ms a radius $R \approx 70$ nm for the protein particle is obtained. This value would suggest that the protein aggregate consists of the individual casein micelle. It was found previously that at low pH (6.0 and 5.5) the size of the

casein micelle is approximately 154 nm (Sinaga et al., 2017), which is in very good agreement with the value obtained using DWS.

To compare between the different samples, τ_{slow} is plotted as a function of the time at which the measurement was taken (Figure 5.2). This time includes the time for equilibration to room temperature (30 min). The longest relaxation time, τ_{slow} increases with the heat treatment and with milk concentration. Note that at the highest concentrations (>15%), the long-time dynamics becomes temporally heterogeneous and the shoulder in $g_1(t)$ is observed at longer times (around 400 s on the blue curve in Figure 5.1). Such behaviour is expected to be related to the microscopic reorganization of an attractive network induced by stress relaxation.

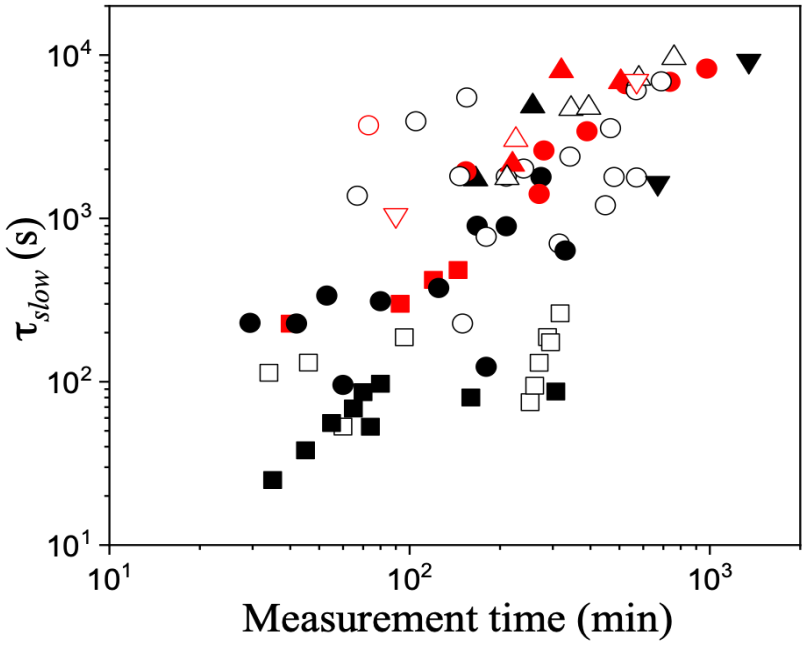

Figure 5. 2. Slow half-life τ_{slow} for different acid gels made with unheated milks (black symbols) and heated milks (red symbols) as a function of the time at which the measurements were carried out (after incubation at 30 ^{o}C and 30 min equilibration to room temperature). Milks are A2 (open symbols) and A1A2 (solid symbols). Milk concentrations are: 5 (■), 10 (●), 15 (▲), and 20 (▼) %.

While clearly milk gels made with low milk concentration (5%) and unheated milks showed lowest values of τ_{slow}, it is very difficult to discriminate between acid milk gels made with A1A2 and A2 milks. Recently, it was reported that acid milk gels made from A2 milk have

lower elasticity that those made of A1 milks (Nguyen et al., 2018). A probable explanation to the differences between the present study and the study by Nguyen et al. (2018) is the difference between A2 milk and A1A2 milk is not as different as between A2 and A1 milks. Further, it is noticed that the measurement time influences the value of τ_{slow}. In general, τ_{slow} increases with the time, indicating that the structure of the gel is continuously evolving. Particularly for low concentration milk gels τ_{slow} increases markedly with time. For example, the gel made with 5 wt% unheated milk (square solid sample, bottom left in Figure 5.2) increased nearly 10 folds. These results show that DWS-MSDWS measurements of the set acid milk gels depend on the aging of the sample.

DWS-MSDWS measurements were also carried out on commercial stirred yoghurts (Figure 5.3). The behaviour of $g_1(t)$ is markedly different from that of the model set acid milk gels, as $g_1(t)$ does not exhibit a fast decay time but only a long decay time. This indicates that these samples can be consider not as gels but rather as highly viscous dispersions. In order to analyse the behaviour of these commercial yoghurts, the measured relaxation time τ as a function the product of the viscosity by particle size ($\eta \times a$), based on equation (1) which indicates that these two parameters should be proportional. Please note that the particle size measured ($D_{4,3}$) in the study is not a hydrodynamic size but a volume average size obtained by static light scattering. In addition, for simplicity we replace the value of τ_{long} by the half-life time, the time at which $g_1(t)$ =0.5. As can been appreciated in the inset to Figure 5.3, excluding two commercial yoghurts, there is a linear relationship between τ_{long} and $\eta \times D_{4,3}$, showing as expected that the relaxation time increases with the increase of particle size and viscosity. The two excluded yoghurt samples from the analysis are the Biofarm (very low half-life time) and Symbio (very high half-life time. While Biofarm yoghurt has the lowest viscosity (~15 Pa.s) and a large particle size (~49 μm), Symbio has a viscosity of ~50 Pa.s and a particle size of ~38 μm, in the range of others commercial yoghurts, however contains a starch based thickener. Therefore, it is still unclear why these two yoghurts behaved differently in comparison to other yoghurts.

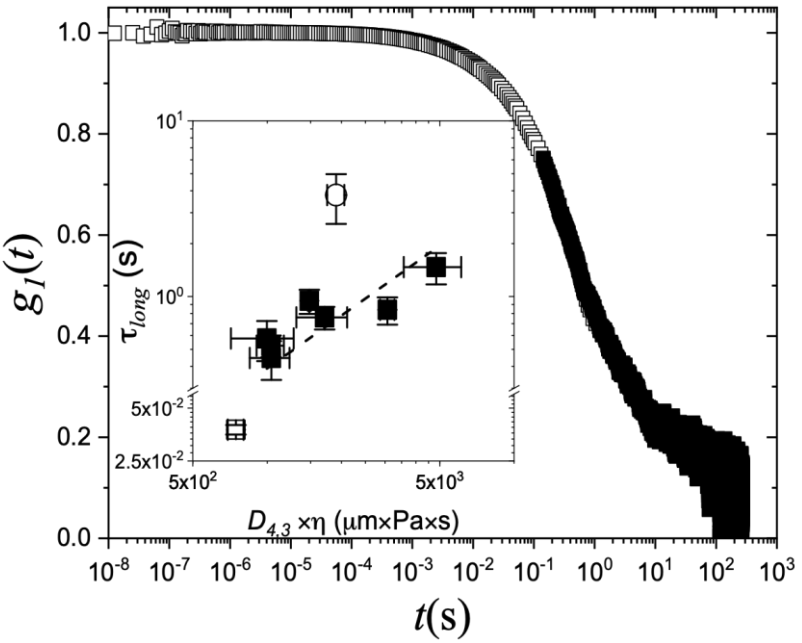

Figure 5. 3. Typical DWS and MSDWS correlation function of a commercial stirred yoghurt. Inset: slow relaxation τ_{long} measured by MSDWS as the function of the product of the viscosity and the mean volume size ($\eta \times D_{4,3}$).

While the relationship between τ_{long} and $\eta \times D_{4,3}$ is not extremely good (a linear fit results with an intercept set to zero and excluding the outliers samples results in R^2=0.64), This could be due to several factors, including the fact that the particle size measured is not a hydrodynamic radius (required in equation 1), and yoghurt particles are not spherical but are rather made of particulate aggregate. Further their size is very large and thus may not undergo Brownian motion. Nevertheless, DWS-MSDWS can be used as a quality control method for commercial yoghurts.

5.4. Summary

In this study, DWS was combined with MSDWS (DWS-MSDWS) to investigate model set-acid milk gels and commercial yoghurts. DWS-MSDWS allowed to probe the dynamics of these systems in a range from the few nanoseconds to few seconds. This revealed that set-acid milk gels show two dynamics; a fast one around 2 ms which is likely due to the diffusion of the individual protein aggregate (likely the casein micelle according to the calculated radius of the aggregate) which is part of the protein network; and a slow dynamic (>10 s) which reflects the dynamics of the whole system. It is shown that the time at which the measurement is performed is extremely important, as these systems are dynamic and continue to evolve with

time. There is no indication from this study that the dynamics of milk gels made of A2 milks are different from those made from A1A2 milks. This could be due to the fact that the difference in the amount of A2 β-CN present in both milks is not very different.

This study also showed that DWS-MSDWS has a potential to investigate commercial stirred yoghurt. In comparison to the model acid-set yoghurts, they exhibit only a slow relaxation time, making their autocorrelation function easy to analyze. This study suggests that the DWS-MSDWS technique can be implemented as a tool to monitor the physical quality of commercial yoghurts.

Chapter 6.

Effect of high pressure on milks

6.1. Introduction

The application of high hydrostatic pressure (HHP) has long been considered a potential alternative to heat treatment in the food industry. HHP can achieve the destruction of microorganisms to prolong shelf-life without impacting colour, flavour and nutritional quality (Cheftel, 1992). According to Chawla et al., (2011) the first report of high hydrostatic pressure (HHP) being applied to increase the shelf-life of milk was by Hite in 1899. It was also reported that HHP increased the shelf-life of milk by up to 4 days by treating the milk with 600 MPa at room temperature for 1 h (Bridgman, 1914). However, the lack of advancement in equipment technology meant more intensive research couldn't be conducted till the 1990's (Lopez-Fandino, 2006). Since observing egg albumin protein was denatured under HHP treatment in 1914 (Bridgman, 1914), research has been undertaken on the application of HHP to diverse food systems (Lau, 2010). Consumer demand for minimally processed high quality food products has also led to considerable research interests in HHP technology (Lau, 2010). HHP processing is now being used for commercial products such as fruit jams, jellies, sauces, juices, avocado pulp, guacamole, and cooked ham, for example, although there are not yet many commercially available HHP-treated dairy products (Lau, 2010).

HHP treatment can influence many properties of the proteins in food. It is reported that pressure treatment can impact the activity and structure of proteins. Pressure-induced changes are governed by Le Chatelier principle, which states that changes that result in a decrease in volume are favoured by an increase in pressure (Mozhaev et al., 1996). The ability of proteins to withstand pressure is based on its compressibility which is governed by the compression of its internal cavities (Balny & Masson, 1993). Upon application of high pressure, the volume of a cavity decreases due to compression of internal cavities under pressure being favoured by Le Chatelier principle and could lead to the unfolding of globular proteins (Mozhaev et al., 1996). It is known that milk contains two main classes of proteins: caseins and whey proteins. Caseins represent approximately 80% of the proteins while whey proteins account for the remaining 20% (Fox & Mulvihill, 1982). The caseins are predominantly present in the form of colloidal particles known as micelles. These casein micelles are loose, highly hydrated and are composed of α_{s1}-, α_{s2}-, β-, and κ-CNs, and minerals primarily in the form of colloidal calcium phosphate (CCP) (de Kruif et al., 2012). The shape of casein micelles in bovine milk, as observed by electron microscopy, is relatively spherical, polydisperse in size ranging from 50 to 500 nm in diameter with an average around 120 nm and an average molecular mass from 10^6 to 10^9 Da

(Phadungath, 2005). A combination of hydrophobic interactions and electrostatic interactions via micellar clusters of CCP help maintain the integrity of casein micelles (Horne, 2006). Due to the importance of casein and casein micelles in the functional behaviour of milk and dairy products, the nature and structure of casein micelles have been studied extensively, albeit many details of the exact structure are still under debate (Day et al., 2017).

Interactions between protein molecules are divided into electrostatic interactions, hydrogen bonds, hydrophobic interactions, and covalent bonds. HHP is known to induce protein denaturation by influencing the delicate balance between these interactions which help stabilize the folded protein (Boonyaratanakornkit et al., 2002). HHP treatments can influence the functional properties of milk proteins through the disruption and reformation of hydrogen bonds, electrostatic and hydrophobic interactions (Boonyaratanakornkit et al., 2002). These changes are dependent on many properties including the protein structure, concentration, pressure amplitude, temperature, pH, and ionic strength (Boonyaratanakornkit et al., 2002). HHP induced changes to protein structure are usually reversible within the range of 100 to 300 MPa. However, proteins can undergo irreversible denaturation with pressures greater than 300 MPa (Rastogi et al., 2007). Pressures greater than 700 MPa have also been reported to disrupt secondary protein structure inducing irreversible denaturation (Balny & Masson, 1993).

Hydrophobic interactions play an important role in the stabilization of the quaternary structure in proteins. Quaternary structures have been reported to be pressure sensitive because of a large negative volume change upon globular unfolding, with changes taking place at relatively low pressures ~150 MPa (Balny & Masson, 1993). Tertiary and secondary structures are also affected by high pressures with a pressure induced an incomplete unfolding being reported (Gekko & Hasegawa, 1989). Stabilizing H-bonds are stable at low pressures but can be disintegrated at very high pressures. At pressures >200 MPa, tertiary structure of proteins which are maintained by hydrophobic and ionic interactions have been observed to undergo significant changes (Patel & Creamer, 2008).

Casein micelles can be significantly influenced by HHP treatment. One of the first studies conducted, reported a decrease in the size of casein micelles upon HHP treatment as observed by electron microscopy (Schmidt & Buchheim, 1970). Casein micelle size is affected only slightly by HHP treatment at pressures $\leq$ 200 MPa due to the minimal amount of secondary and tertiary structures (Huppertz et al., 2004b). However, Needs et al., (2000) reported a slight

increase in casein micelle size in untreated milk collected directly from the farm after 15 mins of HHP treatment at 200 MPa. A variety of methods have been used to determine casein micelle size in HHP-treated milk such as laser diffraction granulometry, transmission electron microscopy (TEM) and photon correlation spectroscopy (PCS), as well as turbidimetry, an indirect method (Huppertz et al., 2002). More recently scattering methods such as small angle X-ray scattering (SAXS) and small angle neutron scattering (SANS) have been used (Holt et al., 2003).

Disintegration of casein micelles under HHP has been attributed to two main factors; firstly, solubilisation of the colloidal calcium phosphate (CCP) (Schrader et al., 1997), which is responsible for crosslinking caseins and neutralizing the negatively charged phosphoserine groups. Consequently, CCP dissociation disrupts micelle stability (Horne, 2006). Secondly, HHP causes the disruption of hydrophobic interactions (Schrader et al., 1997), which are integral in the binding of individual caseins within casein micelles (Horne, 2006). Under higher pressures ≥ 300 MPa, fragmentation of casein micelles takes place, whereby micelles disintegrate into its soluble components the α_{s1}, α_{s2}, ß- and κ-CNs (Schrader et al., 1997). HHP treatment can result in a milk with a more translucent appearance, with lower turbidity and an increased viscosity (Gaucheron et al., 1997).

It is found that many factors can influence the effect of HHP treatment on milk proteins. For example, the increase in micelle size at pressures between 200 to 300 MPa has been reported to depend on the pH of the milk, temperature, pressure and length of pressure treatment (Huppertz et al., 2004b). This increase in size has been attributed to the interactions between casein micelles and the denatured whey proteins and/or the formation of casein aggregates (Huppertz et al., 2004b). Initial reports suggested that aggregation could be due to interactions between denatured whey proteins and casein micelles (Huppertz et al., 2004b). However, subsequent studies on whey protein depleted systems indicate that casein aggregation is primarily due to hydrophobic interactions (Anema et al., 2005; Huppertz et al., 2004b). This aggregation is more evident with an increase in temperature, pressure, and length of pressurization (Anema et al., 2005; Huppertz et al., 2004b). This could be due to the reformation of micellar particles from fragments of HHP-disrupted casein micelles. This re-association could be facilitated by the re-formation of hydrophobic bonds, as hydrophobic bonds might be favoured under prolonged moderate pressurization from 200 to 300 MPa (Needs et al., 2000).

The behaviour of whey proteins when they are HHP treated either individually in solution or as part of whey protein products such as whey protein concentrates (WPC) or whey protein isolate (WPI) has been studied extensively (Huppertz et al., 2004a; Johnston et al., 1992; Lopez, 1996). In one of the first studies, it was reported that the amount of non-casein nitrogen decreased in milk serum with increased pressure, indicating denaturation and precipitation of whey proteins (Johnston et al., 1992). It has also been reported that under HHP treatment, whey proteins can undergo unfolding of monomeric proteins, aggregation and gelation (Huppertz et al., 2004a), via the re-forming of intra and inter molecular bonds via disulphide bridges (Balny & Masson, 1993; Cheftel, 1992). This pressure induced unfolding of proteins is influenced by the type of protein, protein concentration and treatment conditions such as pressure, temperature, duration of pressurization, pH, and ionic strength (Balny & Masson, 1993; Huppertz et al., 2004a).

Out of all the whey proteins, β-lactoglobulin (β-lg) is the most sensitive to HHP and it plays a significant role in the denaturation, aggregation and gelation of whey proteins (Lopez-Fandino, 2006). Treatment of untreated milk collected directly from the farm up to 100 MPa does not cause denaturation of β-lg (Lopez, 1996). Application of pressures over 100 MPa at room temperature, results in progressive denaturation, which is a measure of the loss in solubility, compared to α-lac and BSA which are both resistant to pressures up to 400 MPa (Lopez, 1996). It has been proposed that pressures greater than 100 MPa, initiates unfolding of β-lg along with exposure of free sulphide (SH)-groups, which may interact with κ-CN or other unfolded β-lg molecules (Funtenberger et al., 1997). β-lg has two SH-groups and one free thiol group which may play a crucial role in HHP-induced β-lg aggregation via thiol-disulphide interchange reactions (Funtenberger et al., 1997). Application of higher pressures enhanced denaturation of whey proteins which reached 70 to 80% after HHP treatment at 400 MPa (Huppertz et al., 2004a; Lopez, 1996). However little further denaturation of β-lg occurs at 400-800 MPa (Needs et al., 2000).

Compared to β-lg, α-lac is much more resistant to denaturation under pressure. The greater stability of α-lac towards HHP could be attributed to differences in their secondary structures, number of sulphide bonds and Ca^{2+} binding sites. The presence of four disulphide bonds along with the lack of free thiol group also makes α-lac more rigid, enhancing its resistance to denaturation (Gaucheron et al., 1997; Lopez, 1996). It has also been reported that both whey proteins, β-lg and α-lac, are more prone to denaturation in milk compared to whey (Huppertz

et al., 2004a). In addition, the ability of denatured whey proteins to remain soluble in HHP treated casein-free milk serum, would suggest that denatured β-lg, in pressurised milk is interacting with casein micelles (Huppertz et al., 2004b).

In-situ methods have been used in this chapter to get a better understanding of the behaviour of milk proteins under pressure, and its effect on the reversibility of the physical and chemical changes induced by pressure. In the first part small angle X-ray scattering (SAXS) was used in combination with a diamond anvil cell (DAC) to monitor *in-situ* the change in the structure of skim milk. This part has been published by Yang et al., in 2018. In the second part, a high-pressure cell equipped with sapphire windows was used to measure the change in turbidity of milks at different pHs.

6.2. Materials and methods

6.2.1. Materials

One of the milks used in this work was a laboratory freeze dried commercial Anchor skim milk and the other three types of milk were spray dried, low-heat skim milk powder, two of them were regular A1A2 powders and one was an A2 milk powder. The two A1A2 low-heat skim milk powders were obtained from Westland Milk Products (Hokitika, New Zealand) and Fonterra Ltd. (Auckland, New Zealand). A2 low-heat skim milk powder was obtained from Synlait Milk Ltd. (Rakaia, New Zealand).

The details of the milks' compositional information are given in Section 3.1.1. The chemicals used including HCl, NaOH, premixed acrylamide: bis-acrylamide solution, tris-HCl, sodium dodecyl sulphate, ammonium persulfate, tetramethylethylenediamine, premixed electrophoresis buffer (running buffer), Laemmli buffer (sample buffer), 2-mercaptoethanol, Coomassie brilliant blue R-250, methanol and glacial acetic acid were all of analytical grade and purchased from Sigma Aldrich (Auckland, New Zealand) and Sigma Aldrich (St. Louis, Missouri, The United States).

6.2.2. Samples and experimental methods

The details for preparing the milk samples are presented in Sections 3.2.1.5 and 3.2.1.7. The experiments set up can be found in sections 3.2.2.6.1, 3.2.2.6.2, and 3.2.2.6.3. The Figure below illustrates the types of milk and methods used for each milk samples.

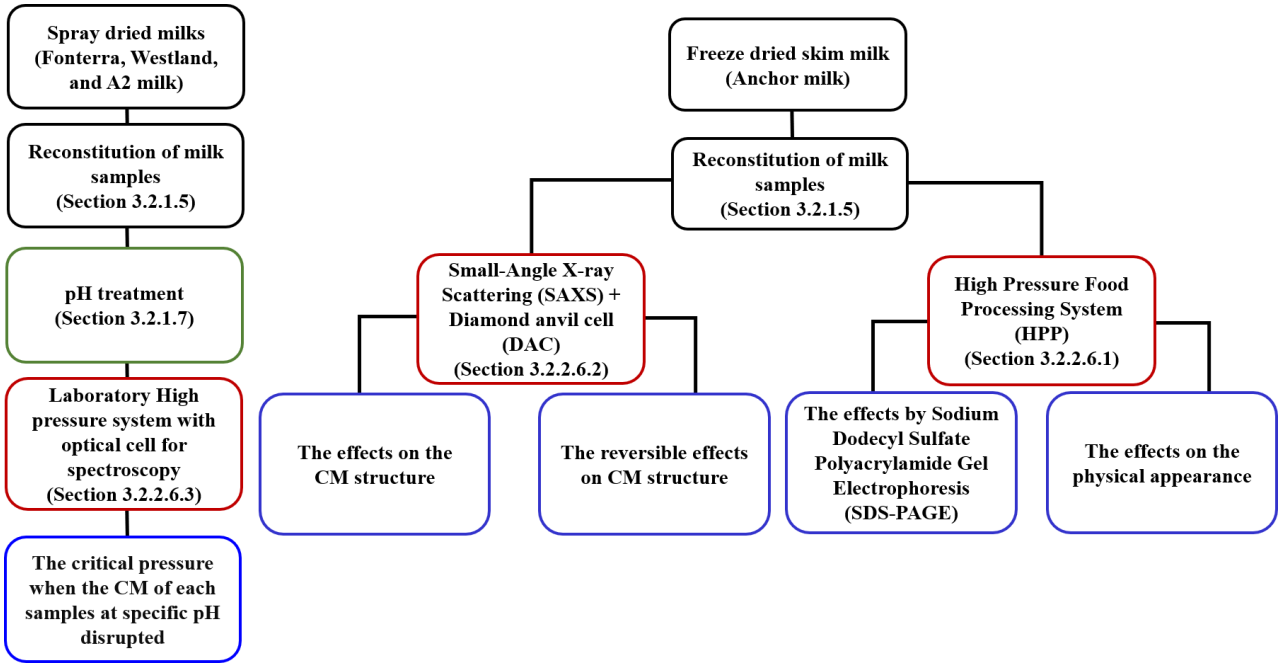

Figure 6. 1. Flow diagram of the experimental procedures used in this chapter.

6.3. Results and discussion

The first part of this section will report on the physical appearance, SDS-PAGE, and Small Angle X-ray Scattering (SAXS) of the reconstituted freeze-dried Anchor skim milk. The second part will investigate the dissociation of the casein micelles in reconstituted milk samples prepared from three different types of milk powders at different pHs as monitored using an *in-situ* turbidity method.

6.3.1. Physical appearance of milks

Treating the milk with high pressure can induce changes in its turbidity and colour. These changes can be a result, for example, of HHP causing changes in the mineral balance, the hydration level and the protein structures in the casein micelles in the milk. The turbidity value has been used to represent the average light scattered by the micelles in the sample (Orlien et al., 2010).

The white colour of milk is due to the scattering of light by fat globules and casein micelles (Naik, 2013). It is observed that the white colour of skim milk decreases with increasing the pressure up to 600 MPa (Figure 6.2). Treatment up to 200 MPa had only a slight effect on the appearance of skim milk with the most noticeable change taking place from 200 to 400 MPa

and little further changes from 400 to 600 MPa. This change in translucency is in agreement with observations by Johnston et al. (1992) who reported a decrease in the Hunter Luminance value (L* value), which is a measure of whiteness. Similar observations were made by Naik, (2013), who reported a significant decrease in L* value after treatment between 250 and 450 MPa of skim milk. Gervilla et al. (2006) observed the same, with a reported decrease of L* and an increase of greenness (a*) and yellowness (b*) upon HHP treatment of ewe's milk (Gervilla et al., 2006). Needs et al., (2000) observed that when skim milk was treated at 600 MPa, milk underwent significant changes as measured through the L*, b* and a* values (Needs et al., 2000).

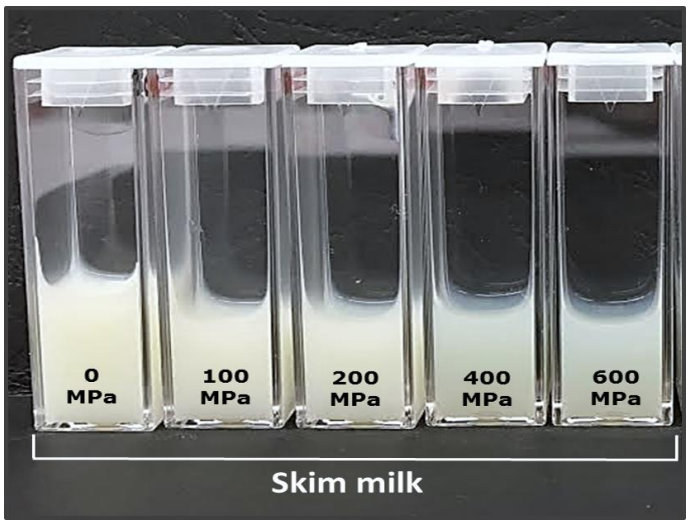

Figure 6. 2. Reconstituted freeze-dried Anchor skim milk samples treated by different pressure (0, 100, 200, 400, and 600 MPa) using the Avure 2L high pressure food processing system (QFP 2L-700, Avure Technologies, Ohio, USA). Picture was taken at atmospheric pressure after 1 h after pressure treatment.

The size of casein micelles in milk play an important role in light scattering. Upon application of high pressure, non-covalent forces (hydrogen bonds, ionic interactions, and hydrophobic forces) undergo disruption along with solubilisation of colloidal calcium phosphate (CCP) (Needs et al., 2000; Orlien et al., 2010; Schrader et al., 1997). This casein micelle disruption leads to a reduction in light scattering, affecting L* values (Johnston et al., 1992), which could explain the increase in light transmittance of skim milk as seen in Figure 6.2.

6.3.2. Sodium Dodecyl Sulphate Polyacrylamide Gel Electrophoresis (SDS-PAGE)

SDS-PAGE was used to give an indication of the protein content (caseins and whey proteins) and highlighting the protein distribution patterns in 10% (w/w) reconstituted freeze-dried Anchor skim milk samples treated with different pressures (0, 100, 200, 400, and 600 MPa).

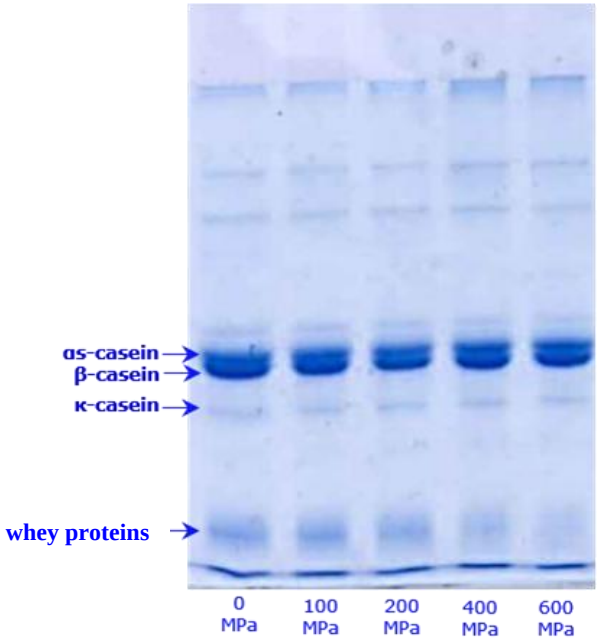

Figure 6. 3. SDS-PAGE of 10% (w/w) reconstituted freeze-dried Anchor skim milk samples after pressure treatment at 0, 100, 200, 400, and 600 MPa at room temperature (~25 °C) for 30 min.

Even though, caseins micelles were expected to dissociate with increasing pressure treatment above 200 MPa, the indevidual band intensity of each casein (α_s-CN, β-CN and κ-CN) in SDS-PAGE did not show any changes. Similar result has been detected by Marciniak et al., (2018) under reduced SDS PAGE. In fact, there is no change in the molecular weight of the caseins (no appearance of other bands indicating smaller molecular weights). This confirms that while the casein micelles is dissociated by HHP, the casein molecules are not cleaved. In addition, a visible difference in the intensity of whey protein bands were expected upon increasing the pressure. Although, α-lac and β-lg are not well separated in this SDS-PAGE experiment, a progressive decreas in the band intensity of whey proteins with increase in the pressure from 0 MPa to 600 MPa can be seen (please compare lowest band in Figure 6.3).

Whey proteins are known to undergo denaturation and solubilisation, as evidenced by the decrease in non-casein nitrogen in milk serum upon increase in pressure (Johnston et al., 1992). Pressures up to 100 MPa result in some partial unfolding of β-lg, which would explain the minimal change in intensity between 0 and 100 MPa. Increase in pressure from 100 to 200 MPa results in a decrease in band intensity, indicating initiation in structural changes, as unfolding of β-lg starts exposing any free SH groups, resulting in the possibility of interaction with κ-CN or other unfolded β-lg (Lopez, 1996). Subsequent increase in pressure (up to 400 MPa) results in a fairly visible decrease in band intensity, indicating considerable denaturation. Application of higher pressures (up to 400 MPa) has been reported to denature β-lg by 70% to 80% (Huppertz et al., 2004a; Lopez, 1996). Similar band intensity between 400 and 600 MPa, would indicate little further denaturation of ß-lg which is consistent with reported findings (Needs, et al., 2000). In comparison, α-lac is more resistant to denaturation for pressures up to 500 MPa (Gaucheron et al., 1997; Needs et al., 2000), which would suggest that the more sensitive β-lg has is the protein which played a significant role in the decrease in band intensity of whey proteins upon increase in pressure.

6.3.3. *In-situ* study of milk structure changes under HHP using synchrotron SAXS

The *in-situ* effect of HHP on the internal structures of the casein micelle up to ~1000 MPa was studied *in-situ* under HHP using synchrotron SAXS (Yang et al., 2018). Synchrotron SAXS is particularly advantageous in comparison to lab bench SAXS, due to enhanced intensity, allowing fast real-time recording of scattering patterns. Compared to SANS, for example, SAXS is also more efficient as it offers fast measurements whilst using smaller sample volumes. A diamond anvil cell (DAC) was used to hold the sample and apply different pressures. The reversible effects that took place upon pressure release to ambient conditions were also studied. *In-situ* SAXS patterns of HHP induced skim milk can be seen in Figure 6.4 (A) presented below. At atmospheric pressure, the obtained SAXS spectra are in line with earlier studies of casein micelles, with scattering in the low-*q* region correlating to the overall casein micelle size (Ingham et al., 2016; Shukla et al., 2009). This is followed by a decay in scattering intensity upon further increase in *q* region between 0.008 and 0.02 $Å^{-1}$, which would indicate a relatively smooth and sharp casein micelle interface (Mata et al., 2011). The presence of a distinctive shoulder at *q* region 0.08 $Å^{-1}$, has been attributed to the scattering of CCP

nanoclusters (Bouchoux et al., 2010; Marchin et al., 2007).

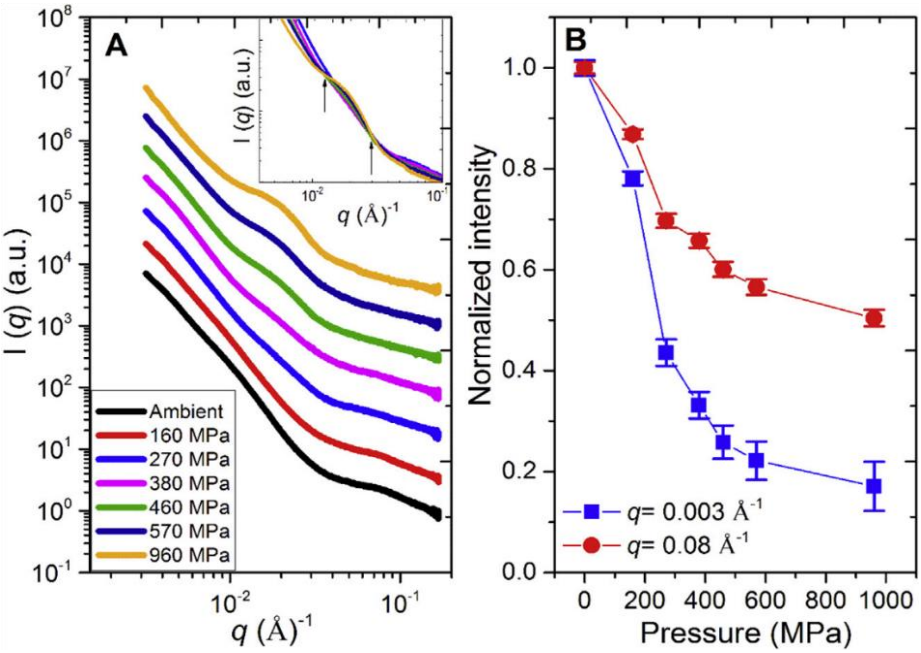

Figure 6. 4. (A) *In-situ* synchrotron SAXS patterns of skim milk solution (10 wt%) under various pressures. Inset: the isosbestic points are indicated by arrows. The scattering curves are vertically shifted for clarity. (B) Normalized scattering intensities at low-*q* (0.003 $Å^{-1}$) and high-*q* (0.08 $Å^{-1}$) with increasing pressures from atmospheric pressure to 960 MPa.

As seen in Figure 6.4 (A), application of HHP impacts the observed scattering patterns greatly. An increase in pressure impacts the power law exponent of -4. This resulted in a peak forming at *q* region of 0.02 $Å^{-1}$, while at the same time the peak at ~0.08 $Å^{-1}$, gradually disappeared. The decrease in normalised scattering intensity as a function of increasing pressure at low (0.003 $Å^{-1}$) and high (0.08 $Å^{-1}$) *q* values is displayed in Figure 6.4B. The HHP induced changes in scattering intensity for both 0.003 $Å^{-1}$ and high 0.08 $Å^{-1}$ are similar, albeit the rate of decrease is greater at 0.003 $Å^{-1}$ than 0.08 $Å^{-1}$. Previous reports have linked the decrease in scattering intensity at $q \sim 0.003$ $Å^{-1}$ to pressure induced disruption of casein micelles (Jackson & McGillivray, 2011; Tromp et al., 2014). The decrease in scattering intensity at $q \sim 0.08$ $Å^{-1}$ has been attributed to the HHP induced solubilisation of the CCP clusters. HHP induced solubilisation of CCP nanoclusters along with disruption of hydrophobic and electrostatic interactions between micelles is largely responsible for disruption of casein micelles under HHP treatment (Huppertz et al., 2006; Needs et al., 2000; Schrader et al., 1997). Hubbard et

al., (2002) also observed similar findings using ^{31}P nuclear magnetic resonance (NMR), whereby an increase in the NMR peak for soluble inorganic phosphate occurred with increased pressure from 100 to 300 MPa indicating gradual solubilisation of CCP as a function of pressure.

The dramatic increase of the scattering peak at ~0.02 $Å^{-1}$ from 460 MPa to 960 MPa could be considered one of the most significant features of the graph as seen in Figure 6.4A. Previous *in-situ* SANS studies of HHP treated casein micelles have also reported this distinctive feature, which has been attributed to the disassociation of casein micelles leading to the creation of "sub-micelles" with a diameter ranging from 20 to 40 nm (Jackson & McGillivray, 2011; Tromp et al., 2014). Needs et al., (2000) also reported similar findings using transmission electron microscopy (TEM), where casein micelles underwent disassociation from 150-200 nm to ~40 nm upon application of 600 MPa pressure for 15 mins. Cryo-TEM analysis of HHP treated milk at 400 MPa at 20 ^{o}C for 20 mins also resulted in smaller casein assemblies with sizes ranging from 30 to 100 nm (Knudsen & Skibsted, 2010). The inset in Figure 6.4 (A) also shows isosbestic points for which all scattering curves, crossed over at q ~0.013 $Å^{-1}$ and q ~0.030 $Å^{-1}$. The presence of one isosbestic point at q ~0.01 $Å^{-1}$ and one of q ~0.019 $Å^{-1}$ have also been reported (Jackson & McGillivray, 2011; Tromp et al., 2014).

The differences in the reported q positions of iso-scattering points as observed in the different studies, could be due to differences in sample preparation and scattering methods. For example, Tromp et al., (2014), incorporated SANS analysis on casein micelles which were free of fat and whey protein and were reconstituted in D_2O. In contrast Jackson & McGillivray, (2011) used skim milk or casein pellets reconstituted in D_2O. Despite the fact that this study used SAXS measurements of skim milk samples reconstituted in H_2O, the presence of these isosbestic points would imply that, the changes in casein micelle ratio would be due to pressure induced disassociation into "sub-micelles". In addition, the fact that there is no change in the peak position at q ~0.020 $Å^{-1}$ (Figure 6.4), would indicate there is no change in "sub-micelle" size with pressure (Tromp et al., 2014). The presence of two isosbestic points at two different q values, could be due to changes in symmetry of scattering objects due to two different factors such as the appearance of "sub-micelles" and the disassociation of CCP nanoclusters under HHP conditions.

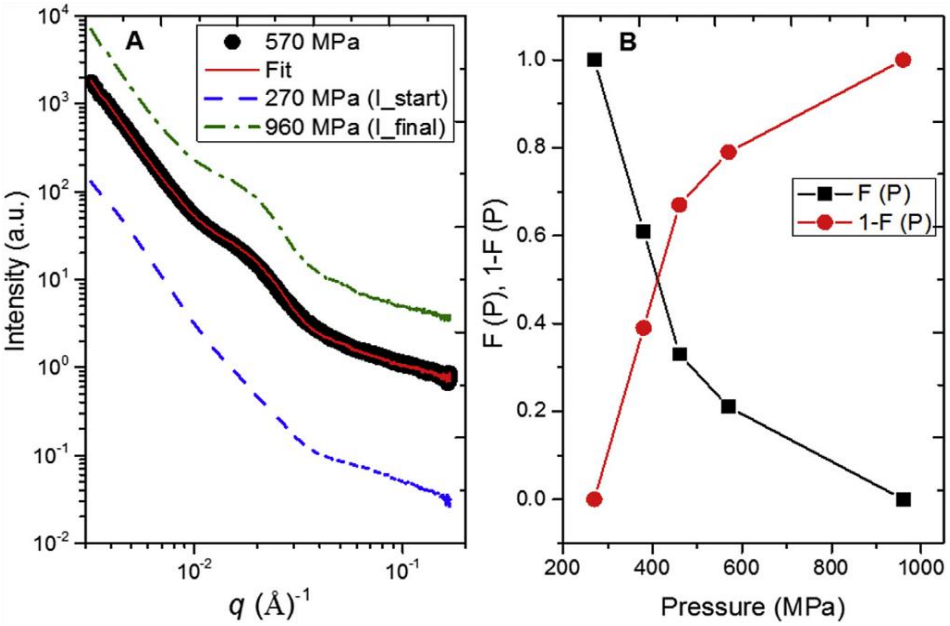

Figure 6. 5. (A) Example of SAXS scattering curve at 570 MPa (black symbol) with fit (solid red line) through two-state analysis using equation (6.1) mentioned below, along with the initial (270 MPa) and final (960 MPa) scattering curves. The scattering curves are vertically shifted for clarity. (B) Fitting parameters F(P) and 1-F(P) plotted as a function of pressure.

Liu et al. (2012) also reported on appearance of two isosbestic points in the SAXS analysis of annealed polymer. The scattering pattern of the HHP induced system has been described as the linear combinations of two constituents (Hirai et al., 1998; Nicolai et al., 2006; Sauter et al., 2016).

$$I(q) = F(P)I_{start}(q) + [1\text{-}F(P)]I_{final}(q) \quad (6.1)$$

$$F(P) = \frac{I - Ifinal}{Istart - Ifinal} \quad (6.2)$$

Where F(P) is the unitless variation of the scattering intensity, $I(q)$ is the scattering intensity of the system, $I_{start}(q)$ is the initial scattering curve showing iso-scattering point at 270 MPa and $I_{final}(q)$ final scattering curve at 960 MPa. The unit for scattering intensities is cm^{-1}. All SAXS scattering curves fit in well within the whole q range with corresponding Chi-square (χ^2) values of 26.3, 11.1 and 8.6 for skim milk under 380 MPa, 460 MPa, and 570 MPa, respectively. Figure 6.5 (A) above shows the scattering intensity fitting for HHP induced milk sample at 570 MPa. The resultant F(P) and 1-F(P) is displayed in Figure 6.5 (B). This analysis indicates that

HHP induced disintegration of casein micelles between 270 and 960 MPa is comprised of two state processes.

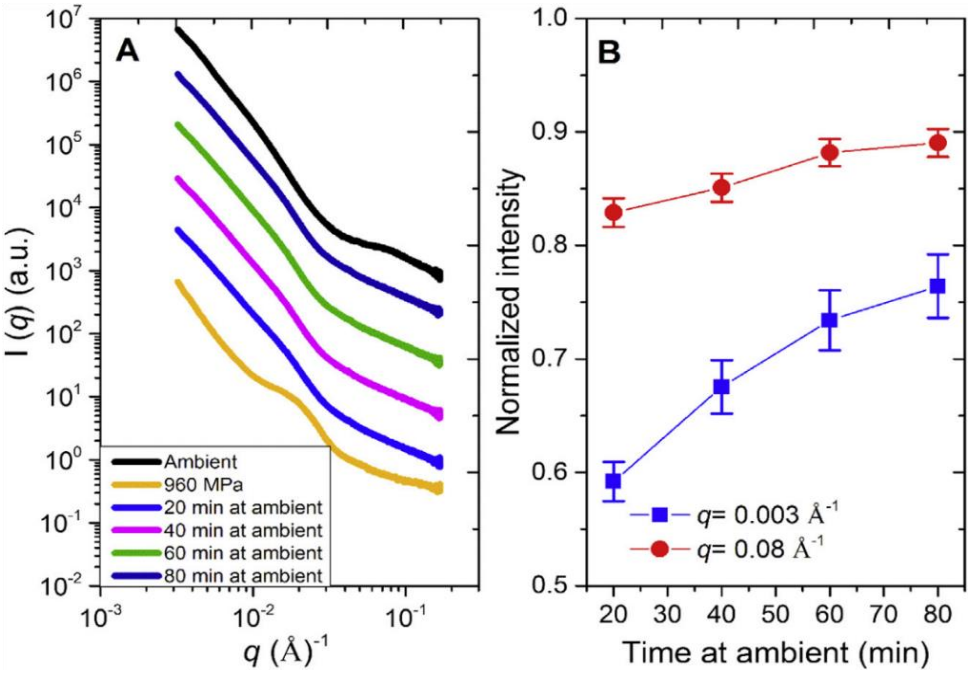

Figure 6. 6. (A) Time-evolution of the SAXS patterns after release of a pressure from 960 MPa to atmospheric pressure. The scattering curves are vertically shifted for clarity. (B) Values of the ambient normalized scattering intensities at low- (0.003 Å1) and high-*q* (0.08 Å1) at different time after pressure release to ambient pressure.

To explore the reversibility of casein disintegration, the high pressure in the DAC was brought back to atmospheric pressure after the measurements of the maximum pressure. To determine relaxation kinetics of the sample, SAXS measurements following pressure release was conducted for a period of up to 80 min. From the results obtained, it was found that within the first 20 mins, rearrangement of the primary structure took place, followed by slight changes in the sample upon further increase in time (Figure 6.6 (A)). To gain further insight on reversible effects, the evolution of the normalized (to the intensity measured under ambient condition) scattering intensity at 0.003 $Å^{-1}$ and 0.08 $Å^{-1}$ are displayed in Figure 6.6 (B). Whilst the scattering intensity did partially return to the original scattering behaviour at ambient pressure, full recovery wasn't observed. Jackson & McGillivray (2011) and Tromp et al. (2014) also reported similar findings in *in-situ* SANS studies of HHP treated casein micelles. It has to be noted that partial dissolution of CCP nanoclusters under HHP conditions has been suggested

to be largely reversible (Huppertz et al., 2002).

In summary, this study demonstrates that at different length scales, pressure does affect casein micelle structural properties, and these HHP induced changes are only partially reversible upon release to ambient pressure over 80 min at least. In addition, the potential use of synchrotron SAXS with a DAC to examine *in-situ* and real time HHP induced structural variation of milk samples has also been demonstrated.

6.3.4. *In-situ* investigation of the change in milks at different pHs using a high-pressure unit fitted with an optical cell

The casein micelles dissociation pressure for three different type of milk was investigated using a High-pressure system with an *in-situ* optical cell. A simple turbidity method using a HeNe laser and a spectrophotometer was implemented. The maximum operating pressure of the system was 700 MPa. In this experiment, two A1A2 milks and one A2 milk were investigated. The milk samples studied were reconstituted at pHs ranging from 5.7 ± 0.1 to 10.5 ± 0.1. During the experiment, the pressure was varied in increments of 5 MPa. Figure 6.7 shows an example of the transmitted intensity as a function of the wavelength for an A1A2 milk obtained from Fonterra at pH 6.7 ± 0.1 for different applied pressures. It could be seen that the transmitted intensity has a peak that occurs at 632.7 ± 0.2 nm which corresponds to the HeNe laser wavelength. Note that a filter was used to select only this wavelength by the detection system. From this example, it can be seen that the maximal transmitted intensity increase as the pressure increases from 170 MPa to 195 MPa but does not change once the pressure applied reaches 195 MPa. This pressure will be defined as the threshold pressure at which this milk is fully dissociated.

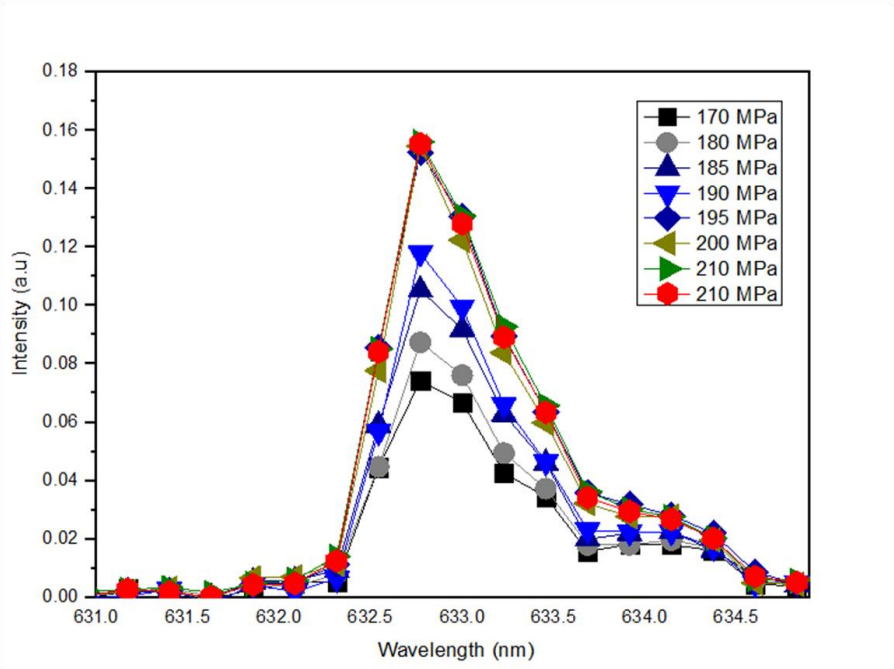

Figure 6. 7. Transmitted intensity as a function of wavelength for A1A2 milk at pH 6.7 for different applied pressures as indicated in the legend in MPa.

While in the previous example (Figure 6.7) the maximum transmitted intensity increases with the pressure, different behaviour of the change in maximal intensity with pressure can be observed for milks at different pHs (Figure 6.8). For example, while milk at pH 5.7 show an increase in maximal transmitted intensity with pressure similarly to the milk at pH 6.7. In contrast, pressurisation of milks under alkaline conditions results in the decrease in the transmitted intensity. This can be explained by the state of the casein micelles under different pHs. At alkaline pHs, the casein micelles dissociate into smaller casein particles, and thus the milk becomes transparent (Lam et al., 2018). In turn, this affects the way light is scattered by these milks. The threshold pressure is defined, as with milk at pH 6.7, the pressure at which there is no longer variation in the maximal transmitted intensity as pressure is increased.

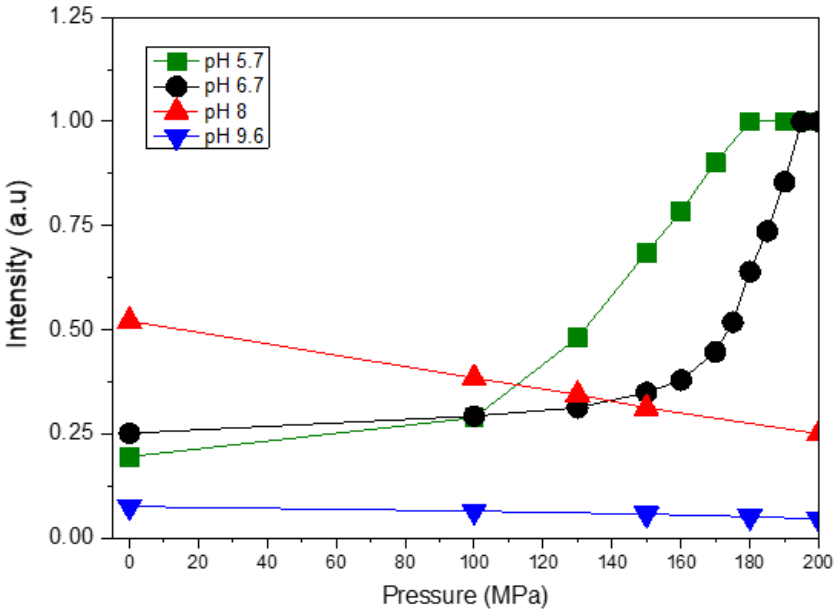

Figure 6. 8. Transmitted maximal intensities as a function of pressure for A1A2 milk at different pHs.

The pressure threshold of the three different milks as a function of initial pH is plotted in Figure 6.9. Firstly, the results show that it is very difficult to discriminate between the three different milks, and that there is no clear difference between the behaviour of A2 milk when compared to A1A2 milks. This is maybe because A1A2 milk also contain a large amount of A2 β-CN. A better experiment would be to compare A2 milk to A1 milk. Unfortunately, we were not able to source during the course of this thesis A1 bovine milk. Secondly, for the three investigated milks, it can be seen that the pressure threshold increases when the pH increases from 5.7 ± 0.1 to 8.7 ± 0.1, then remains constant when the pH is further increased. Note that, the pressure threshold increases linearly from 180 to 195 MPa and from 200 to 250 MPa when the pH increases from 5.7 to 6.5 and from 7.5 to 8.7 respectively. However, the pressure threshold remains nearly constant between 195 and 200 MPa, when the pH increases between 6.5 and 7.5.

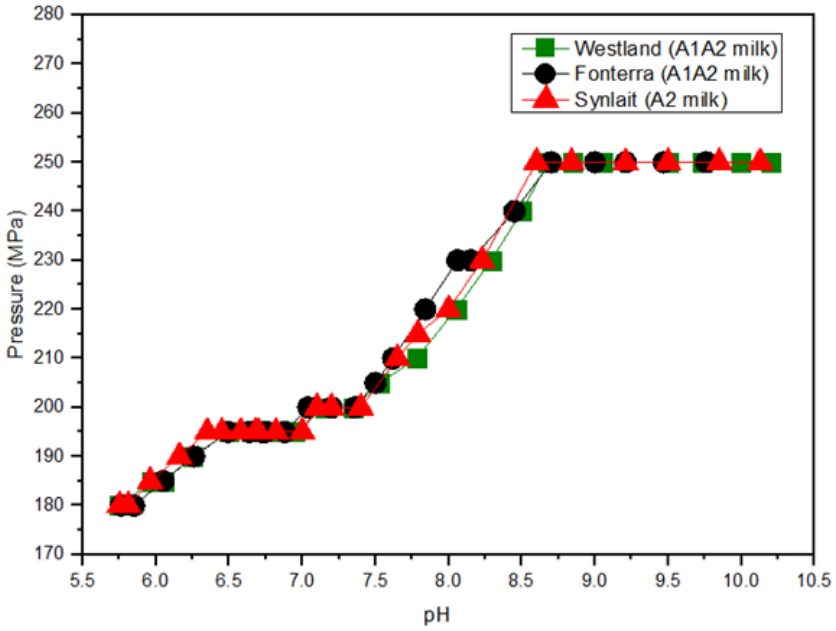

Figure 6. 9. Pressure threshold as a function of A1A2 (Westland, and Fonterra milks) and A2 milk's initial pH.

A similar experimental setup was also used previously to monitor changes in reconstituted skim milk at pH from 5.5 to 7.5 (Orlien et al., 2010). A similar optical high pressure cell (SITEC Sieber Engineering AG, Maur-Zürich, Switzerland) was used, but with a shorter (2 mm) path length and the turbidity was measured at 600 nm. In their work, the authors calculated the turbidity as a function of the applied pressure and defined the pressure threshold as the pressure at which the turbidity reaches a half-value between an initial (at 0.1 MPa) and final (500 MPa) pressures. They reported that the pressure threshold is shifted toward higher pressures when the pH is increased from 5.5 to 7.7, in agreement with this study. However, they reported higher pressure thresholds; for example, 250 MPa in their study and 195 MPa in this work, for milk at pH 6.7. These discrepancies in the values of the values of pressure threshold could be due to the difference in the milks used, and possibly in the difference in path length of the high-pressure cells. Nevertheless, both studies show clearly that the pressure threshold increases with pH and demonstrate the possibility of using a simple experimental setup to monitor change in milk under HHP.

6.4. Summary

This chapter comprises two parts dealing with the effect of HHP on different milk systems. Both parts involve the use of *in-situ* methods. The first part of the work involved using

synchrotron X-ray scattering and a diamond anvil cell to monitor the dissociation of casein micelles at the pressures up to approximately 1 GPa. The measurements demonstrated that the scattering due to the dissociation of the casein micelles showed two isosbestic points indicating that the scattering could be described two state model with two-step process. Further the study also showed that, the casein reassociates rapidly (within 20 min) but not completed upon release of pressure to atmospheric pressure, the casein reassociates within the first 20 min.

In the second part of this chapter a simple turbidity method was used to monitor *in-situ* the intensity of the transmitted light in milks at different pHs subjected to pressures up to 250 MPa. This study showed that firstly there is no evidence that A2 milk behaves differently from A1A2 milk under HHP. Secondly, an increase in the milk initial pH from 5.7 up to 8.7 also resulted in the increase of the pressure threshold from 180 to 250 MPa.

Chapter 7.

Conclusions and Future works

7.1. General Conclusions

Milk and dairy products represent a big part of the global food industry. Therefore, a lot of studies have been performed for understanding the behaviour of their components. A large amount of debates has been raised few years ago on the health benefits of A2 milk containing only A2 β-casein (A2 β-CN) compared to the regular cow's milk containing A1 and A2 β-CN variants. Although, the cost of A2 milk is currently around twice the price of the regular A1A2 milk, many consumers are interested to buy it due to the claimed health benefits. The main focus of this study is to compare some physicochemical properties of A1A2 and A2 milks to determine if they are different when obtain as an ingredient such as SC, or used as product (acid milk gels) or raw milk under pressures.

In ***chapter 4***, sodium caseinates (SCs) extracted from both types A1A2 and A2 milks were used to investigate their physicochemical properties. This study showed that the viscosity of the SC increased, as expected, when the concentration increased, especially when the concentration was >1 wt%. Particle size analysis also showed that the size of SC particles increased with concentration. This is due to the fact that the size was determined based on intensity and that likely some large aggregates formed when the concentration was higher than 1 wt%. The adsorption behaviour of SC onto latex particles showed that SC adsorbs as a layer of approximately 10 nm and that the full surface coverage was approximately 16.5 mg/m^2. These results are in agreement with the published literature (Dalgleish, 1992, Yang & Schoemaker, 1990).

Small angle X-ray scattering (SAXS) showed that the SC particles had approximately a radius of gyration of 7 nm and that the internal structure had protein inhomogeneities of approximately 3 nm. The size of SC particle is nearly 10 folds smaller than that determined by light scattering (diameter of approximately of 70 nm, even at dilute SC concentrations). These discrepancies are likely due to the fact as indicated above of the contribution of the large aggregate in the light scattering measurements. And due to the limit of the lowest q achievable in the SAXS measurements, as these large aggregates cannot be determined.

The most important finding of this study is that all the experimental methods used showed that, within experimental error, there is no differences between SC obtained from A1A2 and A2 milks.

In ***chapter 5*** acid milk gels made from heated and non-heated A1A2 and A2 milks with total solid concentrations from 5 to 20 wt%, were investigated to obtain the dynamic behaviour differences between the milk gels of both type of milks. Set acid milk gels and commercially sourced stirred yoghurts were investigated by diffusing-wave spectroscopy (DWS) coupled with multiple speckle diffusing-wave spectroscopy (MSDWS) for their dynamics from few nanoseconds to several seconds. Both DWS and MSDWS were developed in-house. Acid milk gels proved to be very challenging to measure as they are on one hand non-ergodic (which limits the use of DWS alone). In addition, the structure of those gels evolves with time, making the time at which the measurement is taken very important. Despite these drawbacks, DWS-MSDWS showed the acid milk gels possess a fast (around 2 ms) and a slow (>10 s) relaxation times. The fast relaxation time was assigned to the diffusion of the casein particle within the gel network, while the slow relaxation time was ascribed to the overall dynamic of the gel (i.e. it depends on the overall mechanical properties of the gel). DWS-MSDWS was found to be very adequate in characterising stirred yoghurt, where only a slow relaxation time is observed. The study showed that in the case of stirred yoghurt, this relaxation time is likely dependent of the product of the viscosity by the protein aggregate size. This study was not able to show any clear differences between the dynamic behaviour of the milk gels made from A2 milks and A1A2 milks.

Chapter 6 was dedicated to establishing High Hydrostatic Pressure methods to *in-situ* investigate the effect of pressure on milk system of both types of milk. This chapter was divided to two parts. Firstly, *in-situ* SAXS with a diamond anvil cell (DAC) was used to monitor the dissociation of casein micelles under the pressures up to approximately 1 GPa. As a result of the dissociation of the casein micelles under pressure two isosbestic points were appeared. These indicate that the casein micelle dissociates into “sub-micelles” and to individual casein molecules. In addition, releasing the pressure to the atmospheric pressure causes a partial reassociation of casein structure within the first 20 min. While the potential of the SAXS-DAC method was demonstrated, its application to differentiate between the behaviour of A1A2 and A2 milks was not performed. This is mainly due to the limit in the beamtime time allocated by the Synchrotron.

In the second part of this study, purpose-built apparatus to study of high pressure on milk was set up. This apparatus is made by coupling a simple turbidity measurement system with an HHP unit (up to 700 MPa) having two spectroscopic windows. The effect of HHP on A1A2

and A2 milks with different pHs was carried out. The measurements showed that the change in turbidity was dependent on the pH; with the pressure threshold needed to dissociate the milk increasing from 180 MPa to 250 MPa when the pH increased from 5.7 to 8.7. Further increase in pH up to 11 did not affect the value of the pressure threshold. Here again, this study showed that the dissociation behaviour of A1A2 and A2 milks at different pHs under HHP is the similar.

The overall results of the three chapters presented in this study showed that the physicochemical behaviours of A1A2 and A2 milks, as ingredient (SC) or product (acid milk gel) and under HHP, are very similar. This would indicate that the difference in the amount of A1 β-CN and A2 β-CN in the milks is not high enough to impact marked changes. In fact, LC-MS/MS measurements showed that only a small amount (approximately 10%) of A1 β-CN is present in the A1A2 milks used to prepare SCs.

7.2. Future Works

In the context for the results of this work, some research areas can be considered.

7.2.1 Comparing A2 milk to A1 milk (rather than A1A2 milk to A2 milk)

This study was unable to demonstrate any marked differences in some of the physicochemical behaviour of A1A2 and A2 milks and the SCs obtained from these milks. It is speculated that this likely due to the low amount of A1β-CN present in the A1A2 milk. Ideally this study should compare A2 to A1 milk. Unfortunately, we were unable to source A1 milk. However, the work performed in this study is highly relevant since most of the commercially available milk worldwide is of A1A2 milk.

7.2.2. Improving the DWS-MSDWS setup

The DWS-MSDWS method applied in ***chapter 5*** is a very promising method to investigate milk gels. However, one of the limits was the limit of DWS to study these systems. In the future, it will be important to develop translating or rotating sample holder which will allow averaging spatially the DWS measurement on the sample. This will improve further the accuracy of the DWS-MSDWS technique.

7.2.3. Study the effect of β-CN variant on the physicochemical properties and sensory attributes of model milk products.

The acid milks and SCs made from milks with different β-CN genotypes have been compared in terms of mechanical properties and structural characteristic. However, the physicochemical properties and sensory attributes of other popular dairy products such as cheese and milk protein concentrate (MPC) made from the milks with different β-CN genotypes have not been investigated. Contrary to the yoghurt production, where the casein micelles are aggregated through acidification; during the cheese manufacture, the casein micelles are coagulated due to the action of rennet. MCP is different from milk as it is nearly devoid of lactose. Therefore, this study will enable comparing the stability and coagulation behaviours of casein micelles with different β-CN genotypes under renneting, and the performance of MPC in dairy products. The texture and flavors of the milk product should be also evaluated.

7.2.4 Study the effect of thermal processing on the physicochemical properties and structural characteristics of milks with different β-CN genotypes.

Thermal processing including pasteurization and UHT have been employed extensively in the dairy industry to inactive microorganism and enzymes in milks for extending shelf life. For this reason, it is important to understand the impact of thermal processing on the physicochemical properties, structural characteristics, and digestion behaviours of the milks with different β-CN genotype. It is expected that many significant changes include whey protein aggregation, whey protein-casein micelle complex formation, and solubilization of colloidal calcium phosphate nanocluster may occur during thermal treatment. Until now, the effect of thermal processing on the A2 milk is still scant. Future studies will be conducted to identify whether A1A2 and A2 milks have different susceptibility toward thermal treatment.

7.2.5. Investigate the effect of β-CN variant on the digestion behaviours and nutrients absorption in dairy products including milk, yoghurt and cheese.

The impact of utilizing milks with different β-CN genotype, and the consequences of interactions between the resultant structural assemblies, on digestion still unclear, and as a result nutritional outcome are often poorly understood. In the future studies, digestibility and nutritional absorption of the dairy products made from the milk protein with different β-CN genotype will be evaluated both *in vitro* and *in vivo*. This will provide rigorous scientific

evidence to address key questions about whether different β-CN genotypes could affect the digestion behaviour and the absorption and delivery of nutrients.

7.2.6. In-situ study the milks with different β-CN genotypes under various external stressors

Investigating the structural response of milk proteins to various external stressors such as HHP, high-pressure homogenization, and ultrasonication will help us to understand the structural assemblies and the behaviour of milk under processing conditions. In this thesis, regular A1A2 milk under high hydrostatic pressure was investigated *in-situ using* synchrotron SAXS. It will be interesting to conduct similar study on A2 milk in the future in comparison preferably to A1 milk. This will allow identifying if any differences exist in casein micelles disintegration pattern under HHP between A1 and A2 milk.

7.2.7. Effect of enzymatic and chemical cross-linking on milks with different β-CN genotypes

Enzymatic (transglutaminase) and chemical (genipin) cross linking has been employed to create casein nanogels, which are stable in the presence of calcium chelation agent like EDTA. While the cross-linking on the structure of regular milk is well documented, its effect on the A2 milk has not been studied yet. Future studies can be conducted to confirm whether the cross-linking lead to different structures in A1A2, A1, and A2 milks, and its effect on preserving the integrality of casein micelles against calcium chelation by EDTA.

References

Ahmad, S., Piot, M., Rousseau, F., Grongnet, J. F., & Gaucheron, F. (2009). Physico-chemical changes in casein micelles of buffalo and cow milks as a function of alkalinisation. *Dairy Science & Technology, 89*, 387-403.

Alexander, M., & Dalgleish, D. G. (2005). Interactions between denatured milk serum proteins and casein micelles studied by diffusing wave spectroscopy. *Langmuir, 21*, 11380-11386.

Alexander, M., Piska, I., & Dalgleish, D. G. (2008). Investigation of particle dynamics in gels involving casein micelles: a diffusing wave spectroscopy and rheology approach. *Food Hydrocolloids, 22*, 1124-1134.

Amenu, B., & Deeth, H. (2007). The impact of milk composition on cheddar cheese manufacture. *Australian Journal of Dairy Technology, 62*, 171-184.

Anema, S. G., Lowe, E. K., & Stockmann, R. (2005). Particle size changes and casein solubilisation in high-pressure-treated skim milk. *Food Hydrocolloids, 19*, 257-267.

Atamian, S., Olabi, A., Kebbe Baghdadi, O., & Toufeili, I. (2014). The characterization of the physicochemical and sensory properties of full-fat, reduced-fat and low-fat bovine, caprine, and ovine Greek yoghurt (Labneh). *Food Science & Nutrition, 2*, 164-173.

Augustin, M. A., Oliver, C. M., & Hemar, Y. (2011). Casein, caseinates, and milk protein concentrates. R. C. Chandan & A. Kilara, Ed. Wiley-Blackwell: *In Dairy Ingredients for Food Processing*; pp161-178.

Badem, A., & Uçar, G. (2017). Production of caseins and their usages. *International Journal of Food Science and Nutrition, 2*, 4-9.

Balny, C., & Masson, P. (1993). Effects of high pressure on proteins. *Food Reviews International, 9*, 611-628.

Beaucage. (1995). Approximations leading to a unified exponential/power-law approach to small-angle scattering. *Journal of Applied Crystallography, 28*, 717-728.

Beaucage. (1996). Small-angle scattering from polymeric mass fractals of arbitrary mass-fractal dimension. *Journal of Applied Crystallography, 29*, 134-146.

Boonyaratanakornkit, B. B., Park, C. B., & Clark, D. S. (2002). Pressure effects on intra- and intermolecular interactions within proteins. *Biochim Biophys Acta, 1595*, 235-249.

Bouchoux, A., Gésan-Guiziou, G., Pérez, J., & Cabane, B. (2010). How to Squeeze a Sponge: Casein Micelles under Osmotic Stress, a SAXS Study. *Biophysical Journal, 99*, 3754-3762.

Brew, K. (2013). α-Lactalbumin. In P. L. H. McSweeney & P. F. Fox (Eds.), *Advanced Dairy Chemistry: Volume 1A: Proteins: Basic Aspects, 4th Edition*, pp. 261-273. Boston, MA: Springer US.

Bridgman, P. W. (1914). The coagulation of albumen by pressure. *Journal of Biological Chemistry, 19*, 511-512.

Broyard, C., & Gaucheron, F. (2015). Modifications of structures and functions of caseins: a scientific and technological challenge. *Dairy Science & Technology, 95*, 831-862.

Caroli, A. M., Savino, S., Bulgari, O., & Monti, E. (2016). Detecting beta-Casein Variation in Bovine Milk. *Molecules, 21*, 141.

Carr, A., & Golding, M. (2016). Functional milk proteins production and utilization: casein-Based Ingredients. In P. L. H. McSweeney & J. A. O'Mahony (Eds.), *Advanced Dairy Chemistry: Volume 1B: Proteins: Applied Aspects*, pp. 35-66. New York, NY: Springer. New York.

Chandan, R. (1997). CHAPTER 1: Properties of Milk and its components. *Dairy-Based Ingredients*, pp. 1-10. American Association of Cereal Chemists.

Chandan, R. C., & Kilara, A. (2011). Fermented dairy ingredients. *Dairy ingredients for food processing. (Eds)*. Wiley-Blackwell, Oxford, UK.

Chawla, R., Patil, G. R., & Singh, A. K. (2011). High hydrostatic pressure technology in dairy processing: a review. *Journal of Food Science And Technology, 48*, 260-268.

Cheftel, J. C. (1992). Effects of high hydrostatic pressure on food constituents: an overview. *High Pressure Biotechnology*, 195-209.

Chen, B., Grandison, A. S., & Lewis, M. J. (2017). Best use for milk - a review I-effect of breed variations on the physicochemical properties of bovine milk. *International Journal of Dairy Technology, 70*, 3-15.

Chu, B., Zhou, Z., Wu, G., & Farrell, H. M. J. (1995). Laser light scattering model casein solutions: Effect of high temperature. *Journal of Colloid & Interface Science, 170*, 102-112.

Cintineo, H. P., Arent, M. A., Antonio, J., & Arent, S. M. (2018). Effects of protein supplementation on performance and recovery in resistance and endurance training. *Frontiers in Nutrition, 5*, 83.

Creamer, L. K., Loveday, S. M., & Sawyer, L. (2011). Milk proteins | β-lactoglobulin. *Encyclopedia of Dairy Sciences (2nd ed)*, 787-794.

Creamer, L. K., Plowman, J. E., Liddell, M. J., Smith, M. H., & Hill, J. P. (1998). Micelle stability: kappa-casein structure and function. *Journal of Dairy Sciences, 81*, 3004-

3012.

Cucheval, A., Vincent, R. R., Hemar, Y., Otter, D., & Williams, M. A. K. (2009). Diffusing wave spectroscopy investigations of acid milk gels containing pectin. *Colloid and Polymer Science, 287*, 695-704.

Cucheval, A. S. B., Vincent, R. R., Hemar, Y., Otter, D., & Williams, M. A. K. (2009). Multiple particle tracking investigations of acid milk gels using tracer particles with designed surface chemistries and comparison with Diffusing Wave Spectroscopy studies. *Langmuir, 25*, 11827-11834.

Dalgleish, D. G. (1992). The size and conformations of the proteins in adsorbed layers of individual caseins on lattices and in oil-in-water emulsions. colloids and surfaces b. *Biointerfaces, 1*, 1-8.

Dalgleish, D., Alexander, M., & Corredig, M. (2004). Studies of the acid gelation of milk using ultrasonic spectroscopy and diffusing wave spectroscopy. *Food Hydrocolloids, 18*, 747-755.

Dalgleish, D. G., & Corredig, M. (2012). The structure of the casein micelle of milk and its changes during processing. *Annual Review of Food Science and Technology, 3,* 449-467.

Dalgleish, D. G., & Law, A. J. R. (1989). pH-Induced dissociation of bovine casein micelles. II. Mineral solubilization and its relation to casein release. *Journal of Dairy Research, 56*, 727-735.

Dalgleish, D. G., Spagnuolo, P. A., & Goff, H. D. (2004). A possible structure of the casein micelle based on high-resolution field-emission scanning electron microscopy. *International Dairy Journal, 14*, 1025-1031.

Darewicz, M., & Dziuba, J. (2007). Formation and stabilization of emulsion with A1, A2 and B β-casein genetic variants. *European Food Research and Technology, 226*, 147-152.

Day, L., Raynes, J. K., Leis, A., Liu, L. H., & Williams, R. P. W. (2017). Probing the internal and external micelle structures of differently sized casein micelles from individual cows milk by dynamic light and small-angle X-ray scattering. *Food Hydrocolloids, 6*9, 150-163.

De Kruif, C. (2014). The structure of casein micelles: a review of small-angle scattering data. *Journal of Applied Crystallography, 47,* 1479-1489.

de Kruif, C. G. (1998). Supra-aggregates of Casein Micelles as a Prelude to Coagulation. *Journal of Dairy Science, 81*, 3019-3028.

de Kruif, C. (1999). Casein micelle interactions. *International Dairy Journal, 9,* 183-188.

de Kruif, C., and Holt, C. (2003). Casein micelle structure, functions and interactions. *In* "Advanced Dairy Chemistry: Proteins" (P. F. Fox and P. L. H. McSweeney, eds.), Vol. 1, pp. 233-276. Academic/Plenum Publishers, New York.

de Kruif, C. G., Huppertz, T., Urban, V. S., & Petukhov, A. V. (2012). Casein micelles and their internal structure. *Advances in Colloid and Interface Science, 171-172,* 36-52.

Dickinson, E, Golding, M, & Povey, M. J. W. (1997). Creaming and Flocculation of Oil-in-Water Emulsions Containing Sodium Caseinate. *Journal of Colloid & Interface Science, 185,* 515-529.

Donato, L., Alexander, M., & Dalgleish, D. G. (2007). Acid gelation in heated and unheated milks: Interactions between serum protein complexes and the surfaces of casein micelles. *Journal of Agricultural and Food Chemistry, 55,* 4160-4168.

Du, J., & Yarema, K. J. (2010). Carbohydrate Engineered Cells for Regenerative Medicine. *Advanced Drug Delivery Reviews, 62,* 671-682.

Ehssein, C. O., Serfaty, S., Griesmar, P., Caplain, E., Martinez, L., & Gindre, M. (2004, 23-27 Aug. 2004). Kinetic reaction monitoring of acidified milk gels with a quartz resonator: effect of temperature and GDL quantities. *Paper Presented at The IEEE Ultrasonics Symposium, 50th Conf, 2004, 1,* 319-322.

FAO. (2013). Milk and Milk products. *In Food outlook 2013*. Retrieved 2017, from http://www.milkproduction.com/Library/Editorial-articles/FAO-Food-Outlook-Nov-2013---Milk-and-Milk-products.

Faizullin, D. A., Konnova, T. A., Haertlé, T., & Zuev, Y. F. (2017). Secondary structure and colloidal stability of beta-casein in microheterogeneous water-ethanol solutions. *Food Hydrocolloids, 63,* 349-355.

Famelart, M. H., Le, N. H. T., Croguennec, T., & Rousseau, F. (2013). Are disulphide bonds formed during acid gelation of preheated milk?. *International Journal of Food Science and Technology, 48,* 1940-1948.

Farrer, D., & Lips, A. (1999). On the self-assembly of sodium caseinate. *International Dairy Journal, 9,* 281-286.

Farrell, H. M., Kumosinski, T. F., Malin, E. L., & Brown, E. M. (2002). The caseins of milk as calcium-binding proteins. In H. J. Vogel (Ed.), *Calcium-Binding Protein Protocols: Volume 1: Reviews and Case Studies,* pp. 97-140. Totowa, NJ: Humana Press.

Funtenberger, S., Dumay, E., & Cheftel, J. C. (1997). High pressure promotes β-lactoglobulin aggregation through SH/S−S interchange reactions. *Journal of Agricultural and Food Chemistry, 45,* 912-921.

Fox, P. F., & Brodkorb, A. (2008). The casein micelle: historical aspects, current concepts and significance. *International Dairy Journal, 18,* 677-684.

Fox, P. F., Guinee, T. P., Cogan, T. M., & McSweeney, P. L. H. (2017). Chemistry of milk Constituents. *Fundamentals of Cheese Science*, pp. 71-104. Boston, MA: Springer US.

Fox, P.F. and McSweeney, P.L.H. (1998). *Dairy Chemistry and Biochemistry*, Chapman & Hall, London.

Fox, P. F., & McSweeney, P. L. H. (2003). Milk proteins: General and historical aspects. *Advanced Dairy Chemistry.Vol. 1: Proteins. 3rd ed*., pp. 1–48.

Fox, P. F., & Mulvihill, D. M. (1982). Milk proteins: molecular, colloidal and functional properties. *Journal of Dairy Research, 49,* 679-693.

Fox, P. F., Uniacke-Lowe, T., McSweeney, P. L. H., & O'Mahony, J. A. (2015). Heat-Induced Changes in Milk, *Dairy Chemistry and Biochemistry*, pp. 345-375. Cham: Springer International Publishing.

Gamari, B. D., Zhang, D. W., Buckman, R. E., Milas, P., Denker, J. S., Chen, H., Li, H., & Goldner, L. S. (2014). Inexpensive electronics and software for photon statistics and correlation spectroscopy. *American Journal of Physics, 82*, 712-722.

García-Descalzo, L., García-López, E., Alcázar, A., Baquero, F., & Cid, C. (2012). Gel Electrophoresis of Proteins, *Gel Electrophoresis–Principles and Basics. In S. Magdeldin Ed.,* pp. 69-88. Croatia: InTech.

Garcia-Risco, M. R., Olano, A., Ramos, M., & Lopez-Fandino, R. (2000). Micellar changes induced by high pressure. influence in the proteolytic activity and organoleptic properties of milk. *Journal of Dairy Science, 83,* 2184-2189.

Gaucheron, F. (2005). The minerals of milk. *Reprodution Nutrition Development, 45*,473-483.

Gaucheron, F., Famelart, M. H., Mariette, F., Raulot, K., Michela, F., & Le Graeta, Y. (1997). Combined effects of temperature and high-pressure treatments on physicochemical characteristics of skim milk. *Food Chemistry, 59,* 439-447.

Gekko, K., & Hasegawa, Y. (1989). Effect of temperature on the compressibility of native globular proteins. *The Journal of Physical Chemistry, 93,* 426-429.

Gervilla, R., Ferragut, V., & Guamis, B. (2006). High hydrostatic pressure effects on color and milk-fat globule of ewe's milk. *Journal of Food Science, 66*, 880-885.

Gerosa, S., & Skoet, J. (2012). Milk availability: trends in production and demand and medium-term outlook. *FAO Corporate Document Repository, 12,* 1-40.

Goldenberg, D. P., & Argyle, B. (2014). Self crowding of globular proteins studied by small-angle x-ray scattering. *Biophysical Journal, 106,* 895-904.

Grygorczyk, A., Alexander, M., & Corredig, M. (2013). Combined acid- and rennet-induced gelation of a mixed soya milk-cow's milk system. *International Journal of Food Science and Technology, 48,* 2306-2314.

HadjSadok, A., Pitkowski, A., Nicolai, T., BEnyahia, L., & Moulai-Mostefa, N. (2008). Characterisation of sodium caseinate as a function of ionic strength, pH and temperature using static and dynamic light scattering. *Food Hydrocolloids, 22,* 1460-1466.

Hammouda, B. (2010). Probing nanoscale structures-the SANS toolbox. *National Institute of Standards and Technology Center for Neutron Research Gaithersburg,* MD 20899-6102.

Harding, F. (1995). *Adulteration of milk. In F. Harding (Ed.), Milk Quality,* pp. 60-74. Boston, MA: Springer US.

Haug, A., Høstmark, A. T., & Harstad, O. M. (2007). Bovine milk in human nutrition – a review. *Lipids in Health and Disease, 6*, 25.

He, J., Han, Y. M., Liu, M., Wang, Y. N., Yang, Y., & Yang, X. J. (2019). Effect of 2 types of resistant starches on the quality of yoghurt. *Journal of Dairy Science, 102*, 3956-3964.

Hemar, Y., Hebraud, P., Sarcia, R., & Pinder, D. N. (2004). Diffusing-wave spectroscopy of gelling dairy systems. In M. Tokuyama & I. Oppenheim (Eds.), *Slow Dynamics in Complex Systems.Vol. 708,* pp. 434-435. Melville: Amer Inst Physics.

Hemar, Y., Law, A. J. R., Horne, D. S., & Leaver, J. (2000). Rheological investigations of alkaline-induced gelation of skimmed milk and reconstituted skimmed milk concentrates. *Food Hydrocolloids, 14*, 197-201.

Hemar, Y., Pinder, D. N., Hunter, R. J., Singh, H., Hebraud, P., & Horne, D. S. (2003). Monitoring of flocculation and creaming of sodium-caseinate-stabilized emulsions using diffusing-wave spectroscopy. *Journal of Colloid and Interface Science, 264,* 502-508.

Hemar, Y., Singh, H., & Horne, D. S. (2004). Determination of early stages of rennet-induced aggregation of casein micelles by diffusing wave spectroscopy and rheological measurements. *Current Applied Physics, 4,* 362-365.

Hirai, M., Arai, S., Iwase, H., & Takizawa, T. (1998). Small-Angle X-ray Scattering and Calorimetric Studies of Thermal Conformational Change of Lysozyme Depending on pH. *The Journal of Physical Chemistry B, 102*, 1308-1313.

Hite, B. H. (1899). *The effect of pressure in the preservation of milk : a preliminary report.* Morgantown, W.V.: West Virginia Agricultural Experiment Station.

Holt, C., De Kruif, C., Tuinier, R., & Timmins, P. (2003). Substructure of bovine casein micelles by small-angle X-ray and neutron scattering. *Colloids and Surfaces A: Physicochemical and Engineering Aspects, 213*, 275-284.

Horne, D. S. (2003). Casein micelles as hard spheres: limitations of the model in acidified gel formation. *Colloids and Surfaces A: Physicochemical and Engineering Aspects, 213*, 255-263.

Horne, D. (2006). Casein micelle structure: Models and muddles. *Current Opinion in Colloid & Interface Science, 11*, 148-153.

Horne, D. S. (1998). Casein interactions: Casting light on the black boxes, the structure in dairy products. *International Dairy Journal, 8*, 171-177.

Horne, D. S. (1999). Formation and structure of acidified milk gels. *International Dairy Journal, 9*, 261-268.

Horne, D. S. (2002). Casein structure, self-assembly and gelation. *Current Opinion in Colloid and Interface Science, 7*, 456–461.

Horne, D. S. (2006). Casein micelle structure: Models and muddles. *Current Opinion in Colloid & Interface Science, 11*, 148-153.

Horne, D. S. (2011). Milk Proteins | Casein, Micellar Structure. *In Encyclopedia of Dairy Sciences (2nd ed.)*, pp. 772-779. Elsevier, Oxford.

Horne, D. S. (2014). Chapter 6 - Casein Micelle Structure and Stability. In H. Singh, M. Boland & A. Thompson (Eds.), *Milk Proteins (Second Edition)*, pp. 169-200. San Diego: Academic Press.

Hubbard, C. D., Caswell, D., Lüdemann, H. D., & Arnold, M. (2002). Characterisation of pressure-treated skimmed milk powder dispersions: application of NMR spectroscopy. *Journal of The Science of Food and Agriculture, 82*, 1107-1114.

Huppertz, T., Fox, P. F., & Kelly, A. L. (2018). 3 - The caseins: Structure, stability, and functionality. In R. Y. Yada (Ed.), *Proteins in Food Processing (Second Edition)*, pp. 49-92. Woodhead Publishing.

Huppertz, T., Fox, P. F., & Kelly, A. L. (2004). Properties of casein micelles in high pressure-treated bovine milk. *Food Chemistry, 87*, 103-110.

Huppertz, T., Fox, P. F., de Kruif, K. G., & Kelly, A. L. (2006). High pressure-induced changes in bovine milk proteins: a review. *Biochim Biophys Acta, 1764*, 593-598.

Huppertz, T., Fox, P. F., & Kelly, A. L. (2004a). High pressure-induced denaturation of alpha-lactalbumin and beta-lactoglobulin in bovine milk and whey: a possible mechanism. *Journal of Dairy Research, 71*, 489-495.

Huppertz, T., Fox, P. F., & Kelly, A. L. (2004a). High pressure treatment of bovine milk: effects on casein micelles and whey proteins. *Journal of Dairy Research, 71,* 97-106.

Huppertz, T., Fox, P. F., & Kelly, A. L. (2004b). Properties of casein micelles in high pressure-treated bovine milk. *Food Chemistry, 87,* 103-110.

Huppertz, T., Kelly, A. L., & de Kruif, C. G. (2006). Disruption and reassociation of casein micelles under high pressure. *Journal of Dairy Research, 73,* 294-298.

Huppertz, T., Kelly, A. L., & Fox, P. F. (2002). Effects of high pressure on constituents and properties of milk. *International Dairy Journal, 12,* 561-572.

Inagaki, M., Kawai, S., Ijier, X., Fukuoka, M., Yabe, T., Iwamoto, S., & Kanamaru, Y. (2017). Effects of heat treatment on conformation and cell growth activity of alpha-lactalbumin and beta-lactoglobulin from market milk. *Biomedical Research, 38,* 53-59.

Ingham, B., Erlangga, G. D., Smialowska, A., Kirby, N. M., Wang, C., Matia-Merino, L., Haverkamp, R. G., & Carr, A. J. (2015). Solving the mystery of the internal structure of casein micelles. *Soft Matter, 11,* 2723-2725.

Ingham, B., Smialowska, A., Erlangga, G. D., Matia-Merino, L., Kirby, N., Wang, C., Haverkamp, R. G., & Carr, A. (2016). Revisiting the interpretation of casein micelle SAXS data. *Soft Matter, 12,* 6937-6953.

Ion-Titapiccolo, G., Alexander, M., & Corredig, M. (2013). Heating of milk before or after homogenization changes its coagulation behaviour during acidification. *Food Biophysics, 8,* 81-89.

Jackson, A. J., & McGillivray, D. J. (2011). Protein aggregate structure under high pressure. *Chemical Communications, 47,* 487-489.

Jenness, R., Marth, E.H., Wong, N.P., Keeney, M., 1988. Fundamentals of dairy chemistry. Van Nostrand Reinhold, New York, New York, USA.

Jenkins, T. C., & McGuire, M. A. (2006). Major advances in nutrition: impact on milk composition. *Journal of Dairy Science, 89,* 1302-1310.

Jensen, H. B., Holland, J. W., Poulsen, N. A., & Larsen, L. B. (2012). Milk protein genetic variants and isoforms identified in bovine milk representing extremes in coagulation properties. *Journal of Dairy Science, 95,* 2891-2903.

Jensen, R. G., & Pitas, R. E. (1976). Milk Lipoprotein Lipases: A Review1. *Journal of Dairy Science, 59,* 1203-1214.

Johnston, D. E., Austin, B. A., & Murphy, R. J. (1992). Effects of High Hydrostatic-Pressure on Milk. *Milchwissenschaft-Milk Science International, 47,* 760-763

Johnston, D. E., Murphy, R. J., & Birksl, A. W. (1994). Stirred-style yoghurt-type product prepared from pressure treated skim-milk. *High Pressure Research, 12,* 215-219.

Kamiński, S., Cieślińska, A., & Kostyra, E. (2007). Polymorphism of bovine beta-casein and its potential effect on human health. *Journal of Applied Genetics, 48,* 189-198.

Khwaldia, K., Banon, S., Perez, C., & Desobry, S. (2004). Properties of Sodium Caseinate Film-Forming Dispersions and Films. *Journal of Dairy Science, 87,* 2011-2016.

Kitts, D. D. (2005). Antioxidant properties of casein-phosphopeptides. *Trends in Food Science & Technology, 16,* 549-554.

Knudsen, J. C., & Skibsted, L. H. (2010). High pressure effects on the structure of casein micelles in milk as studied by cryo-transmission electron microscopy. *Food Chemistry, 119,* 202-208.

Kumosinski, T. F., Pessen, H., Farrell Jr, H. M., & Brumberger, H. (1988). Determination of the quaternary structural states of bovine casein by small-angle X-ray scattering: submicellar and micellar forms. *Archives of Biochemistry and Biophysics, 266,* 548-561.

Laemmli, U. K. (1970). Cleavage of Structural Proteins during the Assembly of the Head of Bacteriophage T4. *Nature, 227,* 680-685.

Lam, E., McKinnon, I., Marchesseau, S., Otter, D., Zhou, P., & Hemar, Y. (2018). The effect of transglutaminase on reconstituted skim milks at alkaline pH. *Food Hydrocolloids, 85,* 10-20.

Lau, F. (2010). *Biotechnology in Functional Foods and Nutraceuticals.* United States, America: Taylor and Francis Group.

Lee, W. J., & Lucey, J. A. (2010). Formation and Physical Properties of Yoghurt. Asian-Australas *Journal of Animal Science, 23,* 1127-1136.

Li, Z., Yang, Z., Otter, D., Rehm, C., Li, N., Zhou, P., & Hemar, Y. (2018). Rheological and structural properties of coagulated milks reconstituted in D 2 O: Comparison between rennet and a tamarillo enzyme (tamarillin). *Food Hydrocolloids, 79,* 170-178.

Liu, Y., & Guo, R. (2008). pH-dependent structures and properties of casein micelles. *Biophysical Chemistry, 136,* 67-73.

Liu, Y., Horan, J. L., Schlichting, G. J., Caire, B. R., Liberatore, M. W., Hamrock, S. J., Gregory, G. M., Yandrasits, M. A, Seifert. S., & Herring, A. M. (2012). A Small-Angle X-ray Scattering Study of the Development of Morphology in Films Formed from the 3M Perfluorinated Sulfonic Acid Ionomer. *Macromolecules, 45,* 7495-7503.

Lopez-Fandino, R. (2006). Functional improvement of milk whey proteins induced by high

hydrostatic pressure. *Critical Reviews in Food Science and Nutrition, 46,* 351-363.

Lopez-Fandiño, R., Carrascosa, A. V., & Olano, A. (1996). The effects of high pressure on whey protein denaturation and cheese-making properties of raw milk. *Journal of Dairy Science, 79,* 929-936.

López-Fandiño, R., & Olano, A. (1999). Review: Selected indicators of the quality of thermal processed milk / Revisión: Indicadores seleccionados para el control de calidad de la leche tratada térmicamente. *Food Science and Technology International, 5,* 121-137.

Lucey, J. A. (2016). Acid Coagulation of Milk. In P. L. H. McSweeney & J. A. O'Mahony (Eds.), *Advanced Dairy Chemistry: Volume 1B: Proteins: Applied Aspects,* pp. 309-328. New York, NY: Springer New York.

Lucey, J. A., Srinivasan, M., Singh, H., & Munro, P. A. (2000). Characterization of commercial and experimental sodium caseinates by multiangle laser light scattering and size-exclusion chromatography. *Journal of Agricultural and Food Chemistry, 48,* 1610-1616.

Lucey, J. A., Tamehana, M., Singh, H., & Munro, P. A. (1998). A comparison of the formation, rheological properties and microstructure of acid milk gels made with a bacterial culture or glucono - lactone. *Food Research International, 31,* 147-155.

Madadlou, A., Mousavi, M. E., Emam-Djomeh, Z., Sheehan, D., & Ehsani, M. (2009). Alkaline pH does not disrupt re-assembled casein micelles. *Food Chemistry, 116,* 929-932.

Marchin, S., Putaux, J. L., Pignon, F., & Leonil, J. (2007). Effects of the environmental factors on the casein micelle structure studied by cryo transmission electron microscopy and small-angle x-ray scattering/ultrasmall-angle x-ray scattering. *Journal of Chemical Physics, 126,* 045101.

Marciniak, A., Suwal, S., Britten, M., Pouliot, Y., & Doyen, A. (2018). The use of high hydrostatic pressure to modulate milk protein interactions for the production of an alpha-lactalbumin enriched-fraction. *Green Chemistry, 20,* 515-524.

Mata, J. P., Udabage, P., & Gilbert, E. P. (2011). Structure of casein micelles in milk protein concentrate powders viasmall angle X-ray scattering. *Soft Matter, 7,* 3837-3843.

Miluchová M., Gábor, M., Trakovická, A., Hanusová, J. (2016). Bovine beta casein A1 variant as risk factor for human health. *Acta fytotechnica et Zootechnica, 19,* 48-51.

Morisawa, Y., Kitamura, A., Ujihara, T., Zushi, N., Kuzume, K., Shimanouchi, Y., Tamura, S., Wakiguchi, H., Saito, H., Matsumoto, K. (2009). Effect of heat treatment and enzymatic digestion on the B cell epitopes of cow's milk proteins. *Clinical & Experimental Allergy, 39,* 918-925.

Mozhaev, V. V., Heremans, K., Frank, J., Masson, P., & Balny, C. (1996). High pressure effects on protein structure and function. *Proteins, 24,* 81-91.

Mulvihill, D. M. Production, functional properties and utilisation of milk protein products. *In Advanced Dairy Chemistry - 1 Proteins; Fox, P. F., Ed.; Elsevier Applied Science: London, 1992*. pp 369-401.

Nagasawa, D., Azuma, T., Noguchi, H., Uosaki, K., & Takai, M. (2015). Role of interfacial water in protein adsorption onto polymer brushes as studied by SFG spectroscopy and QCM. *The Journal of Physical Chemistry C, 119,* 17193-17201.

Naik, L. (2013). Application of High pressure processing technology for dairy food preservation - future perspective: a review. *Journal of Animal Production Advances, 3,* 232-241.

Nash, W., Oinder, D. N., Hemar, Y. & Singh, H. (2002). Dynamic light scattering investigation of sodium caseinate and xanthan mixtures. *International Journal of Biological Macromolecules, 30,* 269-271.

Needs, E. C., Capellas, M., Bland, P. A., Manoj, P., Macdougal, D., & Paul, G. (2000). Comparison of heat and pressure treatments of skim milk, fortified with whey protein concentrate, for set yoghurt preparation: effects on milk proteins and gel structure. *Journal of Dairy Research, 67,* 329-348.

Needs, E. C., Stenning, R. A., Gill, A. L., Ferragut, V., & Rich, G. T. (2000). High-pressure treatment of milk: effects on casein micelle structure and on enzymic coagulation. *Journal of Dairy Research, 67,* 31-42.

Nicolai, T., Pouzot, M., Durand, D., Weijers, M., & Visschers, R. W. (2006). Iso-scattering points during heat-induced aggregation and gelation of globular proteins indicating micro-phase separation. *EPL (Europhysics Letters), 73,* 299.

Nielsen, S., Toft, K., Snakenborg, D., Jeppesen, M. G., Jacobsen, J., Vestergaard, B., Arleth, L., Nordisk, N., Denmark, S. (2009). BioXTAS RAW, a software program for high-throughput automated small-angle X-ray scattering data reduction and preliminary analysis. *Journal of Applied Crystallography, 42,* 959-964.

Nguyen, D. D., Busetti, F., & Solah, V. A. (2017). Chapter 21 - Beta-Casomorphins in Yoghurt. In N. P. Shah (Ed.), *Yoghurt in Health and Disease Prevention* (pp. 373-386): Academic Press.

Nguyen, H. T. H., Schwendel, H., Harland, D., & Day, L. (2018). Differences in the yoghurt gel microstructure and physicochemical properties of bovine milk containing A1A1 and A2A2 β-casein phenotypes. *Food Research International, 112,* 217-224.

O'Connor, C. B. (1994). Rural dairy technology. ILRI training manual No.1. *International Livestock Research Institute (ILRI),* Addis Ababa, Ethiopia.133.

Orlien, V., Boserup, L., & Olsen, K. (2010). Casein micelle dissociation in skim milk during high-pressure treatment: Effects of pressure, pH, and temperature. *Journal of Dairy Science, 93,* 12-18.

Othman, O. E., El-Fiky, S. A., Hassan, N. A., Mahfouz, E. R., & Balabel, E. A. (2013). Genetic polymorphism detection of two α-Casein genes in three Egyptian sheep breeds. *Journal of Genetic Engineering and Biotechnology, 11,* 129-134.

Patel, H. A., & Creamer, L. K. (2008). Chapter 7 - High-pressure-induced interactions involving whey proteins. In A. Thompson, M. Boland & H. Singh (Eds*.), Milk Protein*. pp. 205-238. San Diego: Academic Press.

Pal, S., Woodford, K., Kukuljan, S., & Ho, S. (2015). Milk intolerance, beta-casein and lactose. *Nutrients, 7,* 7285-7297.

Pedersen, J. S. (1994). Determination of size distribution from small-angle scattering data for systems with effective hard-sphere interactions. *Journal of Applied Crystallography, 27,* 595-608.

Pedersen, J. S. (1997). Analysis of small-angle scattering data from colloids and polymer solutions: modeling and least-squares fitting. *Advances in Colloid and Interface Science, 70,* 171-210.

Permyakov, E. A., & Berliner, L. J. (2000). Alpha-Lactalbumin: structure and function. *FEBS Letters, 473,* 269-274.

Phadungath, C. (2005). Casein micelle structure: a concise review. *Songklanakarin Journal of Science and Technology (SJST), 7,* 201-212.

Philippe, M., Gaucheron, F., Le Graet, Y., Michel, F., & Garem, A. (2003). Physicochemical characterization of calcium-supplemented skim milk. *Le lait, 83,* 45-59.

Piermarini, G. J., Block, S., Barnett, J. D., & Forman, R. A. (1975). Calibration of the pressure dependence of the R1 ruby fluorescence line to 195 kbar. *Journal of Applied Physics, 46,* 2774-2780.

Pitkowski, A., Durand, D., & Nicolai, T. (2008). Structure and dynamical mechanical properties of suspensions of sodium caseinate. *Journal of colloid and interface science, 326,* 96-102.

Post, A. E., Arnold, B., Weiss, J., & Hinrichs, J. (2012). Effect of temperature and pH on the solubility of caseins: environmental influences on the dissociation of alpha(S)- and beta-casein. *Journal of Dairy Science, 95,* 1603-1616.

Poulsen, N. A., Bertelsen, H. P., Jensen, H. B., Gustavsson, F., Glantz, M., Mansson, H. L., Andren, A., Paulsson, M., Bendixen, C., Buitenhuis, A. J., Larsen, L. B. (2013). The occurrence of noncoagulating milk and the association of bovine milk coagulation properties with genetic variants of the caseins in 3 Scandinavian dairy breeds. *Journal of Dairy Science, 96,* 4830-4842.

Raikos, V. (2010). Effect of heat treatment on milk protein functionality at emulsion interfaces. A review. Food Hydrocolloids, 24, 259-265.

Rao, M. A. (2007). Measurement of flow and viscoelastic properties. *In M. A. Rao (Ed.), Rheology of Fluid and Semisolid Foods: Principles and Applications.* pp. 59-151. Boston, MA: Springer US.

Rastogi, N. K., Raghavarao, K. S., Balasubramaniam, V. M., Niranjan, K., & Knorr, D. (2007). Opportunities and challenges in high pressure processing of foods. *Critical Reviews in Food Science and Nutrition, 47,* 69-112.

Raynes, J. K., Day, L., Augustin, M. A., & Carver, J. A. (2015). Structural differences between bovine A1 and A2 β-casein alter micelle self-assembly and influence molecular chaperone activity. *Journal of Dairy Science, 98,* 2172-2182.

Rohart, A., Michon, C., Confiac, J., & Bosc, V. (2016). Evaluation of ready-to-use SMLS and DWS devices to study acid-induced milk gel changes and syneresis. *Dairy Science & Technology, 96,* 459-475.

Rollema, H. S. (1992). Casein association and micelle formation. In Fox, P. F. (Ed.), *Advance Dairy Chemistry, Vol. 1: Proteins,* Elsevier Applied Science, London, 111-140.

Sandra, S., & Corredig, M. (2013). Rennet induced gelation of reconstituted milk protein concentrates: The role of calcium and soluble proteins during reconstitution. *International Dairy Journal, 29,* 68-74.

Sandra, S., Ho, M., Alexander, M., & Corredig, M. (2012). Effect of soluble calcium on the renneting properties of casein micelles as measured by rheology and diffusing wave spectroscopy. *Journal of Dairy Science, 95,* 75-82.

Sarode, A. R., Sawale, P. D., Khedkar, C. D., Kalyankar, S. D., & Pawshe, R. D. (2016). Casein and Caseinate: Methods of Manufacture. In B. Caballero, P. Finglas & F. Toldrá (Eds.), *The Encyclopedia of Food and Health, 1*. pp. 676-682. Oxford: Academic Press.

Sauter, A., Zhang, F., Szekely, N. K., Pipich, V., Sztucki, M., & Schreiber, F. (2016). Structural evolution of metastable protein aggregates in the presence of trivalent salt studied by (V)SANS and SAXS. *The Journal of Physical Chemistry B, 120,* 5564-5571.

Scollard, P. G., Beresford, T. P., Murphy, P. M., & Kelly, A. L. (2000). Barostability of milk plasmin activity, *Lait, 80,* 609 - 619.

Scheffold, F., Skipetrov, S., Romer, S., & Schurtenberger, P. (2001a). Diffusing-wave spectroscopy of nonergodic media. *Physical review. E, Statistical, nonlinear, and soft matter physics, 63,* 061404.

Schmidt, D. G., & Buchheim, W. (1970). Elektronenmikroskopische untersuchung der feinstruktur von caseinmicellen in kuhmilch. *Milchwissenschaft, 25,* 596–600.

Schrader, K., Buchheim, W., & V Morr, C. (1997). High pressure effects on the colloidal calcium phosphate and the structural integrity of micellar casein milk. Part 1. High pressure dissolution of colloidal calcium phosphate in heated milk systems. *Nahrung, 41,* 133-138.

Shukla, A., Narayanan, T., & Zanchi, D. (2009). Structure of casein micelles and their complexation with tannins. *Soft Matter, 5,* 2884-2888.

Sigh, A. K., Borad, S., Meena, G. S., Sharma, H., & Arora, S. (2019). High-Pressure Processing of Milk and Milk Products Non-thermal Processing of Foods, *CRC press.* pp. 75. United States: Taylor & Francls Group.

Sinaga, H., Bansal, N., & Bhandari, B. (2017). Effects of milk pH alteration on casein micelle size and gelation properties of milk. *International Journal of Food Properties, 20,* 179-197.

Slattery, C. W., & Evard, R. (1973). A model for the formation and structure of casein micelles from subunits of variable composition. *Biochimica et Biophysica Acta (BBA) - Protein Structure, 317,* 529-538.

Smialowska, A., Matia-Merino, L., Ingham, B., & Carr, A. (2017). Effect of calcium on the aggregation behaviour of caseinates. *Colloids and Surfaces A: Physicochemical and Engineering Aspects, 522,* 113-123.

Søltoft-Jensen, J., & Hansen, F. (2005). 15 - New Chemical and Biochemical Hurdles. In Sun, D.W. (Ed.), *Emerging Technologies for Food Processing.* pp. 387-416. London: Academic Press.

Southward, C. R. Uses of casein and caseinates. *In Developments in Dairy Chemistry - 4; Fox, P. F., Ed.; Elsevier Applied Science, 1989.* pp 173-24. London.

Stothart, P. H., & Cebula, D. J. (1982). Small-angle neutron scattering study of bovine casein micelles and sub-micelles. *Journal of Molecular Biology, 160,* 391-395.

Swaisgood, H. E. (1992). Chemistry of Caseins. In Fox, P. F (Ed), *Advance Dairy Chemistry, Vol. 1, Proteins.* pp. 63-110. Essex: Elsevier Science Publisher Ltd.

Tiruppathi, C., Miyamoto, Y., Ganapathy, V., Roesel, R. A., Whitford, G. M., & Leibach, F. H. (1990). Hydrolysis and transport of proline-containing peptides in renal brush-border membrane vesicles from dipeptidyl peptidase IV-positive and dipeptidyl peptidase IV-negative rat strains. *Journal of Biological Chemistry Peer-reviewed journal, 265,* 1476-1483.

Titapiccolo, G. I., Alexander, M., & Corredig, M. (2010). Rennet-induced aggregation of homogenized milk: impact of the presence of fat globules on the structure of casein gels. *Dairy Science & Technology, 90,* 623-639.

Titapiccolo, G. I., Corredig, M., & Alexander, M. (2011). Acid coagulation behaviour of homogenized milk: effect of interacting and non-interacting droplets observed by rheology and diffusing wave spectroscopy. *Dairy Science & Technology, 91,* 185-201.

Treweek, T. M., Thorn, D. C., Price, W. E., & Carver, J. A. (2011). The chaperone action of bovine milk αs1- and αs2-caseins and their associated form αs-casein. *Archives of Biochemistry and Biophysics, 510,* 42-52.

Tromp, R. H., Huppertz, T., & Kohlbrecher, J. (2014). Casein Micelles at Non-Ambient Pressure Studied by Neutron Scattering. *Food Biophysics, 10,* 51–56.

Truswell, A. S. (2005). The A2 milk case: a critical review. *European Journal of Clinical Nutrition, 59,* 623.

Tsakali, E., Petrotos, K., D'Allessandro, A., & Goulas, P. (2010). A review on whey composition and the methods used for its utilization for food and pharmaceutical products. Paper presented at the 6th International Conference on Simulation and Modelling in the Food and Bio-Industry (FOODSIM 2010).

Tuinier, R., & De Kruif, C. G. (2002). Stability of casein micelles. *The Journal of Chemical Physics, 117,* 1290-1295.

Vaia, B., Smiddy, M. A., Kelly, A. L., & Huppertz, T. (2006). Solvent-mediated disruption of bovine casein micelles at alkaline pH. *Journal of Agricultural and Food Chemistry, 54,* 8288-8293.

Vasbinder, A. J., van Mil, P., Bot, A., & de Kruif, K. G. (2001). Acid-induced gelation of heat-treated milk studied by diffusing wave spectroscopy. *Colloids and Surfaces B-Biointerfaces, 21,* 245-250.

Vincent, D., Elkins, A., Condina, M. R., Ezernieks, V., & Rochfort, S. (2016). Quantitation and identification of intact major milk proteins for high-throughput LC-ESI-Q-TOF MS analyses. *PLoS One, 11,* 1-21.

Voswinkel, L., & Kulozik, U. (2011). Fractionation of whey proteins by means of membrane

adsorption chromatography. *Procedia Food Science, 1,* 900 - 907.

Walstra, P., Wouters, J. T. M., & Geurts, T. J. (2006). Dairy science and technology, Boca Raton, FL: *CRC Press*.

Wang, F., Zhang, W., & Ren, F. Z. (2016). Effect of carrageenan addition on the rennet-induced gelation of skim milk. *Journal of the Science of Food and Agriculture, 96,* 4178-4182.

Ward, L. S., & Bastian, E. D. (1998). Isolation and identification of β-casein A1-4P and β-casein A2-4P in commercial caseinates. *Journal of Agricultural and Food Chemistry, 46,* 77-83.

Woodford, K. (2007). *Devil in the milk : illness, health and politics : A1 and A2 milk.* Nelson, N.Z: Craig Potton.

Xue, J, Z., Pine, D. J., Milner, S. T., Wu, X. I., & Chaikin, P. M. (1992). Nonergodicity and light scattering from polymer gels. *Pgysical Review A., 46,* 6550-6563.

Yang, Z., Gu, Q., Banjar, W., Li, N., & Hemar, Y. (2018). *In-situ* study of skim milk structure changes under high hydrostatic pressure using synchrotron SAXS. *Food Hydrocolloids, 77,* 772-776.

Ye, A. (2008). Complexation between milk proteins and polysaccharides via electrostatic interaction: principles and applications–a review. *International Journal of Food Science & Technology, 43,* 406-415.

Ye, A., Cui, J., Dalgleish, D., & Singh, H. (2017). Effect of homogenization and heat treatment on the behaviour of protein and fat globules during gastric digestion of milk. *Journal of Dairy Science, 100,* 36-47.

Zhang, F., Roosen-Runge, F., Skoda, M. W., Jacobs, R. M., Wolf, M., Callow, P., Frielinghaus, H., Pipich, V., Prevost, S., & Schreiber, F. (2012). Hydration and interactions in protein solutions containing concentrated electrolytes studied by small-angle scattering. *Physical Chemistry Chemical Physics, 14,* 2483-2493.

Zhang, F., Skoda, M. W., Jacobs, R. M., Martin, R. A., Martin, C. M., & Schreiber, F. (2007). Protein interactions studied by SAXS: effect of ionic strength and protein concentration for BSA in aqueous solutions. *The Journal of Physical Chemistry B, 111,* 251-259.

Zhang, D., Surapaneni, S., & ebrary, I. (2012). ADME-enabling technologies for drug design and development. Hoboken, N.J.: Hoboken, N.J.: Wiley c2012.

Zhao, Z., & Corredig, M. (2016). Influence of sodium chloride on the colloidal and rennet coagulation properties of concentrated casein micelle suspensions. *Journal of Dairy Science, 99,* 6036-6045.

Appendix 1

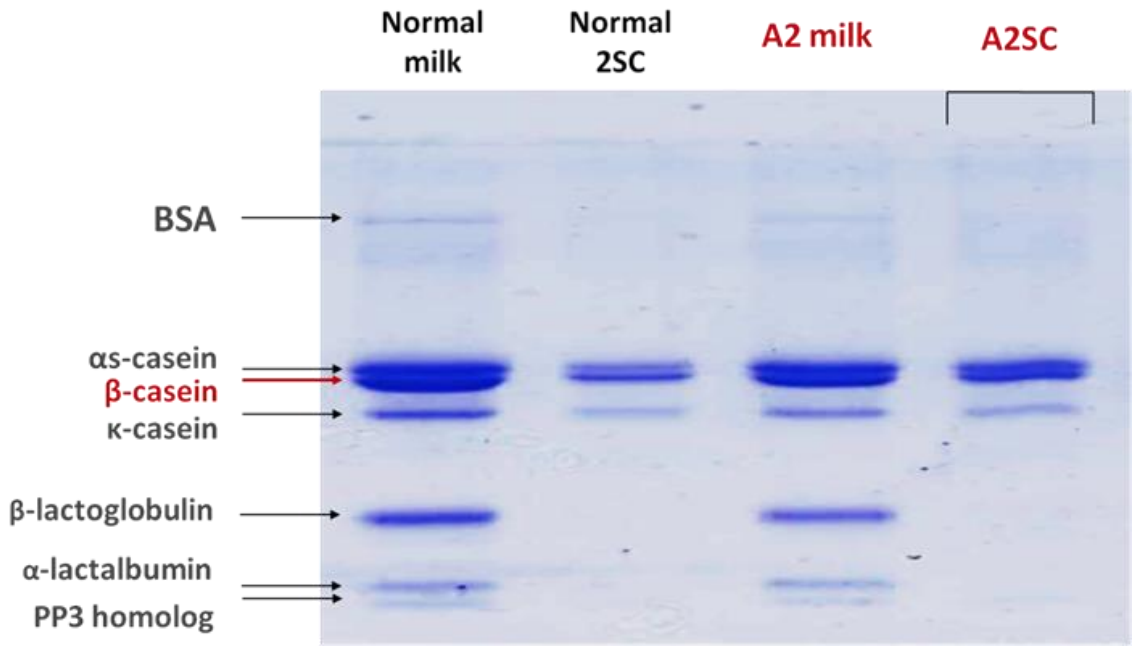

Figure A. 1. SDS-PAGE of normal A1A2 and A2 milks and extracted SCs from both types of milks.

Appendix 2

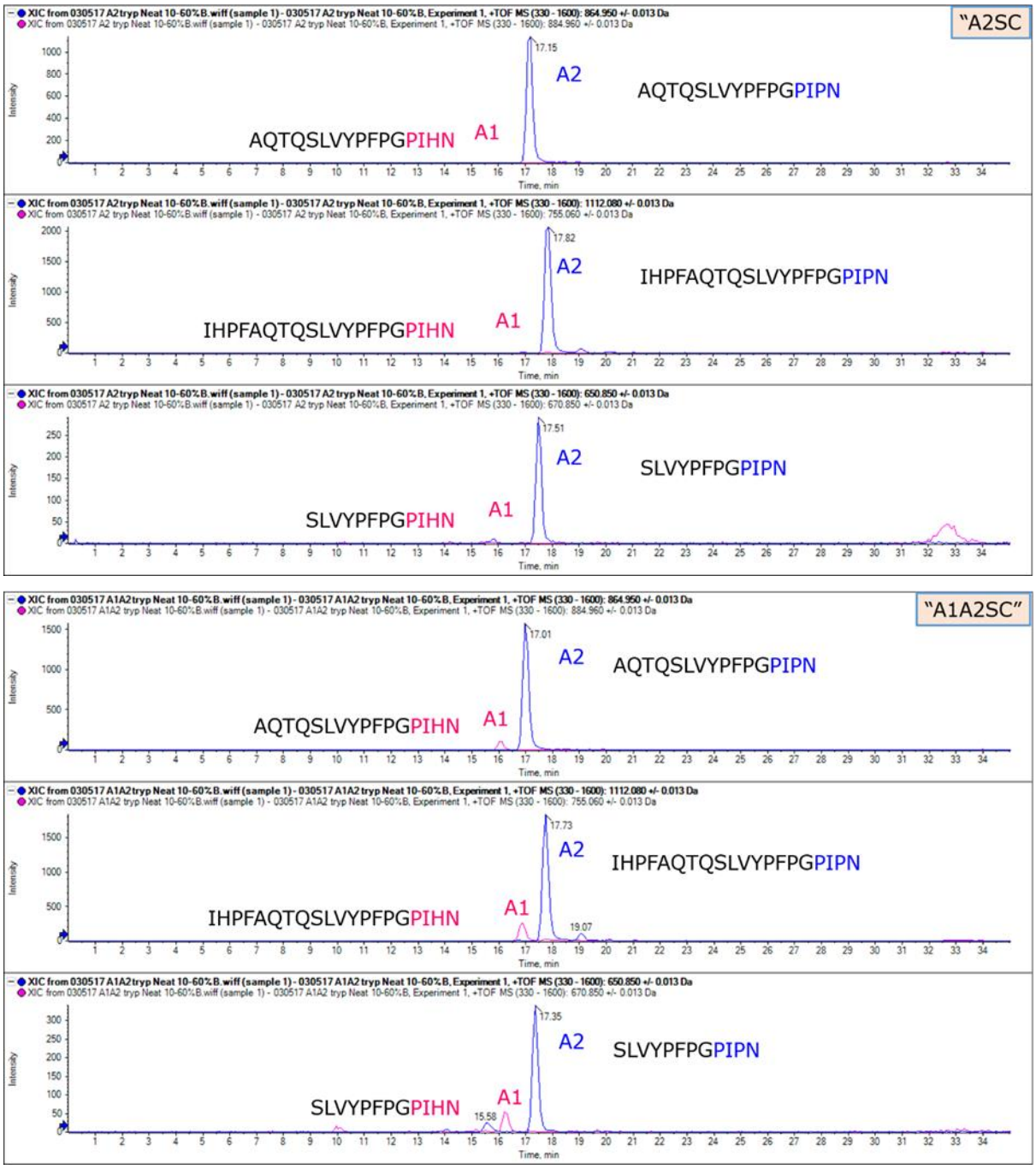

Figure A. 2. Liquid chromatography–tandem mass spectrometry chromatograms (LCMS/MS) of β-CN fractions in A2 and A1A2 SC samples.